EPICUTICULAR WAXES AND THE ENERGY BALANCE OF SORGHUM

[*Sorghum bicolor* (L.) Moench]

A Dissertation

by

HENRIQUE DA ROS CARVALHO

Submitted to the Office of Graduate and Professional Studies of
Texas A&M University
in partial fulfillment of the requirements for the degree of

DOCTOR OF PHILOSOPHY

Chair of Committee,	James L. Heilman
Co-Chair of Committee,	Kevin J. McInnes
Committee Members,	William L. Rooney
	Thomas W. Boutton
	Katie L. Lewis
Head of Department,	David D. Baltensperger

August 2019

Major Subject: Agronomy

ABSTRACT

Epicuticular waxes are hypothesized to enable plants to cope with drought. There is evidence that waxes alter the energy balance of plants through increase in reflectivity of solar radiation and through decrease in conductance of water vapor from the leaf to the atmosphere. Under radiation load from the sun, increase in reflectivity should lead to a decrease in leaf and canopy temperature, whereas decrease in conductance should lead to increase in leaf and canopy temperature because of decrease in evaporative cooling. It is not clear how these competing effects exert control over water use in a crop such as sorghum [*Sorghum bicolor* (L.) Moench], which is known to resist drought.

Experiments were conducted to determine the effects of waxes on spectral reflectivity, stomatal conductance, and energy balance of near-isogenic lines of grain sorghum having different levels of leaf epicuticular wax. Energy balances under field conditions were determined with the Bowen ratio method.

At the leaf level, waxes increased reflectivity of solar radiation, but decreased transmissivity, and, as a result, small differences in absorptivity were observed between waxy and bloomless leaves. Waxes had a negligible effect on the emissivity of longwave radiation. At the canopy level, waxes reduced net radiation of canopies by 3 to 5% compared to that of a non-waxy canopy. An overall 2% increase in albedo was the main driver for those differences, and about 86% of the reflected energy originated from near-infrared wavelengths. Rainfall was an important factor modulating the responses of bloomless plants. When water was non-limiting, waxes caused a relative decrease in

conductance that was greater than the relative increase in reflectivity. Consequently, at the expense of higher canopy temperatures, waxes caused a 5% reduction in latent heat flux. Relative differences in energy partitioning between the phenotypes changed as a drying cycle progressed. These results suggest that epicuticular waxes enabled plants to have a better control over transpiration.

This study helped elucidate the biophysical mechanisms through which epicuticular waxes influence the water and energy relations of sorghum. This information may aid plant scientists in selecting phenotypes that are better suited to cope with water deficits.

DEDICATION

During the course of my doctorate studies, important people in my life passed away. I would like to dedicate this dissertation to them: Hamilton Da Ros, grandfather, Laura Coelho Carvalho, grandmother, Maria José de Carvalho, grandaunt, and Nicanor Carvalho Júnior, uncle. You will always be in my thoughts and memories. Thank you for being examples of integrity, faith, strength, courage, and above all; love.

ACKNOWLEDGEMENTS

I wish to express my gratitude for all the people who contributed, directly or indirectly, to this project:

Drs. J. L. Heilman and K. J. McInnes, co-chairs, for giving me the opportunity to do this work and for my academic training in Environmental Physics. Many were the times I fell short of knowledge and skills; your guidance and support, not to mention patience, were invaluable to me. I would like to thank you for sharing your knowledge and experience with me, as well as for encouraging me to learn new things and to acquire new skills. I could not have asked for better mentors. I am a better professional and person because of you.

Drs. W. L. Rooney, T. W. Boutton, and K. L. Lewis, committee members, for their support throughout the course of this research. I would like to extend my appreciation to Dr. W. L. Rooney for providing the plant material used in this study and for answering my questions about sorghum production in Texas, and to Dr. K. L. Lewis, C. Lewis, and D. Kelley for their friendship and hospitality during my stay in Lubbock.

Dr. S. A. Finlayson for helping with the Li-cor spectroradiometer.

Dr. Y. Deng and B. Fashina for assisting me with the FTIR measurements.

Dr. M. Maeda and A. Maeda for the friendship, help, and support. I will never be able to repay you for all you have done for me. I do not have enough words to thank you.

Dr. J. A. Landivar for always being so accessible, for the help with the experiments in Corpus Christi, and for the encouragement throughout this project.

Finally, I wish to thank my family: Luiz Henrique, father, Vera Lucia, mother, and Rafael, brother. None of this would be possible without you; thank you for all the sacrifices you have made for me and for your endless support, encouragement, and love.

CONTRIBUTORS AND FUNDIND SOURCES

Contributors

This work was supervised by a dissertation committee consisting of Professors James L. Heilman (chair), Kevin J. McInnes (co-chair), William L. Rooney (committee member), and Katie L. Lewis (committee member) of the Department of Soil and Crop Sciences, and Professor Thomas W. Boutton (committee member) of the Department of Ecosystem Science and Management. All other work conducted for the dissertation was completed by the student independently.

Funding Sources

Graduate research assistantship was supported by the Department of Soil and Crop Sciences. This work did not receive external funding from any agency.

NOMENCLATURE

c	Cloud cover (unitless)
c_m	Specific heat capacity of soil minerals (J kg^{-1} K^{-1})
c_p	Specific heat of air at 20 ^oC (J mol^{-1} K^{-1})
C_w	Volumetric heat capacity of water (J m^{-3} K^{-1})
d	Zero plane displacement height (m)
D	Water vapor pressure deficit of air (Pa)
e_a	Actual water vapor pressure of air (Pa)
$e_{sat}(T)$	Saturation vapor pressure at temperature T (Pa)
e_{ss}	Water vapor pressure at the soil surface (Pa)
f_g	Fractional ground cover by the canopy (unitless)
f_{LIVE}	Live fraction of the canopy (unitless)
g_0	Boundary layer conductance when u or h_c is zero (mol m^{-2} s^{-1})
g_{bl}	Boundary layer conductance for any entity (mol m^{-2} s^{-1})
g_{blH}	Boundary layer conductance for heat (mol m^{-2} s^{-1})
g_{blW}	Boundary layer conductance for water vapor (mol m^{-2} s^{-1})
g_c	Canopy conductance (mol m^{-2} s^{-1})
g_{Hr}	Convective-radiative conductance (mol m^{-2} s^{-1})
g_r	Radiative conductance (mol m^{-2} s^{-1})
g_{ss}	Soil surface conductance (mol m^{-2} s^{-1})
g_s	Stomatal conductance (mol m^{-2} s^{-1})
g_v	Total conductance for water vapor (mol m^{-2} s^{-1})

G	Soil heat flux density (W m^{-2})
G_{plate}	Heat flux density through a heat flux plate (W m^{-2})
h	Plant height (m)
h_c	Calculated canopy height (m)
h_{mx}	Maximum canopy height (m)
h_{ref}	Reference height (m)
H	Sensible heat flux density (W m^{-2})
k	Light extinction coefficient (m^2 m^{-2})
k	Thermal conductivity of the soil (W m^{-1} K^{-1})
K_H	Thermal eddy diffusivity of air (m^2 s^{-1})
LAI	Leaf area index (m^2 m^{-2})
LAI_{LIVE}	Live fraction of the canopy (m^2 m^{-2})
LE	Latent heat flux density (W m^{-2})
LE_{eq}	Equilibrium evaporation (W m^{-2})
LE_i	Imposed evaporation (W m^{-2})
L_h	LAI at which h_{mx} is obtained (m^2 m^{-2})
LW	Longwave radiation, 4-100 μm (W m^{-2})
LW_e	Emitted longwave radiation by a canopy, 4-100 μm, (W m^{-2})
LW_i	Incoming atmospheric longwave radiation, 4-100 μm, (W m^{-2})
LWi_{so}	Isothermal net outgoing longwave radiation, 4-100 μm, (W m^{-2})
NIR	Near-infrared radiation (700-1100 nm)
P_a	Atmospheric pressure (Pa)

R_e	Emitted radiation by a surface (W m^{-2})
R_n	Net radiation (W m^{-2})
R_{ni}	Isothermal net radiation (W m^{-2})
R_s	Solar radiation, 0.3-4 μm, (W m^{-2})
$R_s(\lambda)$	Spectral solar radiation, 400-1100 nm, (W m^{-2} nm^{-1})
R_{sr}	Reflected solar radiation by the canopy, 0.3-4 μm, (W m^{-2})
$R_{sr}(\lambda)$	Spectral reflected solar radiation, 400-1100 nm, (W m^{-2} nm^{-1})
SW	Shortwave radiation, 0.3-4 μm, (W m^{-2})
s	Slope of the saturation water vapor mole fraction curve (K^{-1})
t	Time (s)
T_a	Air temperature (K)
T_c	Canopy temperature (K)
T_L	Leaf temperature (K)
T_s	Average soil temperature above a heat flux plate (K)
u	Wind speed (m s^{-1})
u_{ref}	Reference wind speed (m s^{-1})
VIS	Visible radiation (400-700 nm)
z or *Z*	Depth below or height above the soil surface (m)
z_m	Roughness length for momentum transport (m)
z_v	Roughness length for water vapor transport (m)

$\alpha(\lambda)$	Absorptivity for radiation as a function of wavelength (unitless)
β	Bowen ratio (unitless)
γ	Thermodynamic psychrometer constant (K^{-1})
γ^*	Apparent psychrometer constant (K^{-1})
$\delta T/ \delta z$	Vertical temperature difference between two points (K m^{-1})
Δ	Slope of the saturation water vapor pressure curve (Pa K^{-1})
$\Delta T_s/\Delta t$	Change in soil temperature with time (K s^{-1})
$\varepsilon(\lambda)$	Emissivity of a surface as a function of wavelength (unitless)
ε_L	Emissivity of a leaf (unitless)
θ	Volumetric water content (m^3 m^{-3})
λ	Latent heat of vaporization of water (J mol^{-1})
λ	Wavelength (nm or μm)
$\rho(\lambda)$	Reflectivity for radiation as a function of wavelength (unitless)
ρ_b	Soil bulk density (kg m^{-3})
ρ_c	Albedo (unitless)
$\rho_c(\lambda)$	Canopy reflectivity as a function of wavelength (unitless)
$\hat{\rho}$	Molar density of air (mol m^{-3})
$\hat{\rho} c_p$	Volumetric specific heat of air (J m^{-3} K^{-1})
σ	Stefan-Boltzmann constant (W m^{-2} K^{-4})
$\tau(\lambda)$	Transmissivity for radiation as a function of wavelength (unitless)
Ω	Decoupling factor (unitless)
Ω_c	Canopy decoupling factor (unitless)

TABLE OF CONTENTS

Page

LIST OF FIGURES

Page

LIST OF TABLES

Page

CHAPTER I

INTRODUCTION

Epicuticular waxes (*EW*) can be found at the epidermis of all plants. They constitute the last barrier that interfaces plant tissues with their immediate microclimate. Accumulation of *EW* over plant surfaces is generally regarded as a response to a number of biotic and abiotic stresses such as freezing, air pollutants and acid rain, ultra violet radiation (*UV*), drought, mechanical damage, insects and pathogens. *EW* generally are composed of hydrophobic compounds such as long-chained hydrocarbons, alkanes, primary alcohols, aldehydes, secondary alcohols, ketones, esters, and other derived compounds (Shepherd and Griffiths, 2006).

Common visual cues of accumulation of *EW* by plants are the presence of powdery "bloom" or "blueish" glaucousness. According to Jeffree (2006), leaves exhibit glaucousness when the *EW* layer is developed to the point where it is able to scatter light. In this dissertation, the terms "waxy" and "glaucous" will be used to refer to leaves/plants with greater *EW* load compared to "bloomless" and "non-glaucous".

Epicuticular Waxes and Plant-Water Relations

Sanchez-Diaz et al. (1972) proposed two mechanisms to explain the function of waxes in affecting plant-water relations and providing tolerance to drought: increased reflectivity of solar radiation, and decreased conductance of water vapor from the leaf to the atmosphere. These two mechanisms are addressed in the following discussion.

Increased Reflectivity of Solar Radiation

Studies have shown that *EW* increases reflectance of solar radiation. Blum (1975b) investigated differences in reflectivity on waxy and bloomless sorghum (*Sorghum bicolor* (L.) Moench) phenotypes. He found an increase of 4 to 5% in the visible (*VIS*) and near infrared (*NIR*) bands on adaxial leaf surfaces of waxy plants compared to bloomless plants. Reicosky and Hanover (1978) found that *EW* increased reflectivity of glaucous foliage of blue spruce (*Picea pungens* Engel.) by an average 10% over the 0.35 to 0.80 μm waveband. Johnson et al. (1983) worked with near-isogenic lines of wheat (*Triticum aestivum* L.) and found that reflectivity over the 0.40 to 0.70 μm waveband increased linearly with *EW* load. Jefferson et al. (1989) found significant increases in reflectivity on the abaxial surface of glaucous *Triticeae* range grasses over the 0.40 to 0.70 μm waveband. Holmes and Keiller (2002) measured the effects of *EW* on reflectivity of *UV* and *VIS* bands of 45 different species and found that waxy leaves were up to 30% more reflective compared to controls that had waxes removed.

Blum (1975a) found that mean total daily net radiation (R_n) over experimental dryland plots of sorghum was 5 to 6% smaller for a waxy canopy compared to a bloomless one. This appears to be the only attempt reported in the literature to measure differences in R_n between bloomless and waxy phenotypes under field conditions. Grant et al. (1995) studied the scattering effects of *EW* on *UV* and photosynthetically active radiation (*PAR*) on near-isogenic sorghum canopies but did not investigate these effects on the canopy radiation balance. Febrero et al. (1998) measured the reflectivity of barley

(*Hordeum vulgare* L.) isolines differing in glaucousness over irrigated and rain fed plots at the canopy level and found that at *VIS* wavelengths the glaucous canopy was about 20% more reflective than the non-glaucous one.

According to Febrero et al. (1998), increased reflectivity leads to decreased absorptivity of radiation, which can potentially reduce leaf temperature (T_L), and in turn reduce the vapor pressure deficit between the leaf and the atmosphere, thus potentially reducing the driving force for transpiration. Richards et al. (1986) measured differences in T_L and canopy temperature (T_c) between glaucous and non-glaucous isogenic wheat lines in the field and in the greenhouse. The field plants were monitored with thermocouples placed in their leaf sheaths, while an infrared thermometer (*IRT*) was used in the greenhouse. Under drought conditions in the field, the glaucous plants were 0.7 ^{o}C cooler than the non-glaucous ones; glaucous plants were 0.3 ^{o}C cooler than their non-glaucous counterparts in the greenhouse.

Jefferson et al. (1989) evaluated differences in T_L and T_c between glaucous and non-glaucous crested wheatgrass and wheatgrass hybrids in field nurseries and in the greenhouse. Field measurements of T_c were made with an *IRT*, and in the greenhouse T_L was measured with the thermocouple inside the chamber of a leaf porometer that was also used to measure diffusion conductance. Glaucous hybrids had lower temperatures than the non-glaucous ones in the field study. In the greenhouse study, glaucous plants were warmer than air and non-glaucous plants when soil water content was low but were cooler than air and non-glaucous plants under high water content. In field trials in College Station, Corpus Christi, and Weslaco, Texas, Awika et al. (2017) used a hand-

held *IRT* and found that sorghum plants with high *EW* loads had T_c below air temperature (T_a) by as much as 3 to 5 ^{o}C. These authors also showed that the difference in canopy and air temperature is linearly related to wax load, where the higher the wax load the cooler the canopy with respect to T_a.

Decreased Conductance to Water Vapor Flux

Conceptually, epicuticular wax could decrease conductance to water vapor at the leaf level through increased thickness of the leaf boundary layer, occlusion of stomatal pores, and decreased diffusion through the cuticle (Fig. 1.1). Sanchez-Diaz et al. (1972) and Jenks and Ashworth (1999) have suggested that waxes decreased the boundary layer conductance of water vapor of a leaf. However, this mechanism has not been investigated, and experimental evidence in the literature to support this as an appreciable component of leaf conductance to water vapor is lacking.

Jeffree et al. (1971) argued that *EW* reduce stomatal pore conductance by decreasing the cross-sectional area available for vapor diffusion at the stomatal antechamber and reducing the diffusion of gases by means of increased tortuosity of the pathway. These authors calculated the reductions in conductance caused by the waxes for Sitka spruce (*Picea sitchensis* (Bong.) Carr.) by means of anatomical measurements made with optical and transmission electron microscopes. Their calculations show that *EW* could decrease water vapor and CO_2 conductance by 66% and 32%, respectively. This effect may be present in other species (Blum, 1975b; Jenks and Ashworth, 1999).

O'Toole et al. (1979) found that removal of *EW* from rice (*Oryza sativa* L.) leaves by chloroform significantly increased cuticular conductance. Jordan et al. (1984)

collected leaves of field-grown sorghum plants to investigate the effect of *EW* load on cuticular transpiration in the laboratory. The authors found that *EW* loads greater than 0.67 mg dm^{-2} reduced cuticular transpiration and provided an effective barrier to water loss, preventing desiccation when stomata are closed.

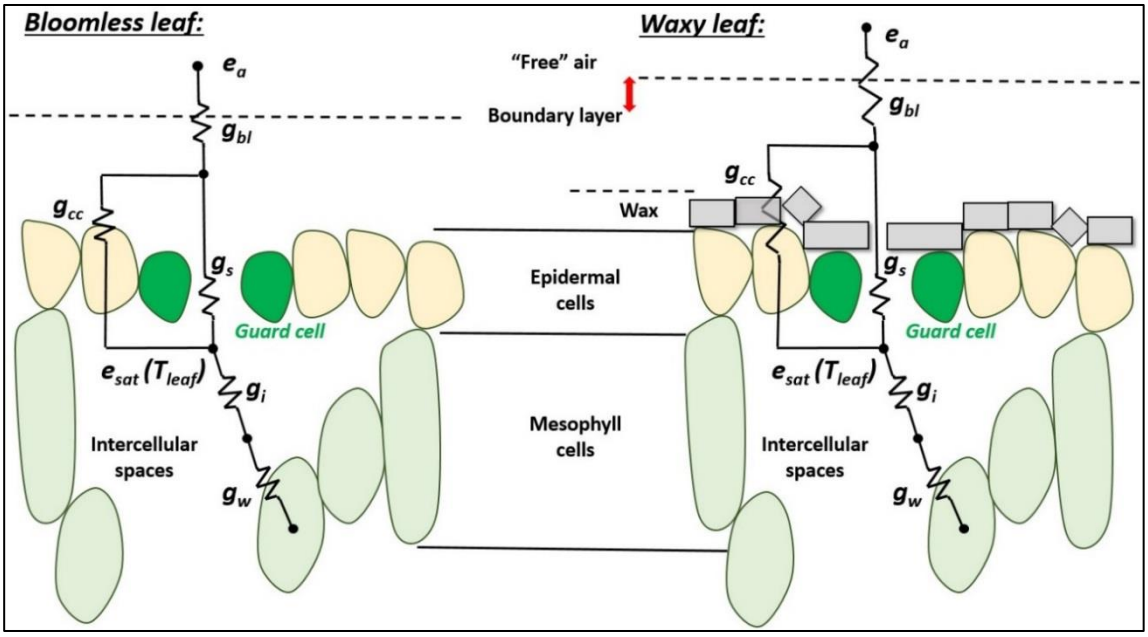

Figure 1.1. Schematic representation of the differences in the conductance network for water vapor transport from a bloomless and a waxy leaf to the surrounding air. Water vapor pressure inside the leaf intercellular spaces (e_{sat} (T_{leaf})) and in air (e_a) are represented by dots. Leaf boundary layer (g_{bl}), cuticular (g_{cc}), stomatal (g_s), intercellular (g_i), and cell-wall (g_w) conductances are represented by resistors symbols. Epicuticular waxes (*EW*) are represented by gray rectangles. The red double arrow represents the increase in boundary-layer thickness due to the presence of the waxes**.**

Effects of *EW* on water vapor fluxes from plants have been investigated mostly under environmentally controlled conditions. In a growth chamber study, Chatterton et al. (1975) assessed differences in leaf gas exchange 23 days after seeding for waxy and bloomless sorghum lines. They found that mean transpiration and mean net carbon dioxide exchange rates were 26% and 18% greater for bloomless phenotypes, respectively, but that the mean ratio of net carbon dioxide exchange to net transpiration was 6% higher for the waxy plants. Saneoka and Ogata (1987) studied the gas exchange parameters of bloom and bloomless sorghum phenotypes grown in pots under well-watered and drought-stressed conditions. They found that the ratio of apparent photosynthetic rate to transpiration rate was greater for the waxy lines in both water regimes. Clarke and Richards (1988) found that the rate of water loss from excised wheat leaves was reduced by 10% due to *EW*. Premachandra et al. (1994) found that water loss from excised leaves was greater in bloomless sorghum lines and that water-use efficiency was linearly related to *EW* load under both irrigated and non-irrigated greenhouse conditions. Hamissou and Weibel (2004) found that waxy sorghum genotypes were able to sustain higher leaf water potentials (-1.43 MPa vs -1.7 MPa) than bloomless ones under drought conditions in a greenhouse study.

These results suggest that *EW* restrict water loss from leaves. It is long and well known by plant physiologists and environmental physicists that transpiration has a cooling effect. Under high radiative load from the sun, leaf temperatures are expected to rise if transpiration decreases. One of the early accounts of the importance of evaporative cooling was reported by Lange (1959) who measured the temperature of

excised and intact leaves of *Citrullus colocynthis*. This author found that during the day, when air temperatures were as high as 50 ^{o}C, an intact leaf was 10 to 12 ^{o}C below air temperature, whereas an excised leaf quickly rose above 46 ^{o}C, the heat tolerance limit for that species, to a maximum of 60 ^{o}C. Cook et al. (1964) investigated the importance of stomatal closure for suppressing transpiration and its effect on leaf temperature under controlled environmental conditions. These authors treated tomato (*Lycopersicon esculentum* Mill.) leaves with a solution of sodium azide (NaN_3) to prevent stomatal opening. After about 17 minutes, the treated leaves were 5 ^{o}C warmer than their untreated counterparts. Ehrler and van Bavel (1967) measured the effect of soil water availability on leaf conductance and temperature of field-grown sorghum plants in central Arizona using a porometer and thermocouples inserted into the leaves. These authors reported that when the soil was dry, leaf conductance was low, and temperatures were 5 ^{o}C above air temperature during the day. Conversely, when the plants were well supplied with water after irrigation, conductance increased, and leaf temperatures were below air temperature by 4 to 6 ^{o}C in the afternoon. Lastly, by means of heat budget analysis, Gates (1968) showed that leaf temperature rises as transpiration rate decreases for a variety of leaf dimensions, stomatal conductances, and environmental conditions.

Hypotheses

There is evidence that *EW* alters the energy balance of plants through changes in leaf reflectivity and leaf conductance, both of which affect leaf temperature. Under radiative load from the sun, increased reflectivity should have the effect of reducing leaf and canopy temperatures, whereas reduced conductance should increase leaf and canopy

temperatures because of a decline in evaporative cooling. It is unclear how *EW*, through their influence on reflectivity and conductance, affect field-scale energy fluxes. I therefore propose the following hypotheses:

i. If the primary mechanism through which *EW* affect the energy balance of plants is by increased reflectivity, then waxy plants should have lower rates of water use and lower temperatures than bloomless plants.

ii. If the primary mechanism through which *EW* affect the energy balance of plants is by decreased conductance, then waxy plants should have lower rates of water use and higher temperatures than bloomless plants.

iii. If increased reflectivity and reduced conductance are co-dominant, then waxy plants should have lower rates of water use than bloomless plants, but similar temperatures.

Canopy temperature should be the variable that indicates which effect prevails under field conditions.

Objectives

Hypotheses will be tested using field-scale measurements of the energy balance of near-isogenic waxy and bloomless phenotypes of grain sorghum by means of the Bowen ratio energy balance method (*BREB*). Specific objectives are:

i. Quantify components of the energy-balance fluxes of waxy and bloomless phenotypes.

ii. Determine the mechanisms that drive the differences in energy flux, if differences exist.

iii. Quantify differences in canopy temperature and water use between waxy and bloomless phenotypes.

Theoretical implications of *EW* for the energy balance of vegetated surfaces are discussed in the following chapter.

CHAPTER II

THEORETICAL EFFECTS OF EPICUTICULAR WAXES ON THE ENERGY BALANCE OF VEGETATED SURFACES

In Chapter I, the effects of epicuticular waxes (*EW*) on the water relations of plants were discussed. Reports from the literature indicate that *EW* are associated with drought tolerance. Increased reflectivity of solar radiation and decreased conductance to water vapor could be mechanisms driving differences in water use by waxy and bloomless plants.

In this chapter, these mechanisms will be extended from leaf to canopy level and the effects of *EW* on the energy balance of vegetated surfaces will be discussed. Specifically, the means through which *EW* could affect the energy balance of a field will be addressed in terms of net radiation (R_n), canopy temperature (T_c), latent heat flux (LE), Bowen ratio (β), and a decoupling factor (Ω_c) which describes the degree of stomatal control over transpiration. The relations developed in this chapter are based on energy balance and environmental physics theory. The adopted approach is based on that of Campbell and Norman (1998) and Monteith and Unsworth (2013). The variables and parameters used throughout this discussion, as well as their definitions and units, are summarized on page vii.

Net Radiation

The radiation balance of a surface is computed as the net amount of radiant energy absorbed by the surface minus the radiant energy emitted by it. The energy

spectrum is commonly divided in two bands of interest, the shortwave R_s (0.3 to 4 μm) and the longwave *LW* (4 to 100 μm). The amount of energy emitted by a surface is a function of its temperature, and for the range of temperatures of earthly bodies, it takes the form of *LW* radiation. The Stefan-Boltzmann law gives emitted *LW* radiation (R_e) as a function of surface temperature as

$$R_e = \varepsilon \sigma T_s^4 \tag{2.1}$$

where ε is the emissivity of the surface, σ is the Stefan-Boltzmann constant ($5.67 \cdot 10^{-8}$ W m^{-2} K^{-4}), and T_s is the absolute temperature of the surface (K). Emissivity values can range from near 0 to 1. For vegetated surfaces an average value of 0.97 is assumed for ε (Campbell and Norman, 1998; Monteith and Unsworth, 2013).

The net radiation of a leaf is given by

$$R_n = \alpha_s SW_t + \alpha_L LW_t - \varepsilon_L \sigma T_L^4 \tag{2.2}$$

where α_s is the absorptivity of shortwave radiation, α_L is the absorptivity of longwave radiation (which is equivalent to its emissivity, ε_L, according to Kirchhoff's law), SW_t and LW_t are the total short and longwave radiation incident on the leaf, and T_L is the leaf absolute temperature. SW_t is commonly described as the sum of incoming solar radiation intercepted by the leaf and the amount that is reflected by the surroundings and reaches the leaf. LW_t is the incoming *LW* that is emitted by the atmosphere and the surroundings of the leaf.

Equation 2.2 shows that what couples a leaf to its radiative environment is absorptivity (Gates et al, 1965). For translucent materials such as non-succulent leaves, absorptivity is calculated as the residual of the following equation

$$\alpha(\lambda) = 1 - \rho(\lambda) - \tau(\lambda) \quad (2.3)$$

where ρ and τ are the reflectivity and transmissivity of the material, respectively. Therefore, in terms of solar radiation, increased ρ caused by *EW* will affect R_n by means of decreased α only if τ remains unchanged.

In the early studies of *EW* and spectral properties of plants, the longwave balance was overlooked, and emphasis was placed on the shortwave balance. Equation 2.2 shows that R_n is affected by the longwave balance through ε_L and T_L. There is no information in the literature about whether the presence of *EW* alters ε_L. It is readily seen in Eq. 2.2 that increasing T_L reduces R_n. Leaf temperature, however, is a dynamic variable which is determined by energy balance, and because of that it can be challenging to make specific predictions about how *EW* influence T_L. From this discussion it is clear that the effects of *EW* on the spectral properties (α, ρ, τ, and ε) of leaves need to be investigated.

Assuming complete soil coverage, R_n for a plant canopy can be written as

$$R_n = (1 - \rho_c)R_s + \varepsilon LW_i - \varepsilon\sigma T_c^4 \quad (2.4)$$

where ρ_c, or albedo, is the canopy reflectivity of solar radiation (ratio of reflected to incoming R_s), LW_i is the incoming longwave radiation emitted by the atmosphere, and T_c is the absolute canopy temperature. Equations 2.2 and 2.4 are very similar. The major difference between them is in the shortwave term, where α_s is replaced by (1 - ρ_c). That means the intercepted solar radiation, i.e. the amount left after reflection by the canopy, will eventually be extinguished due to multiple reflections among leaves and the soil surface (Campbell and Norman, 1998). Therefore, for a dense canopy fully covering the soil, the albedo determines the amount of solar radiation that is absorbed by the surface.

Thus, if the *EW* are effective in increasing albedo, then reductions in R_n can be expected. Similarly, an increase in T_c will lead to a decrease in R_n. Net radiation data from Blum (1975a) do not show how *EW* decreased R_n, whether it was mainly due to an increase in albedo, or increase in T_c, or a combination of both. Mechanisms by which *EW* affect canopy R_n still need to be elucidated, and the effects of *EW* on albedo and T_c need to be quantified.

Canopy Temperature

It was stated previously that the energy balance determines the temperature of a system. Therefore, to understand the mechanisms through which *EW* can affect T_c it is necessary to investigate the energy balance equation for a plant canopy. This equation can be written as

$$R_n + H + LE + G = 0 \qquad (2.5)$$

where *H* is the sensible heat flux density, *LE* is latent heat flux density, and *G* is the soil heat flux density, all in units of W m^{-2}. The sum of the terms in Eq. 2.5 needs to be equal to zero, if the amount of energy stored in photosynthetically derived products is negligible. The sign convention used here is that fluxes directed toward the surface are positive and those away from the surface are negative (Fig. 2.1). Net radiation is positive during the daytime and negative at night. Net radiation of a canopy is partitioned among *H*, *LE,* and *G*.

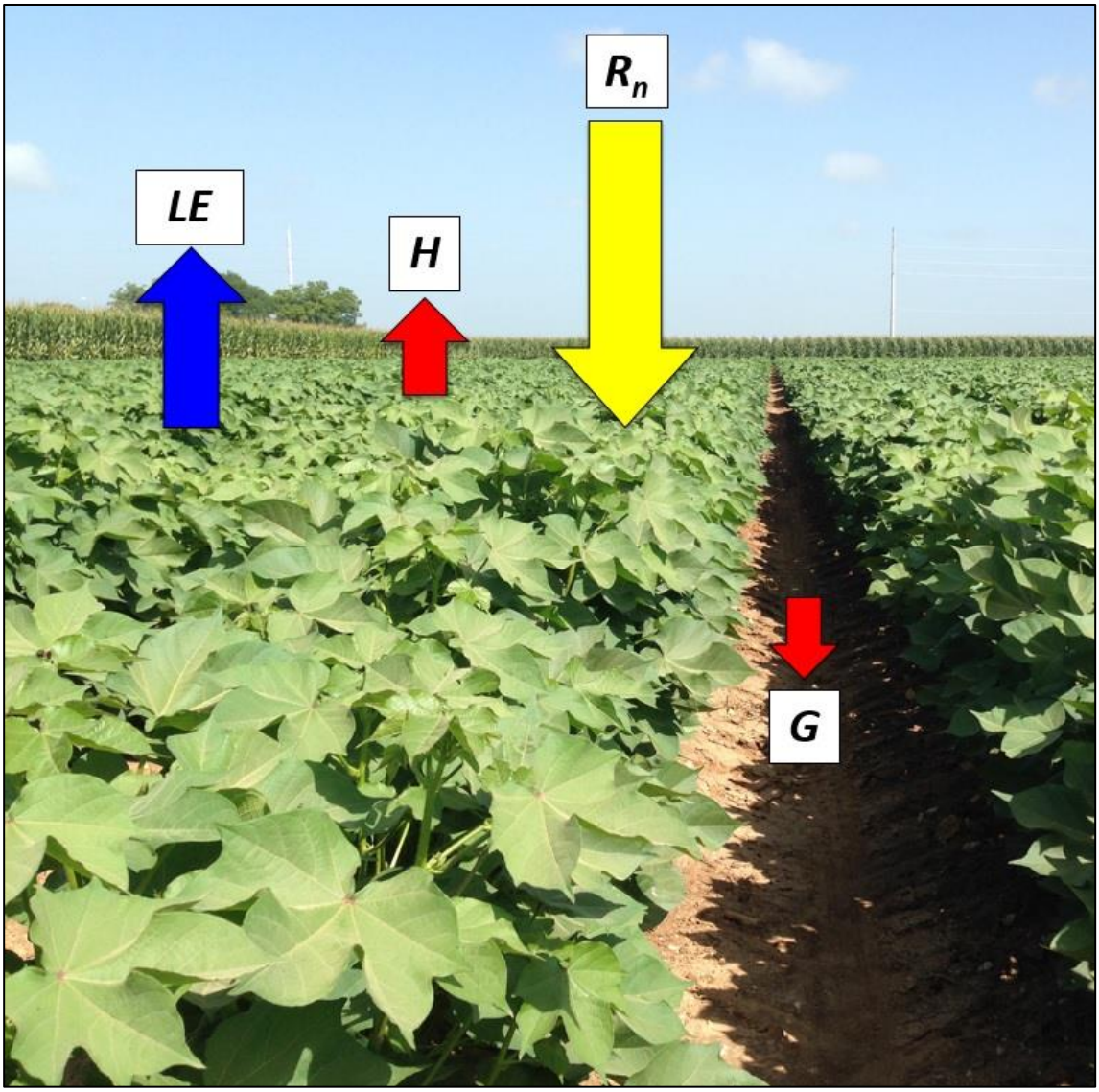

Figure 2.1. Simplified schematic of the daytime energy balance of a crop field. Sign convention dictates that net radiation (R_n) is directed towards the surface, while sensible (H), latent (LE), and soil heat (G) fluxes are directed away from the surface.

Sensible heat flux density can be estimated as

$$H = -g_{blH} c_p (T_c - T_a) \tag{2.6}$$

where g_{blH} is the boundary layer conductance for heat transfer, c_p is the molar specific heat of air, and T_a is the air temperature.

Latent heat flux density can be estimated as

$$LE = -\lambda g_v \frac{e_{sat}(T_c) - e_a}{P_a} \tag{2.7}$$

where λ is the latent heat of vaporization of water, g_v is the total conductance of water vapor, $e_{sat}(T_c)$ is the saturation water vapor pressure at T_c, e_a is the actual vapor pressure of air, and P_a is the atmospheric pressure. It is assumed that the air in the intercellular spaces in the plant is saturated with water vapor. The total water vapor conductance consists of three terms (Fig. 2.2), the canopy conductance (g_c), which incorporates the contributions of all the leaves in the canopy, the soil surface conductance (g_{ss}), and the turbulent boundary layer conductance for water vapor transport (g_{blW}). In dense canopies that fully cover the soil g_{ss} is usually small (Jones, 2014), so it is often neglected and g_v may be treated as a series network between g_c and g_{blW}. This approach is commonly known as the "big leaf" model and was first introduced by Monteith (1965). The soil surface conductance becomes important in sparse canopies, thus making the "big leaf" model inappropriate under those conditions, which often requires a more complex two-source energy balance model that takes into account the canopy and soil energy balances separately (Shuttleworth and Wallace, 1985). However, Ritchie and Burnett (1971) demonstrated that for crops growing under well-watered field conditions as the leaf area

index exceeds 2.7 and the ground cover is in excess of 80%, transpiration will be the determinant factor of *LE*. Therefore, it is reasonable to neglect g_{ss} and approximate g_v as

$$g_v = \frac{1}{\frac{1}{g_c} + \frac{1}{g_{blW}}} \tag{2.8}$$

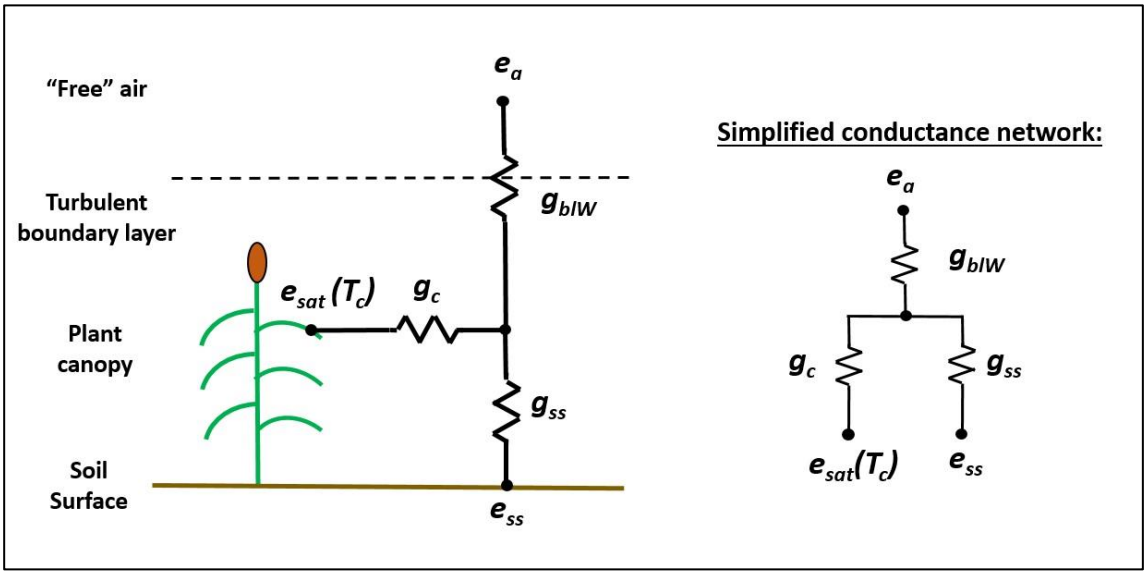

Figure 2.2. Simplified schematic representation of the conductance network in the soil-plant-atmosphere system. In series with the boundary layer (g_{blW}) are the canopy (g_c) and soil surface (g_{ss}) conductances, which are in parallel with respect to each other. The plants and the soil surface are sources of water vapor, while the atmosphere is the sink. Water vapor pressure at the plant canopy (e_{sat} (T_c)), soil surface (e_{ss}), and air (e_a) are represented by dots.

The soil heat flux can be estimated using Fourier's Law for heat transport as

$$G = -k\frac{\delta T}{\delta z} \tag{2.9}$$

where k is thermal conductivity of the soil and $\delta T/\delta z$ is the change in temperature with depth in the soil. It is not expected that EW will have significant short-term effects on G.

After substituting Eqs. 2.4, 2.6, and 2.7 into 2.5, the canopy energy balance equation becomes

$$(1-\rho_c)R_s + \varepsilon LW_i - \varepsilon\sigma T_c^4 - g_{blH}c_p(T_c - T_a) - \lambda g_v\frac{e_{sat}(T_c) - e_a}{P_a} + G = 0 \tag{2.10}$$

Equation 2.10 clearly shows the importance of T_c in determining the energy balance of the surface. However, as is Eq. 2.10 cannot be solved for T_c in an easy way because the terms $\varepsilon\sigma T_c^4$ and $e_{sat}(T_c)$ are non-linear. Therefore, these terms need to be approximated to obtain a solution for T_c.

According to Campbell and Norman (1998), air temperature can be used to approximate T_c^4, so that $T_c^4 = (T_a + \Delta T)^4$, where $\Delta T = T_c - T_a$. Then, $\varepsilon\sigma T_c^4$ can be approximated as

$$\varepsilon\sigma T_c^4 \cong \varepsilon\sigma T_a^4 + 4\varepsilon\sigma T_a^3(T_c - T_a) \tag{2.11}$$

Equation 2.11 can be further simplified by defining the radiative conductance (g_r) as

$$g_r = \frac{4\varepsilon\sigma T_a^3}{c_p} \tag{2.12}$$

Substitution of equation 2.12 into 2.11 yields

$$\varepsilon\sigma T_c^4 = \varepsilon\sigma T_a^4 + c_p g_r(T_c - T_a) \tag{2.13}$$

Substituting Eq. 2.13 into Eq. 2.10 yields

$$(1-\rho_c)R_s + \varepsilon LW_i - \varepsilon\sigma T_a^4 - c_p g_r(T_c - T_a) - g_{bl}c_p(T_c - T_a) - \lambda g_v \frac{e_{sat}(T_c) - e_a}{P_a} + G = 0 \quad (2.14)$$

It is commonly accepted to combine the first three terms into what is called the isothermal net radiation term (R_{ni}). R_{ni} receives this name because the LW balance is calculated by approximating T_c as T_a, so that canopy and air are at the same temperature. The other simplification that is usually adopted is to combine g_r and g_{blH} into a single term, the convective-radiative conductance (g_{Hr}), where $g_{Hr} = g_r + g_{blH}$. Then, equation 2.14 reduces to

$$R_{ni} - g_{Hr}c_p(T_c - T_a) - \lambda g_v \frac{e_{sat}(T_c) - e_a}{P_a} + G = 0 \quad (2.15)$$

The linearization of $e_{sat}(T_c) - e_a$ was first introduced by Penman (1948) who proposed that this term could be approximated as

$$e_{sat}(T_c) - e_a \cong \Delta(T_c - T_a) + D \quad (2.16)$$

where Δ is the slope of the saturation water vapor pressure-temperature curve and D is water vapor pressure deficit of the air. Vapor pressure deficit D is given by

$$D = e_{sat}(T_a) - e_a \quad (2.17)$$

Substituting Eq. 2.16 into 2.15 yields

$$R_{ni} - g_{Hr}c_p(T_c - T_a) - \lambda g_v \frac{[\Delta(T_c - T_a) + D]}{P_a} + G = 0 \quad (2.18)$$

It is useful to define the slope of the saturation water vapor mole fraction as s, where $s = \Delta/P_a$. After substituting s into equation 2.18 and some manipulation, the following balance is obtained

$$R_{ni} + G - \lambda g_v \frac{D}{P_a} - \left(c_p g_{Hr} + \lambda s g_v\right)(T_c - T_a) = 0 \quad (2.19)$$

To solve for ($T_c - T_a$), two more steps must be taken. The first is to define the apparent psychrometer constant (γ^*) as

$$\gamma^* = \frac{c_p g_{Hr}}{\lambda g_v} \tag{2.20}$$

Then, by rearranging the terms in Eq. 2.19 and making the necessary substitutions using Eq. 2.20, the canopy-air temperature difference can be described as

$$T_c - T_a = \frac{\frac{R_{ni} + G}{g_v} - \lambda \frac{D}{P_a}}{\lambda(s + \gamma^*)}. \tag{2.21}$$

The form in which Eq. 2.21 is presented allows us to investigate the consequences of *EW* for the temperature difference between canopy and air in a direct way. Since the effects of the *EW* are associated with reduced net radiation and water vapor conductance, the term of interest in Eq. 2.21 is ($R_{ni} + G$)/g_v. Three scenarios that can be explored are:

1) *EW* are effective in reducing R_{ni} but not g_v.

2) *EW* are effective in reducing g_v but not R_{ni}.

3) *EW* effectively reduce both R_{ni} and g_v.

If everything else is held constant, in the first scenario it can be shown that reductions in R_{ni} should reduce ($T_c - T_a$), which means the difference between T_c and T_a should decrease. Therefore, increases in albedo should lead to a cooling effect and T_c should approach T_a. In semiarid environments where *D* is large, if albedo is increased substantially, then it is possible that ($T_c - T_a$) becomes negative so that the air is warmer than the canopy. This condition, referred to as advection (Kirkham, 2014), has significant implications for the energy balance of plants. It implies that *H* is no longer a

means by which R_{ni} is dissipated, but a source of energy for the plants (Fig. 2.3). Consequently, *LE* can exceed R_{ni} if *G* is low. Advection typically occurs in irrigated fields that are downwind of hot, dry areas, regardless of leaf optical properties and results in high rates of water use.

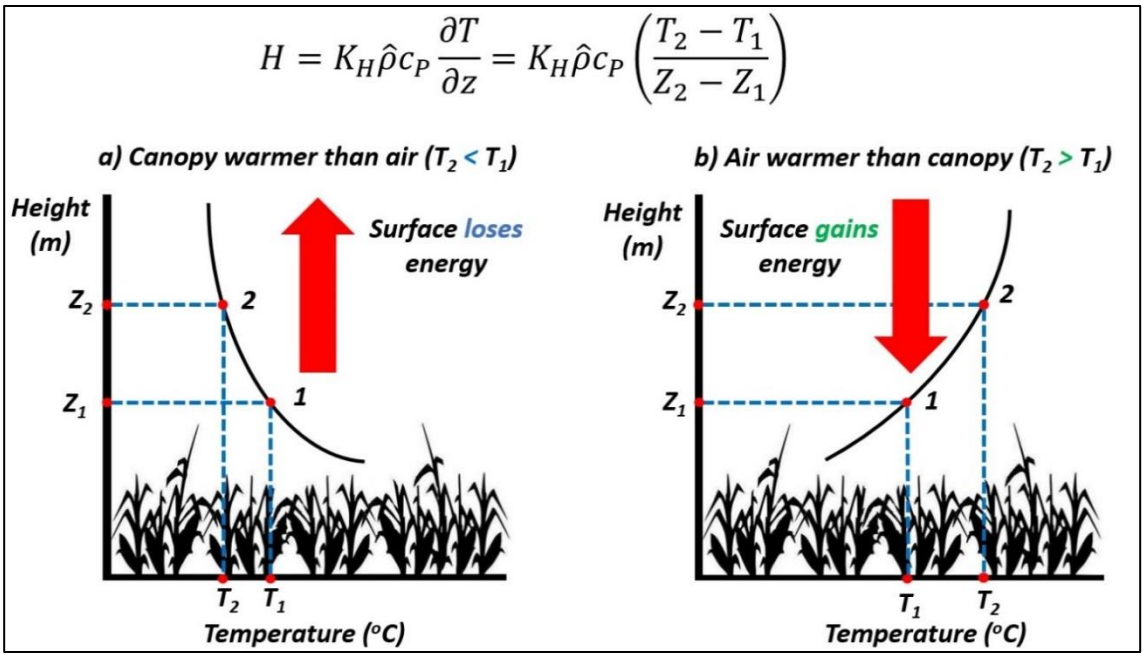

Figure 2.3. Schematic representation of a) convection and b) advection. The aerodynamic equation for sensible heat flux (*H*) is shown for reference; K_H is the thermal eddy diffusivity of air, $\hat{\rho} c_p$ is the volumetric specific heat of air, and $\delta T/\delta z$ is the air temperature gradient between points 1 and 2. According to the sign convention adopted in equation 2.4, $\delta T/\delta z$ in a) is negative, thus making *H* negative, which represents an energy transfer away from the surface. The opposite occurs in b) and *H* becomes a source of energy for the surface.

In the second scenario it is assumed that the waxes will affect g_v through g_c. Even though it has been suggested that at the leaf level *EW* may increase the thickness of the leaf boundary layer, at the canopy level g_{blW} is a function of plant height and wind speed. Therefore, it is not expected that waxes can affect g_{blW}. As g_c decreases, the denominator in Eq. 2.8 increases, thus making g_v small. As consequence, the term $(R_{ni} + G)/g_v$ in Eq. 2.21 should become large because g_v decreases, which indicates that $(T_c - T_a)$ also increases. That means the canopy becomes warmer than air. Therefore, if the waxes are effective in decreasing g_v only, then waxy plants should be expected to have high canopy temperatures.

The third scenario is the mostly likely to happen. Equation 2.21 shows that the influence of *EW* on R_{ni} and g_v have opposing effects on $(T_c - T_a)$. Therefore, the dominant effect will dictate canopy temperature. If albedo increases more than g_v decreases, on a relative basis, then T_c is expected to decrease. In the extreme situation where albedo is substantially increased, and given that *D* is large, then the canopy can be cooler than air. It is important to note, however, that for this condition to be true albedo has to significantly offset g_v. On the other hand, if g_v dominates $(R_{ni} + G)/g_v$, then T_c is expected to rise. At this point, there is no indication in the literature of who wins the "arm wrestling" contest between reflectivity and conductance.

Latent Heat Flux

The energy balance equation can be linearized and rearranged to solve for *LE*. This derivation yields the Penman-Monteith equation. According to Campbell and Norman (1998), this equation can be written in its isothermal form as

$$LE = \frac{s}{s+\gamma^*}(R_{ni} + G) + \frac{\gamma^*}{s+\gamma^*}\left(\lambda g_v \frac{D}{P_a}\right) \quad (2.22)$$

Equation 2.22 shows that *LE* is the weighted sum of the available energy ($R_{ni} + G$) and atmospheric demand for water ($\lambda g_v D/P_a$) terms, where the weighting factors are $s/(s + \gamma^*)$ and $\gamma^*/(s + \gamma^*)$. If everything else is held constant, as R_{ni} and g_v decrease, *LE* should decrease as well. Therefore, as opposed to what was discussed for T_c, in terms of water use, increased albedo and decreased conductance act synergistically to decrease *LE*. Campbell and Norman (1998) explain that *s* is a function of temperature, so that as air becomes warmer R_{ni} is expected to exert an even greater control over *LE*. From this discussion, it is clear that a good strategy for reducing water use by the plant would be if *EW* decreased both R_{ni} and g_v.

Bowen Ratio

Another useful way to analyze the consequences of *EW* to the energy balance of vegetated surfaces is by the Bowen ratio (β), which is expressed as

$$\beta = \frac{H}{LE}. \quad (2.23)$$

The Bowen ratio is the ratio of sensible heat flux to latent heat flux, and it indicates how the available energy of a field is being partitioned. It also forms the basis of a micrometeorological method known as the Bowen ratio energy balance (*BREB*) for determining energy fluxes in the field. The *BREB* method takes advantage of the theoretical development of Bowen (1926) to compute *LE* and *H* (Rosenberg et al., 1983).

When crops are actively growing, water is non-limiting, and environmental conditions are favorable, *LE* is usually larger than *H*, thus making β small. On the other

hand, when water availability is limiting, *LE* becomes smaller than *H*, so β increases. Therefore, the magnitude of β is a good indicator of the water status of a field.

As discussed previously, *EW* may reduce *LE* by means of reduced R_{ni} and g_v. Therefore, it is reasonable to argue that a waxy canopy could show larger values of β than those of a bloomless one. The magnitude of the difference of β between waxy and non-waxy canopies serve as an indicator of how effective the waxes may be in influencing the energy partitioning in the field environment. In the canopy temperature section, the possibility of advection being induced by *EW* was discussed. If that is the case, then β should reflect that, and negative values should be observed for waxy canopies that have T_c lower than T_a.

Decoupling Factor

The decoupling factor (Ω) was first introduced by Jarvis and McNaughton (1986) to investigate the importance of stomatal conductance in determining transpiration at different scales, ranging from leaf to ecosystem level. Omega is a dimensionless quantity that has values between 0 and 1. When Ω approaches 1, the surface is considered to be perfectly decoupled from the atmosphere, whereas when it approaches 0 it is said to be perfectly coupled to the atmosphere. In general, Ω may be interpreted as measure of the degree of stomatal control over transpiration. At the canopy level Ω_c, the decoupling factor can be calculated as

$$\Omega_c = \frac{\frac{s}{\gamma} + 1}{\frac{s}{\gamma} + 1 + \frac{g_{bl}}{g_c}} \tag{2.24}$$

where γ is the psychrometer constant, given as

$$\gamma = \frac{c_p}{\lambda} \tag{2.25}$$

Omega was derived from the Penman-Monteith equation in its original form, i.e. non-isothermal, which is given as

$$LE = \frac{s(R_n + G)}{s + \gamma\left(1 + \frac{g_{bl}}{g_c}\right)} + \frac{c_p g_{bl} \frac{D}{P_a}}{s + \gamma\left(1 + \frac{g_{bl}}{g_c}\right)}. \tag{2.26}$$

Equation 2.26 is similar in form as Eq. 2.22. The difference between them is that R_{ni} is replaced by R_n and γ^* is evaluated as $\gamma^* = \gamma g_{blH}/g_v$. Then, it is assumed that $g_{bl} \approx g_{blH} \approx g_{blW}$, where g_{bl} is the turbulent boundary layer conductance for the transport of any entity, so the apparent psychrometer constant can be rearranged to $\gamma(1+g_{bl}/g_c)$. Equation 2.26 shows that LE is driven by two terms, $s(R_n + G)$ and $c_p g_{bl}(D/P_a)$. The first is commonly called the diabatic term and it describes the effect of solar radiation on evaporation through R_n. The second is called the adiabatic term and it represents the effects of the status of the atmosphere on evaporation in terms of its humidity and turbulence.

To have Eq. 2.26 in the format of that given by Jarvis and McNaughton (1986), it is necessary to divide the denominator and numerator of the terms in the right-hand side of Eq. 2.26 by γ, so that the following is obtained

$$LE = \frac{\frac{s}{\gamma}(R_n + G)}{\frac{s}{\gamma} + 1 + \frac{g_{bl}}{g_c}} + \frac{\frac{c_p}{\gamma} g_{bl} \frac{D}{P_a}}{\frac{s}{\gamma} + 1 + \frac{g_{bl}}{g_c}}. \tag{2.27}$$

The authors consider two scenarios: one where g_{bl} tends to zero, e.g. at low wind speeds and/or very short canopies, and one where g_{bl} tends to infinity, e.g. at high wind speeds

and/or very tall canopies. In the first case, $g_{bl} \rightarrow 0$, it can be seen that equation 2.27 reduces to

$$LE_{eq} = \frac{\frac{s}{\gamma}(R_n + G)}{\frac{s}{\gamma} + 1} \tag{2.28}$$

where LE_{eq} stands for *equilibrium evaporation.* It describes the extreme condition where *LE* is determined by the available energy term (R_n + *G*), which is controlled mainly by solar radiation. In this situation, the canopy is said to be perfectly decoupled from the atmosphere, so that atmospheric humidity and turbulence and stomatal conductance have no effect on *LE*. Conversely, when $g_{bl} \rightarrow \infty$, Eq. 2.27 reduces to

$$LE_i = \frac{\frac{c_p}{\gamma} g_{bl} \frac{D}{P_a}}{\frac{s}{\gamma} + 1 + \frac{g_{bl}}{g_c}} \approx \frac{\frac{c_p}{\gamma} g_{bl} \frac{D}{P_a}}{\frac{g_{bl}}{g_c}} \approx \frac{c_p}{\gamma} g_c \frac{D}{P_a} \tag{2.29}$$

where LE_i is referred to as the *imposed evaporation.* It represents that extreme condition where *LE* is determined by the water vapor saturation deficit of the atmosphere and canopy conductance. The canopy is said to be perfectly coupled from the atmosphere under this condition, and solar radiation has no effect on *LE*. Therefore, *LE* is determined by the conditions "imposed" by the atmosphere and the degree to which the plants can control their canopy conductance.

The Penman-Monteith equation can be rewritten by combining Eqs. 2.24, 2.28, and 2.29 as

$$LE = \Omega_c LE_{eq} + (1 - \Omega_c) LE_i. \tag{2.30}$$

Equation 2.30 shows that *LE* is the weighted sum of LE_{eq} and LE_i, where the weighing factor is Ω_c. Jarvis and McNaughton (1986) explain that forests have low Ω_c, grasslands and pastures have values of Ω_c close to 1, and agricultural crops are intermediate. Forests canopies are exposed to a highly turbulent environment, which means *LE* in forests is mostly determined by the atmosphere and canopy conductance. Grasslands and pastures are smooth surfaces, so they experience less turbulence, and as a result *LE* is determined by solar radiation mostly, indicating poor canopy control over transpiration. Crops may depend on both factors about equally. Based on this discussion it is possible to argue that waxy canopies may show lower Ω_c than non-waxy ones due to lower g_c. Thus, waxy canopies may exert a better control over transpiration and be less sensitive to solar radiation as a driving force for *LE*.

According to Jones (2014), a particular value of the approach developed by Jarvis and McNaughton (1986) is the ability to estimate how changes in conductance affect *LE*. The equation given by Jarvis and McNaughton is

$$\frac{\delta LE}{LE} = (1 - \Omega_c)\frac{\delta g_c}{g_c} \tag{2.31}$$

Equation 2.30 may be used to predict the effect of *EW* on *LE*. Chatterton et al. (1975) found that waxy leaves had transpiration rates 26% lower than bloomless ones. Since the experiment was performed in a growth chamber, where plants were exposed to the same conditions, it is reasonable to assume that these differences were consequences of the effects of *EW* on conductance only. Therefore, at the leaf level $\delta g_l/g_l$ takes the value of 0.26. Extrapolating this value to the whole canopy and assuming and an intermediate value for Ω_c (0.5), from Eq. 2.31 we can estimate that $\delta LE/LE$ may be 0.13, indicating

that the presence of the waxes could potentially reduce *LE* by 13%. Of course, this is a rough estimation; such large differences in $\delta g_c/g_c$ may not be realistic. This calculation was intended to show that *EW* might affect *LE*, but at the same time the limitations imposed by Ω_c need to be taken into consideration. Therefore, the conclusion from this analysis is that *EW* can affect *LE* at the field scale, but it is reasonable to expect rather small differences, if any.

Summary

The consequences of *EW* for the energy balance of vegetated surfaces were discussed to some detail in the previous sections. It was shown how *EW* could affect energy fluxes in the field environment and what the possible consequences are. Lastly, by means of the decoupling factor, it was demonstrated that the differences caused by *EW* at the leaf level should produce an effect of lower magnitude at the field environment. The topics discussed here will be investigated by means of a simulation model and field experiments in the following chapters.

CHAPTER III

SIMULATION OF CANOPY TEMPERATURE AND LATENT HEAT FLUX

In chapter II, the consequences of epicuticular waxes (*EW*) for the energy balance of vegetated surfaces were considered based on energy balance and environmental physics theory. It was shown that, at least in theory, reductions in net radiation (R_n) and conductance to water vapor (g_v) act synergistically to decrease canopy latent heat flux (*LE*) but have opposite effects on canopy temperature (T_c). Therefore, the objective of this chapter is to analyze the consequences of such effects in a quantitative way by means of a simulation model. The adopted simulation scheme is based on the work of Johnson (2013) and Thornley and Johnson (2000). Three different scenarios were considered in the analysis that simulate the hypotheses of this study using standard weather data and values published in the literature.

This chapter is organized in three sections. First, the theoretical aspects of the models are covered in a concise manner. Then, the values used in the simulations are specified. The results of the simulations are discussed in the third section. The variables and parameters discussed throughout these sections, as well as their units and definitions, are summarized on page vii.

Theoretical Considerations

The simulation model developed by Johnson (2013) is based on the isothermal form of the Penman-Monteith equation, but with a few modifications. First, the relevant components of the model will be briefly discussed. Then the equations for *LE* and T_c will

be presented. A detailed derivation of these equations is given by Johnson (2013) and Thornley and Johnson (2000). A simplified flowchart for the simulation is shown in Fig. 3.1. Hourly time steps (Δt) are used.

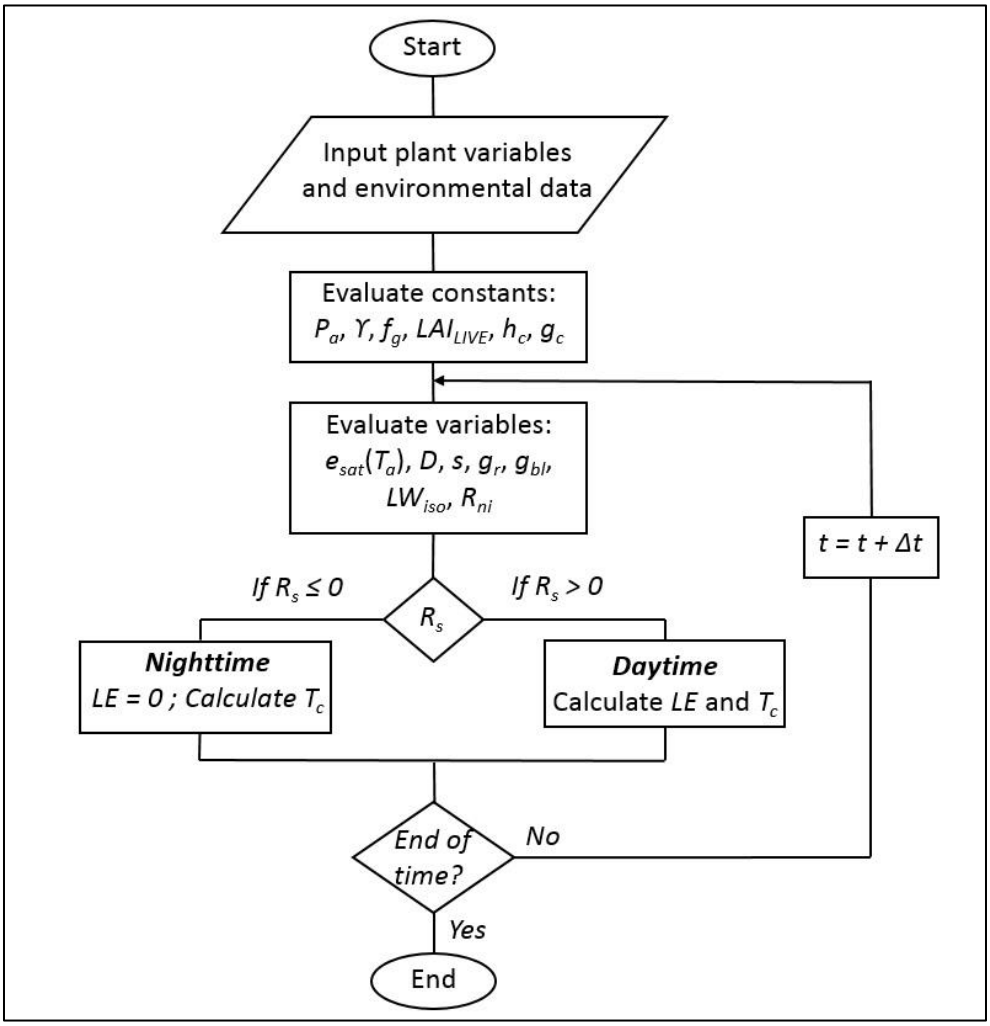

Figure 3.1. Simplified flowchart for simulating canopy temperature (T_c) and latent heat flux (LE).

Weather variables

Hourly weather data from day of year (*DOY*) 196, 2018, from a standard weather station located at the Texas AgriLife Research & Extension Center at Corpus Christi, TX (27.7° N, 97.5° W, 16 m above sea level), were used as input to the calculations (Table 3.1). The input variables were solar radiation (R_s), air temperature (T_a), water vapor pressure (e_a), and wind speed (u). Atmospheric pressure (P_a) was set to 101.3 kPa as the site is near sea level. The water vapor pressure deficit of air (D) was calculated as

$$D = e_{sat}(T_a) - e_a \tag{3.1}$$

where $e_{sat}(T_a)$ is the saturation water vapor pressure of air, calculated as

$$e_{sat}(T_a) = aexp\left(\frac{bT_a}{c + T_a}\right) \tag{3.2}$$

where the coefficients a, b, c are 0.611 kPa, 17.5, and 241 °C, respectively. These values were obtained from Campbell and Norman (1998). The slope of the water vapor saturation mole fraction-temperature curve (s) was evaluated as

$$s = \frac{\frac{bce_{sat}(T_a)}{(c + T_a)^2}}{P_a}. \tag{3.3}$$

The psychrometric constant (γ) was calculated by

$$\gamma = \frac{c_p}{\lambda} \tag{3.4}$$

where c_p is the molar specific heat of air, and λ is latent heat of vaporization of water.

Table 3.1. Hourly weather data for day of year (*DOY*) 196 at Corpus Christi, TX. Solar radiation (R_s), air temperature (T_a), actual water vapor pressure (e_a), and wind speed (u) data were obtained from a standard weather station.

Time	R_s	T_a	e_a	u
-----h-----	-----W m^{-2}----	----^{o}C----	----kPa----	----m s^{-1}----
0	0	26.37	3.10	2.18
1	0	26.11	3.08	1.90
2	0	26.02	3.08	1.83
3	0	25.93	3.08	1.70
4	0	25.71	3.08	1.53
5	0	25.61	3.08	1.60
6	3	25.54	3.08	1.17
7	73	26.03	3.15	1.54
8	234	27.79	3.22	2.56
9	429	29.42	2.98	4.01
10	641	31.02	2.81	3.78
11	784	32.17	2.69	4.05
12	809	32.72	2.78	3.99
13	903	32.94	2.89	4.13
14	873	32.71	2.99	4.61
15	757	32.33	2.98	4.85
16	636	31.92	2.89	5.24
17	470	31.21	2.82	5.50
18	274	30.34	2.74	5.50
19	96	29.13	2.77	5.19
20	7	27.81	2.85	3.97
21	0	27.03	2.90	3.35
22	0	26.48	2.97	2.68
23	0	26.23	3.01	2.43

Plant variables

Johnson (2013) derives the equations in his model in terms of fraction of ground (f_g) covered by the canopy. To calculate f_g, the canopy leaf area index (*LAI*) and light extinction coefficient (*k*) need to be specified. Then, f_g was calculated as

$$f_g = 1 - exp(-kLAI) \tag{3.5}$$

LAI is also used to calculate LAI_{LIVE} and canopy height (h_c), which later will be used in the equations for canopy and boundary-layer conductance. LAI_{LIVE} is the live fraction of the canopy *LAI* and was evaluated as

$$LAI_{LIVE} = LAI \cdot f_{LIVE} \tag{3.6}$$

where f_{LIVE} is the live fraction of leaf area. Canopy height was calculated by

$$h_c = h_{mx}\left[1 - exp\left(-069\frac{LAI}{L_h}\right)\right] \tag{3.7}$$

where h_{mx} is the maximum canopy height attained as *LAI* increases and L_h is the *LAI* at which half maximum height is obtained.

Conductances

Three conductances are required to calculate *LE* and T_c. The first is the radiative conductance (g_r), and was evaluated as

$$g_r = \frac{4\varepsilon\sigma T_a^3}{c_p} \tag{3.8}$$

where ε is the emissivity of the plants, assumed to be 0.97, and σ is the Stefan-Boltzmann constant. Equation 3.8 uses absolute temperature, so T_a needs to be converted to Kelvin.

The second is the canopy conductance (g_c), and was calculated as

$$g_c = g_s \cdot LAI_{LIVE} \tag{3.9}$$

where g_s is the average stomatal conductance of all leaves in the canopy, accounting for both abaxial and adaxial surfaces. It is important to note that the scaling factor between g_s and g_c is LAI_{LIVE}. Johnson (2013) also considers environmental effects on g_s. His approach is similar to that of Ball et al. (1987), where the influence of radiation, humidity, and atmospheric CO_2 concentration on g_s is recognized. For the purposes of this study, these effects were not included and g_c is treated as constant during the day.

Lastly, the boundary layer conductance (g_{bl}) was calculated as

$$g_{bl} = g_0 + \left(g_{ref} - g_0\right)\frac{u}{u_{ref}}\left(\frac{h_c}{h_{ref}}\right)^{0.5} \tag{3.10}$$

where g_0 is the conductance when wind speed or canopy height are zero, g_{ref} is a reference conductance at a reference canopy height (h_{ref}) and reference wind speed (u_{ref}). The values given by Johnson (2013) for g_0, g_{ref}, h_{ref}, u_{ref}, are 0.3 mol m^{-2} s^{-1}, 0.8 mol m^{-2} s^{-1}, 0.3 m, and 2 m s^{-1}, respectively. These values were obtained from the data of Blonquist et al. (2009). Therefore, Eq. 3.10 is a function of wind speed and canopy height. The author argues that even though he derived Eq. 3.10 empirically, it still captures the expected behavior of g_{bl} when calculated using the traditional aerodynamic approach, but without the uncertainties associated with low wind speed and/or canopy height, which makes it useful for simulation purposes. These claims will not be challenged, and Eq. 3.10 will be used in the simulations of the present study.

Isothermal net radiation

The isothermal net radiation (R_{ni}) was evaluated using the equation given by Johnson (2013) as

$$R_{ni} = (1 - \rho_c)R_s - LW_{iso} \tag{3.11}$$

where ρ_c is the albedo (ratio of reflected to incoming solar radiation) of the plant canopy and LW_{iso} is the isothermal net outgoing longwave radiation. LW_{iso} was calculated as

$$LW_{iso} = \sigma T_a^4\left(0.34 - 0.14\sqrt{e_a}\right)[1.35(1 - 0.7c) - 0.35] \tag{3.12}$$

where c is the cloud cover. For cloudless days, c is equal to 0, whereas for completely overcast days c is equal to 1. For the conditions of *DOY* 196 it is assumed c equal to 0.

Canopy temperature and latent heat flux

The simulation scheme treats daytime and nighttime conditions separately. R_s is used as the conditional variable to switch the equations between nighttime and daytime. For daytime conditions, the equations given by Johnson (2013) to calculate LE and T_c are

$$If\ R_s > 0,\ \ then: \qquad LE = \frac{f_g\left[sR_{ni} + \lambda\gamma(g_{bl} + g_r)\frac{D}{P_a}\right]}{s + \gamma f_g(g_{bl} + g_r)\left(\frac{1}{g_c} + \frac{1}{g_{bl}}\right)} \tag{3.13}$$

and

$$T_c = T_a + \frac{f_g R_{ni}\left(\frac{1}{g_c} + \frac{1}{g_{bl}}\right) - \lambda\frac{D}{P_a}}{\lambda\left[s + \gamma s f_g(g_{bl} + g_r)\left(\frac{1}{g_c} + \frac{1}{g_{bl}}\right)\right]}. \tag{3.14}$$

For nighttime conditions, the equations *LE* and T_c are

$$If\ R_s \leq 0,\ \ then\ \ LE = 0 \tag{3.15}$$

and

$$T_c = T_a + \frac{f_g R_{ni}\left(\frac{1}{g_{bl}}\right) - \lambda\frac{D}{P_a}}{\lambda\left[s + \gamma s f_g(g_{bl} + g_r)\left(\frac{1}{g_{bl}}\right)\right]}. \tag{3.16}$$

For nighttime conditions, it is assumed that *LE* is equal to zero because stomata are closed (g_c = 0). Due to the same reason, Eq. 3.14 is reduced to Eq. 3.16.

Simulation Scenarios

To simulate the effects of *EW* on *LE* and T_c the following scenarios were considered:

1) Reflectivity varies and stomatal conductance is held constant.

2) Stomatal conductance varies and reflectivity is held constant.

3) Reflectivity and stomatal conductance vary.

In scenario 1 the *EW* are effective in reducing R_{ni} but not g_c. In scenario 2 the *EW* are effective in reducing g_c but not R_{ni}. In scenario 3 the *EW* effectively reduce both R_{ni} and g_c.

Values used in each simulation are summarized in Table 3.2. A reference ρ_c of 0.20 and reference g_s of 0.20 mol m^{-2} s^{-1} are used to characterize the canopy that has no *EW* (bloomless). According to Campbell and Norman (1998) 0.20 is a representative value of ρ_c for crop canopies. Körner et al. (1979) reported that cultivated C3 and C4 grasses and herbaceous crop plants have an average maximum leaf conductance of about

0.20 to 0.30 mol m^{-2} s^{-1}. Johnson (2013) uses 0.20 mol m^{-2} s^{-1} as the default value of g_s in his model.

The work of Blum (1975b) and Chatterton et al. (1975) are used to specify the values of ρ_c and g_s for the waxy canopy. Blum (1975) investigated the difference between waxy and bloomless sorghum phenotypes in terms of reflectivity of shortwave radiation on adaxial leaf surfaces. He found an increase of 4 to 5% for the waxy type over the bloomless one. Chatterton et al. (1975) found that transpiration, on average, was 26% greater for bloomless sorghum phenotypes compared to waxy ones by means of leaf gas exchange measurements. Since their experiment was performed in a growth chamber, where plants were exposed to the same conditions, it is reasonable to assume that these differences were consequences of the effects of *EW* on conductance only. Based on those results and on the values assumed for the bloomless canopy, the values of ρ_c and g_s given to the waxy canopy are 0.25 and 0.15 mol m^{-2} s^{-1}. The other plant variables were treated as constants for both canopy types. The values assigned to h_{mx}, LAI, k, f_{LIVE}, L_h, are 1, 3, 1, 1, and 1, respectively. The values found by Blum (1975b) and Chatterton et al. (1975) seem to represent the largest differences between bloomless and waxy plants reported in the literature. Therefore, the results of this simulation may indicate the maximum differences that can be expected under field conditions.

Table 3.2. Albedo (ρ_c) and stomatal conductance (g_s) values used for the simulation of the effects of epicuticular waxes (*EW*) on canopy temperature (T_c) and latent heat flux (*LE*).

Scenario	Phenotype	ρ_c	g_s
			-----mol m^{-2} s^{-1}----
1			
	Bloomless	0.20	0.20
	Waxy	0.25	0.20
2			
	Bloomless	0.20	0.20
	Waxy	0.20	0.15
3			
	Bloomless	0.20	0.20
	Waxy	0.25	0.15

Results and Discussion

The output of the simulations is shown in Figs. 3.2, 3.3, and 3.4. The results for scenario 1 show that the waxy canopy had lower *LE* and T_c compared to the bloomless one. The greatest differences occurred at 13h. The difference in T_c and *LE* was 0.36 ^oC and 20 W m^{-2}, respectively. On average, T_c and *LE* were 0.20 ^oC and 10 W m^{-2} greater for the bloomless phenotype than for the waxy one. The daily total difference in *LE* between phenotypes was 0.5 MJ day^{-1}, which means the bloomless canopy exceeded the water use of the waxy canopy by 0.22 mm.

For scenario 2, the simulations showed that the waxy canopy had lower *LE* and higher T_c than the bloomless canopy. At 13h, when the greatest differences were observed, the waxy canopy was 1 ^oC warmer than the bloomless one, but *LE* was lower

by 63 W m^{-2}. The average difference in *LE* between the canopies was 37.9 W m^{-2}. The waxy canopy was 0.57 ºC warmer than the bloomless one on average. The daily total difference in *LE* was 2 MJ day^{-1}, which indicates that the bloomless canopy used 0.84 mm more water than the waxy canopy.

Scenario 3 showed a similar pattern to that of scenario 2, where the waxy canopy uses less water, but is warmer than the bloomless one. At 13h, the phenotypes differed in *LE* by 81 W m^{-2}, while their T_c differed by 0.6 ºC. The average difference in *LE* between the canopies was 46.6 W m^{-2}. The bloomless canopy was 0.36 ºC cooler than the waxy one on average. Scenario 3 is the one that showed the greatest difference in water use between canopy types. The daily difference in *LE* was 2.5 MJ day^{-1}, indicating that the waxy canopy used 1.03 mm of water less than the bloomless canopy. In none of the scenarios was T_c lower than T_a.

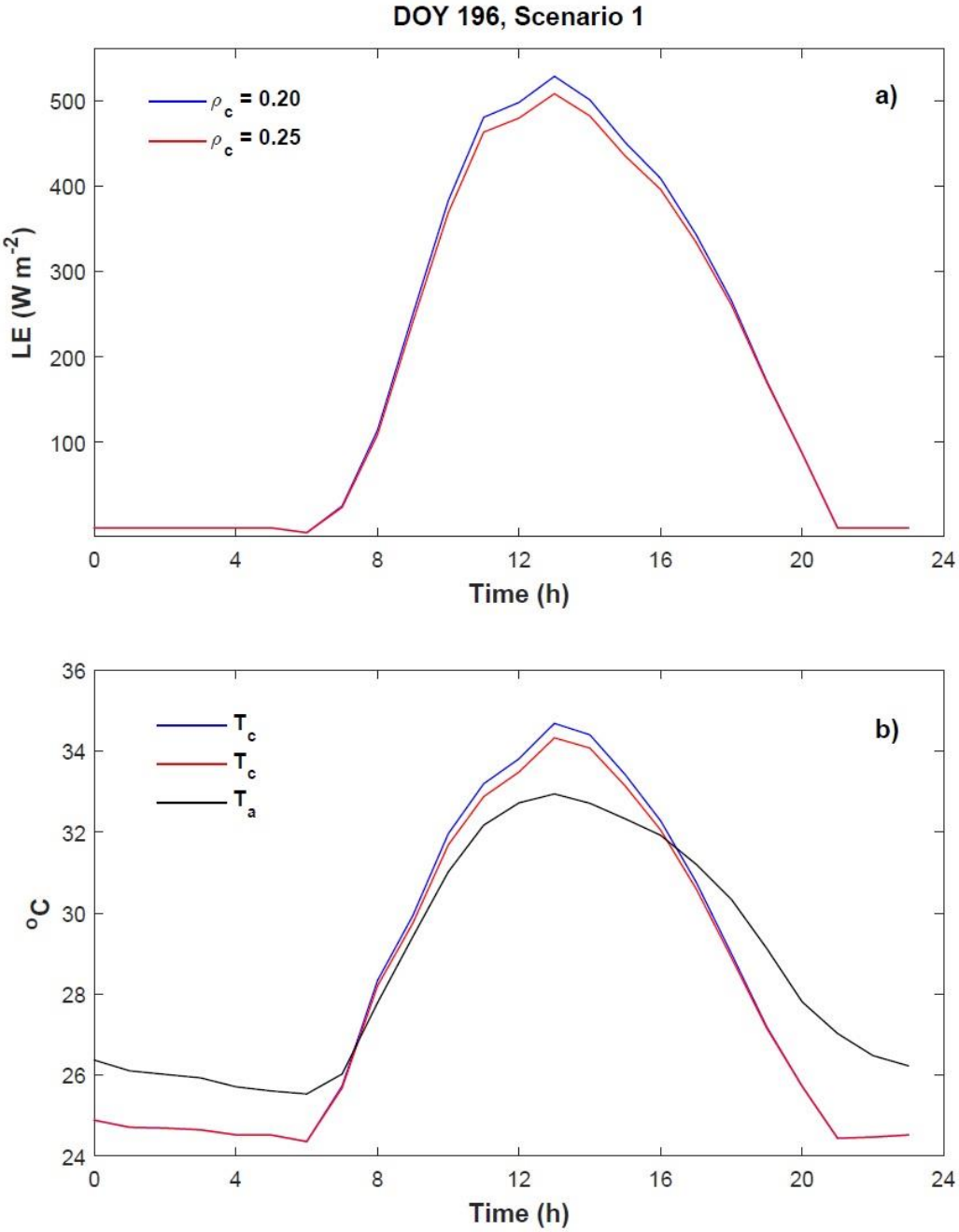

Figure 3.2. Simulation of (a) canopy latent heat flux (*LE*) and (b) canopy temperature (T_c) for day of year (*DOY*) 196. In scenario 1 albedo (ρ_c) varied while stomatal conductance (g_s) was held constant at 0.20 mol m^{-2} s^{-1}. The bloomless and waxy phenotypes are represented by the blue and red lines, respectively. Air temperature (T_a) was plotted for reference.

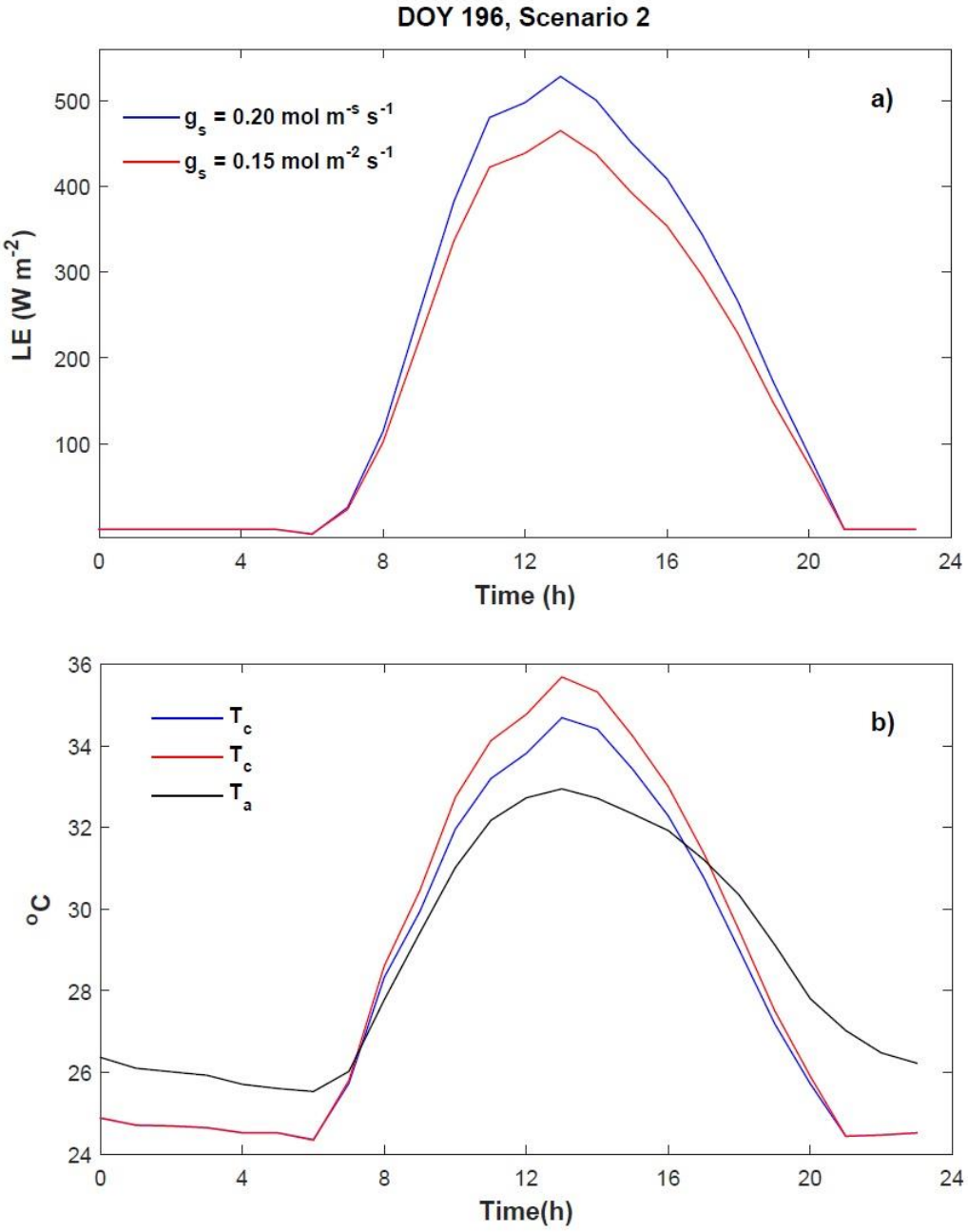

Figure 3.3. Simulation of (a) canopy latent heat flux (*LE*) and (b) canopy temperature (T_c) for day of year (*DOY*) 196. In scenario 2 albedo (ρ_c) was held constant at 0.20 while stomatal conductance (g_s) varied. The bloomless and waxy phenotypes are represented by the blue and red lines, respectively. Air temperature (T_a) was plotted for reference.

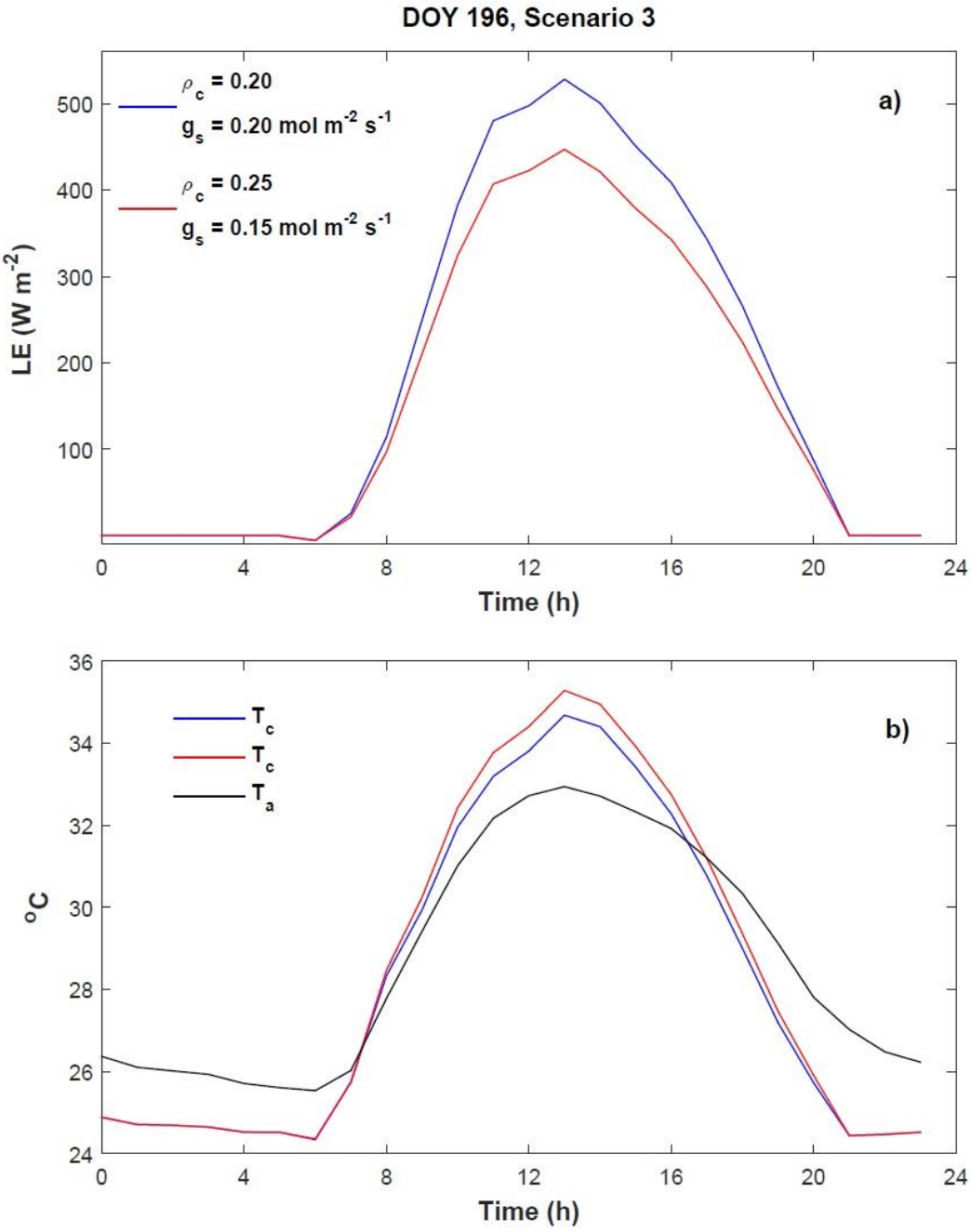

Figure 3.4. Simulation of (a) canopy latent heat flux (*LE*) and (b) canopy temperature (T_c) for day of year (*DOY*) 196. In scenario 3 albedo (ρ_c) and stomatal conductance (g_s) varied. The bloomless and waxy phenotypes are represented by the blue and red lines, respectively. Air temperature (T_a) was plotted for reference.

The simulations revealed that albedo is a weak driver for differences in *LE* and T_c. Scenario 1, where albedo was the main driver, showed the least amount of change in those variables. Scenario 1 also showed that an increase in albedo much greater than 5% will be required to bring T_c below T_a. This simulation indicates that an albedo of 0.50 to 0.60 would cause T_c to be smaller than T_a, which represents an increase in albedo of 30 to 40%. Therefore, it seems unlikely that albedo alone will be responsible for cooling the canopy below air temperature. Stomatal conductance was the dominant factor driving the differences in *LE* and T_c. That was observed in scenarios 2 and 3.

Scenarios 2 and 3 also show that if stomatal conductance is low, a higher albedo may reduce the associated increase in T_c. Results from this simulation show that the most efficient water saving strategy is that in which the plant is able to reduce its stomatal conductance and increase its albedo. In that way, the plant optimizes the balance between reducing latent heat flux and overheating. Increasing albedo alone does not lead to significant changes in *LE* and T_c. Decreasing stomatal conductance alone reduces *LE* significantly, but leads also to extra warming, which is undesirable. These topics will be investigated experimentally in the following chapters.

CHAPTER IV

EFFECTS OF EPICUTICULAR WAXES ON LEAF SPECTRAL PROPERTIES

Introduction

In the first chapters of this dissertation, the effects of epicuticular waxes on plant-water relations were discussed. Specifically, two mechanisms to explain the function of waxes as a means of providing tolerance to drought were investigated: increased reflectivity of solar radiation and decreased conductance to water vapor flux.

Increased reflectivity due to *EW* has been found in sorghum (Kanemasu and Arkin, 1974; Blum, 1975b), blue spruce (Reicosky and Hanover, 1978), wheat (Johnson et al., 1983), and many other species (Holmes and Keiller, 2002). Increased reflectivity can lead to decreased radiation absorptivity (Febrero et al., 1998) and changes in the leaf radiation balance. Reductions in absorptivity could reduce leaf temperature (Richards et al., 1986; Jefferson et al., 1989; Awika et al., 2017), and in turn reduce the vapor pressure deficit between the leaf and the atmosphere through effects on leaf temperature, thus reducing the driving force for transpiration. The radiation balance of a leaf is described by its net radiation (R_n), which is given by the equation

$$R_n = \alpha_s SW_t + \alpha_L LW_t - \varepsilon_L \sigma T_L^4 \quad (4.1)$$

where α_s is the absorptivity of shortwave radiation, α_L is the absorptivity of longwave radiation, which is equivalent to its emissivity (ε_L), SW_t and LW_t are the total short and longwave radiation incident on the leaf, and T_L is the absolute temperature of the leaf. Equation 4.1 shows that what couples a leaf to its radiative environment is absorptivity

(Gates et al, 1965). Increased shortwave ρ caused by *EW* will affect R_n by means of decreased α only if τ remains unchanged. Equation 4.1 also shows that R_n is affected by the longwave balance through ε and T_L. There is no information in the literature on the impact of *EW* on ε. It is readily seen in Eq. 4.1 that changes in T_L affect R_n. Leaf temperature, however, is a dynamic variable which is determined by its energy balance and because of that, it can be challenging to make specific predictions about how *EW* influence T_L. It is possible that reductions in evaporative cooling caused by *EW* may elevate T_L, offsetting the impact of reductions in absorptivity. From this discussion it is clear that the effects of *EW* on the spectral properties (α, ρ, τ, and ε) of leaves need to be further investigated.

The objective of this study was to determine how *EW* affect the spectral properties (α, ρ, τ, ε) of leaves. To do that, spectral properties of leaves from greenhouse and field-grown, near-isogenic lines of sorghum contrasting in *EW* load were measured. The consequences for the energy balance of leaves are discussed.

Materials and Methods

Plant material

Three near-isogenic lines of sorghum [*Sorghum bicolor* (L.) Moench] contrasting in *EW* content were used. These lines are similar in terms of growth pattern, plant height, and other phenotypic traits. The lines Martin and White Martin have the presence of waxy bloom, whereas Bloomless Martin does not.

Greenhouse and field studies

Spectral measurements were made on plant material that was obtained from greenhouse-grown and field-grown plants. Plants in the greenhouse were grown at the Norman E. Borlaug Center for Southern Crop Improvement, College Station, TX, in 2017. The pots were laid out in the greenhouse in a completely randomized design. Eight plants were grown per line. Materials were planted in 6-L pots filled with a soil mixture consisting of vermiculite, bark, and other constituents (Sun Gro Metro-Mix 360 RSI, Agawam, MA). Pots were watered routinely. Samples from field plants were obtained in 2017 and 2018 from research fields at the AgriLife Research Extension Centers at Lubbock (33.6^{o} N, 101.8^{o} W, 1000 m above sea level) and Corpus Christi (27.7^{o} N, 97.5^{o} W, 16 m above sea level), respectively. In both locations, each line was grown in a 50 by 50 m plot. Row spacing was 0.5 m and areal density of plants was 150,000 ha^{-1}. Planting in Lubbock occurred on 6 June 2017, whereas in Corpus Christi planting date was on 1 May 2018. Fields were flood-irrigated in Lubbock and drip-tape irrigation was used in Corpus Christi. Plants were irrigated to ensure adequate vegetative growth and complete canopy cover to minimize soil exposure to solar radiation. In Lubbock, the soil was classified as Olton clay loam series (fine, mixed, superactive, thermic Aridic Paleustolls) and rows followed north-south orientation. In Corpus Christi, the soil was classified as Raymondville clay loam series (fine, mixed, superactive, hyperthermic Vertic Calciustolls), and rows followed east-west orientation. Management practices in both locations such as weed and pest control were performed as needed.

Epicuticular wax contents

Measurements of wax concentration were made when plants were at the flowering stage in all years and locations. The quantity of wax on the leaf blades was determined gravimetrically following the procedure described by Ebercon et al. (1977). The leaves sampled were the first and/or second leaf below the flag leaf. One sample consisted of four leaf blades. Four samples were processed per line on the greenhouse and Corpus Christi experiments, whereas three samples per line used in Lubbock. First, the area of the leaf blades was measured using an area scanner (model 3100C, LI-COR, Lincoln, NE). Then the leaves of one sample were immersed in 100 mL of chloroform for 15 seconds. The extracts were evaporated in a fume hood over a period of 24 hours at room temperature. The amount of wax was calculated as the weight difference of the glassware. Wax concentration on the leaves was calculated as the weight difference divided by the sum of the areas of the leaves in the sample.

Spectral measurements

Leaf samples were collected for determinations of absorptivity, reflectivity, transmissivity, and emissivity. Plants were sampled when they were at the flowering stage in all years and locations. The leaves sampled were the first and/or second leaf below the flag leaf.

Four leaves per line were sampled on the field studies, whereas 16 leaves were analyzed in the greenhouse study. The leaf blades were collected in the morning, around 9h, when no dew was present on the leaves. After being excised, the leaves were immediately placed in plastic bags and then stored in a cooler with ice. Measurements

were made no longer than 2 h from the moment the samples were collected. A spectroradiometer (model LI-1800, LI-COR, Lincoln, NE) and integrating sphere (model LI1800-12, LI-COR, Lincoln, NE) were used for the measurements of ρ and τ. Absorptivity was calculated as the residual in the equation

$$\alpha(\lambda) = 1 - \rho(\lambda) - \tau\,(\lambda) \tag{4.2}$$

where λ is the wavelength being measured. The instrument was set up to take readings in the waveband of 400-1100 nm with spectral resolution of 2 nm. The measurements were made on both abaxial and adaxial surfaces. The values from both surfaces were averaged to represent the whole leaf.

Wax extracts were obtained from the Corpus Christi plants to obtain reflectivity scans of the waxes. The extracts were scanned with the spectroradiometer and integrating sphere using black and a white backgrounds, so that the "true" ρ of the wax could be calculated from a system of linear equations, which can be simplified as

$$\rho(\lambda) = [\rho_w(\lambda)\rho_{abk}(\lambda) - \rho_{bk}(\lambda)\rho_{aw}(\lambda)]/[\rho_{abk}(\lambda) - \rho_{aw}(\lambda) + \rho_w(\lambda) - \rho_{bk}(\lambda)] \tag{4.3}$$

where ρ_w and ρ_{bk} are the reflectivity of the white and black backgrounds, respectively, and ρ_{aw} and ρ_{abk} are the apparent reflectivity of the wax sample when measured with the white and black backgrounds, respectively. It was assumed in Eq. 4.3 that the wax sample covered the same fractional area of the backgrounds during the measurements.

Determinations of ε were done only on leaf samples from the greenhouse plants. The Fourier transform infrared (FTIR) spectroscopy technique was used. The instrument (model Spectrum 100 with diffuse reflectance sampling accessory, PerkinElmer, Shelton, CT) was configured to take ρ readings in the 1.28-22 μm spectral range, with a

resolution of 0.32 nm at a rate of 32 scans per measurement. According to Kirchhoff's law, ε was calculated as

$$\varepsilon(\lambda) = 1 - \rho(\lambda) \quad (4.4)$$

Four leaves per line were analyzed. The measurements were done in three distinct positions in each leaf sample (at 15, 30, and 45 cm from the leaf collar) and in both abaxial and adaxial surfaces. Samples of 9 cm^2 were cut from the leaves and placed on the sample holder for the measurements. Values of $\rho(\lambda)$ over the 8-14 μm waveband were averaged across leaves, positions, and surfaces to represent whole leaf ε. The interval between 8-14 μm corresponds to the wavelengths of peak emittance of most terrestrial objects at earthly temperatures according to Wien's law.

Results and Discussion

The *EW* concentrations for the lines are shown in Table 4.1. As expected, the bloomless isoline had a much lower *EW* concentration than its waxy counterparts. The variability in *EW* concentration between locations and years was small. Therefore, data were combined and average values for each line were obtained. The average wax concentration on the leaves of Bloomless Martin, Martin, and White Martin were 0.34, 1.99, and 2.13 mg dm^{-2}, respectively. The observed concentrations were within the range of values previously reported for sorghum in the literature. Ebercon et al. (1977) showed that *EW* load on sorghum leaves ranged from 1.14 to 1.99 mg dm^{-2} for different waxy genotypes, Powell et al. (1977) reported a range of 1.74 to 2.19 mg dm^{-2} for waxy sorghum lines, Jordan et al. (1983) showed that *EW* concentration of different waxy genotypes varied from 0.65 to 2.25 mg dm^{-2} across different years and locations in

Texas, and Premachandra et al. (1994) found *EW* loads up to 2.5 mg dm^{-2} for sorghum grown in a greenhouse.

Table 4.1. Leaf blade epicuticular wax (*EW*) concentration for the three lines. Concentrations were determined gravimetrically.

Year	Location	Line	Wax concentration ± SD[†]
			----------mg dm^{-2}----------
2017	**Greenhouse**		
		Bloomless Martin	0.34 ± 0.03
		Martin	1.92 ± 0.15
		White Martin	2.14 ± 0.27
2017	**Lubbock**		
		Bloomless Martin	0.37 ± 0.07
		Martin	2.11 ± 0.07
		White Martin	2.19 ± 0.04
2018	**Corpus Christi**		
		Bloomless Martin	0.31 ± 0.03
		Martin	1.97 ± 0.18
		White Martin	2.13 ± 0.19
	Average		
		Bloomless Martin	0.34 ± 0.04
		Martin	1.99 ± 0.15
		White Martin	2.13 ± 0.19

[†] SD = standard deviation

The reflectivity spectra of the wax extracts are shown in Fig. 4.1. Both materials had high ρ across the 400-1100 nm waveband. The highest reflectivity of the materials occurred between 410-430 nm, whereas the lowest reflectivity was observed between 460-500 nm. In the visible portion (*VIS*) of the spectrum (400-700 nm) the reflectivity of the Martin wax had an average value of 0.93, whereas in the near-infrared (*NIR*) waveband (700-1100 nm) it was 0.95. For the White Martin wax the average ρ over the *VIS* and *NIR* was 0.90 and 0.93, respectively. The average ρ across the 400-1100 nm waveband for the Martin and White Martin waxes were 0.94 and 0.92, respectively.

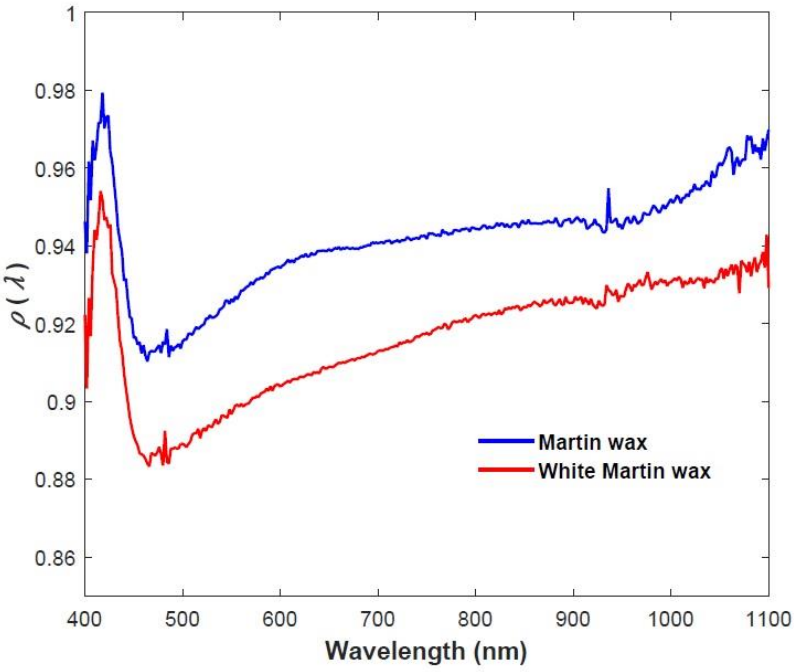

Figure 4.1. Reflectivity [$\rho(\lambda)$] of wax extracts collected from the 2018 study.

Reflectivity, transmissivity, and absorptivity spectra of leaves from the isolines are shown in Fig. 4.2, and their average values are reported in Table 4.2. Because the *EW* concentration in the leaves did not vary significantly between locations, spectral data of each line was also combined and averaged. As expected, the waxy lines had greater whole leaf ρ throughout the 400-1100 nm waveband (Fig. 4.2a and 4.2b). The average reflectivity of Bloomless Martin, Martin, and White Martin in the *VIS* band were 0.12, 0.14, and 0.15, respectively. In the *NIR* band the average reflectivity of Bloomless Martin, Martin, and White Martin were 0.40, 0.42, and 0.42, respectively. The data demonstrated that *EW* increased the whole leaf reflectivity by about 2% across the 400-1100 nm waveband (Table 4.2). Although lower in magnitude, these results are in agreement with those of Blum (1975b), who found that the adaxial surface of waxy sorghum leaves had a 4 to 5% greater reflectivity than their bloomless counterparts.

Bloomless leaves had higher transmissivities than the waxy ones, especially in the *NIR* band (Figs. 4.2c and 4.2d). Average transmissivities of Bloomless Martin, Martin, and White Martin in the *VIS* band were 0.04, 0.03, and 0.04, respectively. In the *NIR* band average transmissivities of Bloomless Martin, Martin, and White Martin were 0.49, 0.47, and 0.47, respectively. The bloomless leaf transmitted on average 1 to 2% more radiation across the 400-1100 nm band than the waxy ones (Table 4.2). The reduced transmissivity of waxy leaves is probably explained by the fact that waxes were present in both adaxial and abaxial surfaces. Therefore, as both surfaces become more reflective due to the presence of *EW*, they also reduce their ability to transmit radiation. Similar effects have been observed for leaves that were treated with reflective materials.

Abou-Khaled et al. (1970) coated citrus leaves (*Citrus sinensis* var. *Valencia*) with 225 mg dm^{-2} of kaolinite and found that the treatments significantly increased reflectivity, but transmissivity was lower than that of the untreated controls across the 400-2400 nm band.

Little change was observed in absorptivity (Figs 4.2e and 4.2f). The main differences in α between waxy and non-waxy leaves were observed in the *VIS* band, whereas in the *NIR* the leaves were found to be very similar. The average absorptivity in the *VIS* band for Bloomless Martin, Martin, and White Martin were 0.84, 0.83, and 0.81, respectively. In the *NIR* band the average absorptivity of Bloomless Martin, Martin, and White Martin are 0.10, 0.11, and 0.10, respectively. On average, the *EW* had an effect of about 1% on absorptivity only when comparing Bloomless Martin and White Martin. There was no difference in absorptivity between Bloomless Martin and Martin (Table 4.2). The data suggests that there is a compensation mechanism where increased reflectivity is offset by decreased transmissivity, so that absorptivity remains relatively unchanged.

Table 4.2. Average spectral properties of leaves from Bloomless Martin, Martin, and White Martin. Reflectivity (ρ), transmissivity (τ), and absorptivity (α) represent averages of both leaf surfaces. Emissivity (ε) was calculated using only the greenhouse data.

Line	ρ	τ	α	ε
	400-1100 nm			8-14 µm
Bloomless Martin	0.2844	0.2994	0.4162	0.9717
Martin	0.3028	0.2810	0.4161	0.9719
White Martin	0.3050	0.2898	0.4053	0.9771

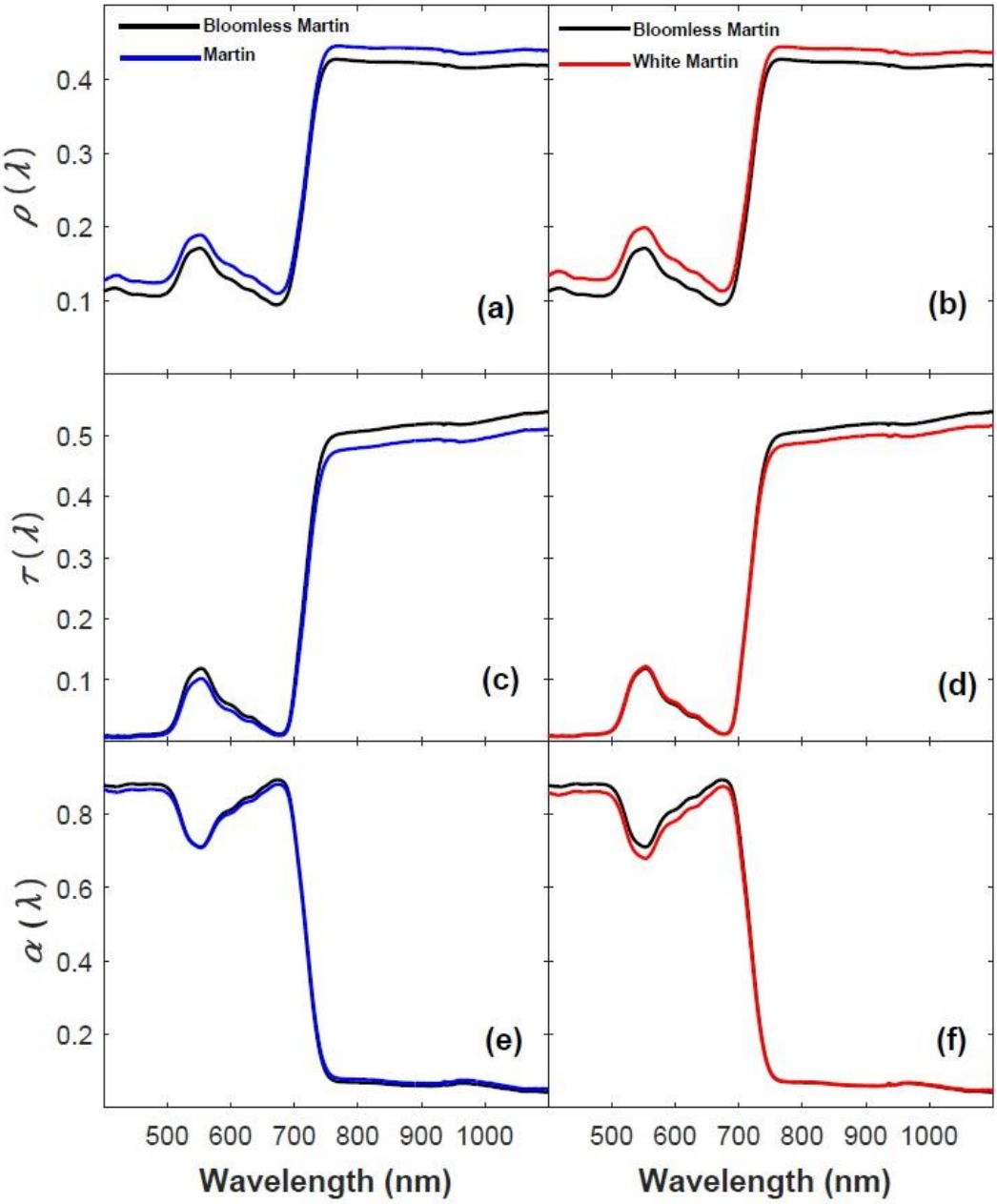

Figure 4.2. Whole leaf spectral properties of Bloomless Martin (black line), Martin (blue line), and White Martin (red line). Data from all three studies were combined to calculate reflectivity [$\rho(\lambda)$], transmissivity [$\tau(\lambda)$], and absorptivity [$\alpha(\lambda)$]. Values represent the average of abaxial and adaxial surfaces over the 400-1100 nm waveband.

Reference spectral irradiance data (G-173) was obtained from the American Society for Testing and Materials (https://www.nrel.gov/grid/solar-resource/spectra-am1.5.html, accessed 15 January 2018) to estimate the magnitude of the differences in reflected, transmitted, and absorbed radiant energy between the leaves of the lines (Fig. 4.3) assuming a normal angle of incidence. The spectral energy flux density of reflected, transmitted, and absorbed radiation of each line was calculated by multiplying the energy in each wavelength to the corresponding reflectivity, transmissivity, and absorptivity at that wavelength for each material (Figs. 4.3b through 4.3g). The total energy across the 400-1100 nm band that was reflected, transmitted, and absorbed by each line was calculated by means of numerical integration using the trapezoidal method (Table 4.3). The total energy in the solar irradiance spectra is 758.5 W m^{-2} (Fig. 4.3a). Bloomless Martin absorbed 2 and 11.4 W m^{-2} more energy than Martin and White Martin, respectively. That represents a difference in absorbed radiation of 0.26 and 1.5%.

Table 4.3. Estimates of total reflected (ρ), transmitted (τ), and absorbed (α) solar energy for the leaves of each line using reference spectral irradiance data (G-173) obtained from the American Society for Testing and Materials (ASTM).

Line	ρ	τ	α
	----------W m^{-2}----------		
Bloomless Martin	184.1	175.7	398.7
Martin	197.9	163.9	396.7
White Martin	200.3	170.8	387.3

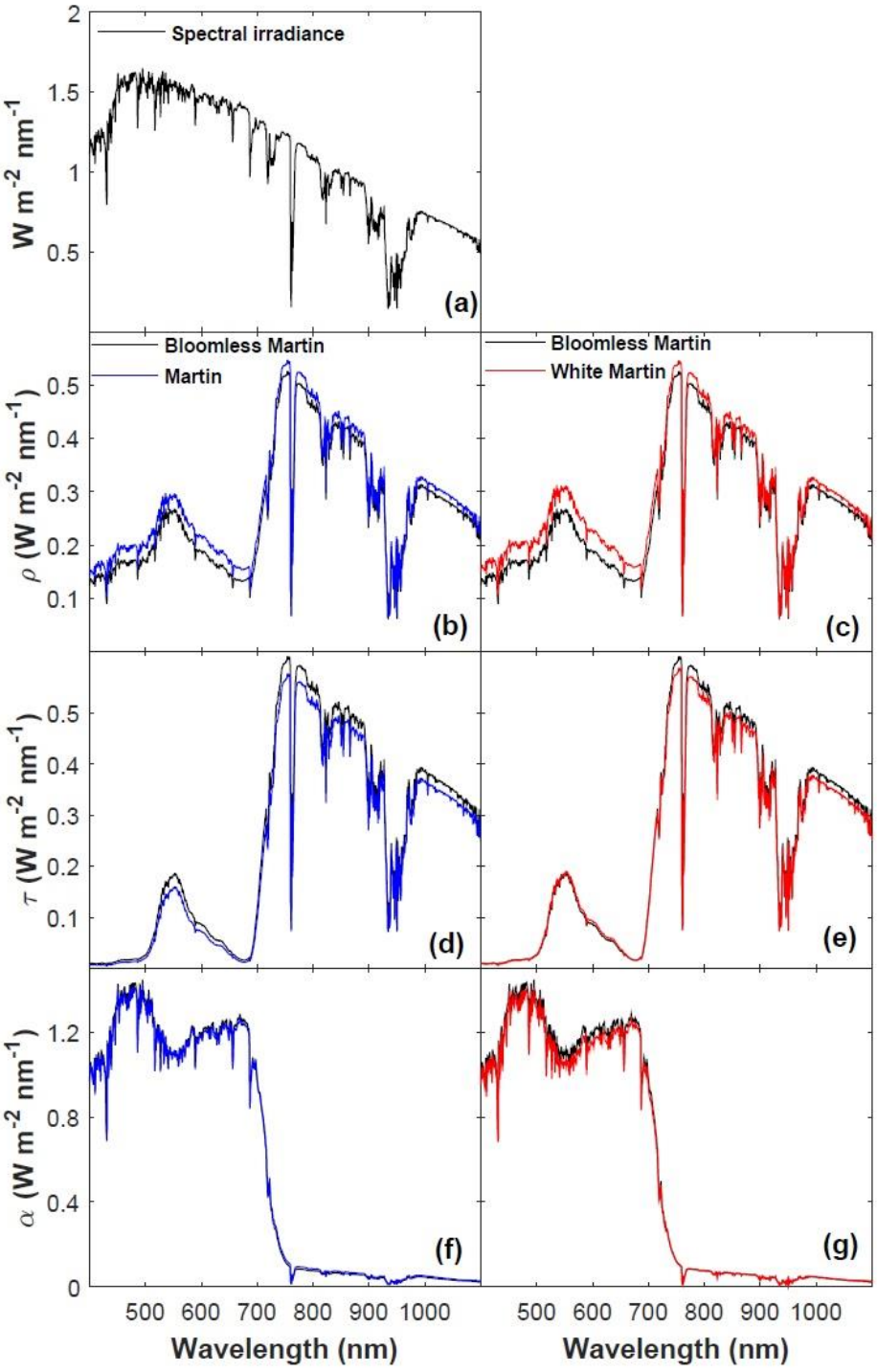

Figure 4.3. Comparison of leaf spectral energy flux density estimates of reflectivity (ρ), transmissivity (τ), and absorptivity (α) for Bloomless Martin (black line), Martin (blue line), and White Martin (red line). Reference solar spectral irradiance (G-173) for an absolute air mass of 1.5.

These results indicate that *EW* has a limited effect on the shortwave radiation balance of a leaf. The work of Gates et al. (1965) with desert species is often referenced in regard to the effect of waxes on radiative energy load on plants. However, as pointed out by those authors, the desert species they analyzed were succulent and did not transmit radiation, so that absorptivity was only controlled by reflectivity. In such cases, increased reflectivity leads to decreased absorptivity. Results from this study suggest that for translucent non-succulent species such as sorghum, where transmission is an important mechanism controlling the degree of coupling of a leaf to its radiative environment, *EW* showed a limited ability to alter absorptivity. Thus, any changes in leaf temperature due to reductions in absorbed shortwave radiation caused by *EW* are likely to be minor. The kaolinite treatments used by Abou-Khaled et al. (1970) successfully decreased leaf absorptivity, mainly in the *VIS* band. These authors were able to reduce the amount of radiant energy reaching leaf tissue by 40%, which cooled leaves by about 4 ^{o}C. Such large reductions for naturally occurring *EW* seem unlikely; the kaolinite concentration used by those authors is about a hundred times greater than the wax concentrations measured in the present study and in those reported by other investigators. One caveat of the experiment conducted by Abou-Khaled et al. (1970) is that they treated only the adaxial surface of the leaves of the species they studied. Out of the three species they analyzed, two were hypostomatous (*Citrus sinensis* var. *Valencia* and *Ficus elastica*) with the stomata present only on the abaxial surface, and one was amphistomatous (*Phaseolus vulgaris*). Therefore, their results represent a condition where the reflective materials affected the spectral properties of the leaves only. The

leaves were transpiring freely, since the stomata were not obstructed. That is not the case with naturally occurring *EW*, which were found to decrease transpiration (Chatterton et al., 1975), occlude stomatal pores (Jeffree et al., 1971; Blum, 1975b; Jenks and Ashworth, 1999), and decrease cuticular conductance (O'Toole et al., 1979; Jordan et al., 1984).

Emissivity spectra of the isolines are shown in Fig. 4.4. The leaves of all lines had high ε over the 8-14 μm band. The average whole leaf ε for Bloomless Martin, Martin, and White Martin were 0.97, 0.97, and 0.98, respectively (Table 4.2). These values are similar to what has been reported in the literature. Heilman et al. (1976) measured the emissivity of a sorghum canopy and found its average value to be 0.97. There was little difference in the emissivity spectra between Bloomless Martin and Martin (Fig. 4.4a). Martin had slightly higher ε than Bloomless Martin between 10.6 and 13.4 μm, but lower ε between 8 and 9 μm. However, these differences did not impact the average ε of these lines. White Martin had higher ε than Martin from 9 to 14 μm. Overall, *EW* had a small effect on the emissivity of the leaves.

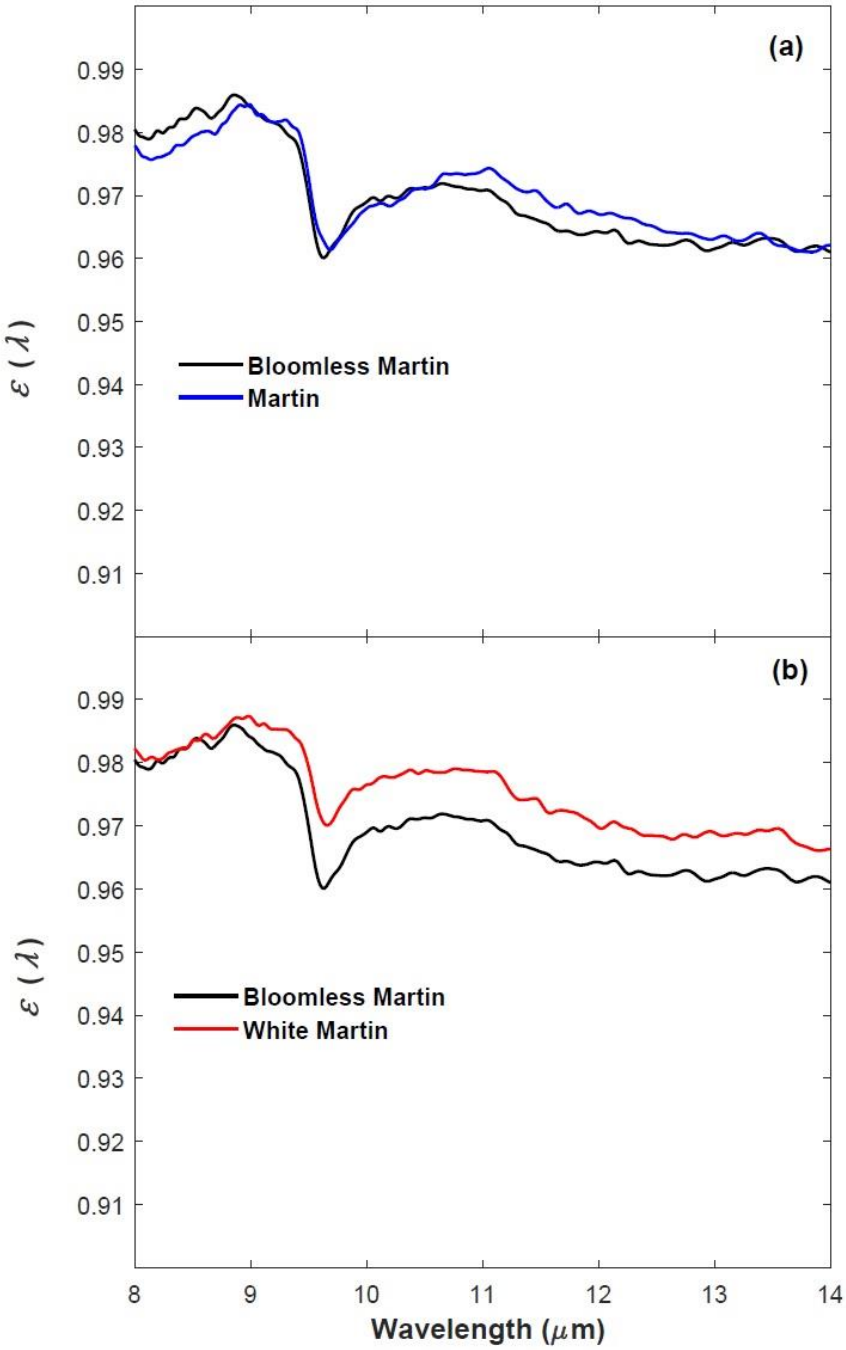

Figure 4.4. Whole leaf emissivity [$\varepsilon(\lambda)$] of Bloomless Martin (black line), Martin (blue line), and White Martin (red line). Values represent the average of abaxial and adaxial surfaces over the 8-14 μm waveband. Scans from the 2017 Greenhouse study were used.

Using the Stefan-Boltzmann law and Eq.4.1, it is possible to analyze the consequences of increased ε on the longwave radiation balance of a leaf. Considering a leaf that has a temperature of 30 ^{o}C, a difference in emissivity of 0.01 produces a difference in emitted radiation of 4.8 W m^{-2}. If this same leaf has 400 W m^{-2} of incident longwave radiation from the atmosphere, which is a common value, a difference in emissivity of 0.01 would generate a difference in absorbed longwave radiation of 4 W m^{-2}. Consequently, a difference in emissivity of 0.01 produces a difference in net longwave radiation of only 0.8 W m^{-2}. Thus, differences in ε due to *EW* likely have little effect on the longwave radiation balance of the leaf and net radiation. Hence, for most practical purposes the consequences of increased ε may be considered negligible. According to Campbell and Norman (1998), the emissivity of plant surfaces is usually assumed to be 0.97. Therefore, a value of 0.97 can be adopted for both bloomless and waxy.

The results reported here are in agreement with previous reports in the literature that showed that *EW* increased the reflectivity of leaves. However, our data suggest that increased reflectivity does not imply decreased absorptivity for translucent non-succulent species. Therefore, it is unlikely that shortwave spectral properties of *EW* can significantly affect leaf temperature and net radiation. Similarly, the effects of *EW* on emissivity were observed to be small and should have an insignificant effect on the longwave radiation balance of a leaf. If large differences in net radiation are to be found between waxy and non-waxy leaves, it is most likely because they have different

temperatures. In the next chapter, the effects of *EW* on the radiation balance of plant canopies will be investigated.

CHAPTER V

EFFECTS OF EPICUTICULAR WAXES ON THE RADIATION BALANCE OF A PLANT CANOPY

Introduction

In Chapter IV of this dissertation, the means through which epicuticular waxes (*EW*) influenced the spectral properties of leaves were investigated. There, I showed that even though *EW* have an effect on the spectral properties of leaves, the impact on leaf net radiation (R_n) would be small because waxy and bloomless leaves had similar absorptivity for solar radiation and longwave radiation. At the canopy scale, Blum (1975a) found that mean total daily R_n over experimental dryland plots was about 5% less for a waxy sorghum canopy compared to a bloomless one. Febrero et al. (1998) measured canopy reflectivity (ρ) of barley isolines differing in wax concentrations in irrigated and rain-fed fields and found that at visible (*VIS*) wavelengths the waxy canopy had about 20% higher ρ than the non-waxy one. In canopies, the impact of transmissivity is minimized because the canopy or the soil ultimately absorbs most of the transmitted shortwave radiation.

Assuming complete soil coverage, R_n for a plant canopy can be written as

$$R_n = (1 - \rho_c)R_s + \varepsilon LW_i - \varepsilon\sigma T_c^4 \qquad (5.1)$$

where ρ_c, albedo, is the canopy reflectivity of solar radiation, R_s is solar radiation, LW_i is the incoming longwave radiation emitted by the atmosphere, and T_c is the absolute canopy temperature. For a dense canopy fully covering the soil surface, albedo should

determine the amount of absorbed solar radiation. Thus, if *EW* are effective in increasing albedo, then reductions in R_n can be expected. The longwave balance is assumed to be mainly controlled by T_c, since ε is not expected to have a significant effect. An increase in T_c would necessarily lead to a decrease in R_n. The net radiation data from Blum (1975a) do not show how *EW* decreased R_n, whether it was mainly due to an increase in albedo, or increase in T_c, or a combination of both. Thus, the mechanisms by which *EW* affect canopy R_n still need to be elucidated, and the effects of *EW* on albedo and T_c need to be quantified. Therefore, the objective of this study was to determine how *EW* affect R_n at the field scale using near-isogenic lines of sorghum contrasting in *EW* load.

Materials and Methods

Experimental site and plant material

The study was conducted during the 2018 growing season at the Texas A&M AgriLife Research and Extension Center at Corpus Christi, TX (27.7^o N, 97.5^o W, 16 m above sea level). The soil was classified as Raymondville clay loam series (fine, mixed, superactive, hyperthermic Vertic Calciustolls). Average annual minimum and maximum temperature and precipitation are 17.1 ^{o}C, 27.6 ^{o}C, and 805 mm, respectively (https://www.ncdc.noaa.gov/climateatlas/, accessed 24 April 2019). Three near-isogenic lines of sorghum [*Sorghum bicolor* (L.) Moench] contrasting in leaf *EW* content were used. These lines were similar in terms of growth pattern, plant height, and other phenotypic traits. Additionally, it was assumed that these materials were similar in terms of leaf angle distribution, so that heterogeneity in plant form and architecture should be minimal. The lines Martin and White Martin produce waxy blooms, whereas Bloomless

Martin does not. Each line was grown in a 50 by 50 m plot. Row spacing was 0.5 m and followed east-west orientation. The lines were planted on 1 May, day of year (*DOY*) 121, at a density of 150,000 ha^{-1}. Drip tapes were installed in the plots after planting. Emergence occurred on *DOY* 131. Plants were irrigated after emergence to ensure adequate vegetative growth and complete canopy cover to minimize soil exposure to solar radiation. Irrigation was withheld after crop establishment so that the plots were rain fed for the remaining of the growing season. Management practices such as weed and pest control were performed as needed.

Net radiation measurements

Net radiation (R_n) was calculated from the output of a four-channel net radiometer (model CNR1, Kipp & Zonen, Delft, Netherlands) as

$$R_n = R_s - R_{sr} + LW_i - LW_e \tag{5.2}$$

where R_{sr} is solar radiation reflected by the canopy, and LW_e is the longwave radiation emitted by the canopy, all in units of W m^{-2}. Radiometers were installed at a height of 1.8 m above the soil surface on masts that were placed at the center of each plot. Albedo was calculated as the ratio of R_{sr} to R_s. The sensors were controlled by data loggers (model CR1000, Campbell Scientific, Logan, UT, USA) and the measurements were averaged over a 30-minute period. Daytime totals for the energy fluxes were calculated by integrating the 30-minute averages over sunrise to sunset. The daytime total differences (Δ) in R_n, R_{sr}, and LW_e between isolines were calculated as

$$\Delta R_n = 0.0018 \cdot \left[\sum_{t=sunrise}^{sunset} R_{n,B}(t) - \sum_{t=sunrise}^{sunset} R_{n,W}(t) \right], \tag{5.3}$$

and

$$\Delta R_{sr} = 0.0018 \cdot \left[\sum_{t=sunrise}^{sunset} R_{sr,B}(t) - \sum_{t=sunrise}^{sunset} R_{sr,W}(t) \right], \quad (5.4)$$

and

$$\Delta LW_e = 0.0018 \cdot \left[\sum_{t=sunrise}^{sunset} LW_{e,B}(t) - \sum_{t=sunrise}^{sunset} LW_{e,W}(t) \right] \quad (5.5)$$

where 0.0018 is an integration constant that has units of MJ s J^{-1}, $R_{n,B}$, $R_{sr,B}$, and $LW_{e,B}$ are the net radiation, reflected solar radiation, and emitted longwave radiation by the bloomless canopy, respectively, and $R_{n,W}$, $R_{sr,W}$, and $LW_{e,W}$ are the net radiation, reflected solar radiation, and emitted longwave radiation by the waxy canopies, respectively.

Spectral measurements

Spectral measurements were measured over the canopies on select days during solar noon when the plants were at the flowering stage. The measurements were made using two field portable spectroradiometers (models SS-110 and SS-120, Apogee Instruments Inc., Logan, UT). The instruments were set up to measure spectral irradiance and reflectance in the 400-1100 nm waveband with spectral resolution of 1 nm. The sensors were installed at the end of a 2.5 m long aluminum boom that was mounted on a survey tripod at a height of 0.5 m above the plant canopy. Sensors were pointed upward to measure spectral irradiance $R_s(\lambda)$. The measurements were made under clear skies. All plots were able to be scanned in less than 40 minutes. Four to six scans were taken per plot in areas within the field of view of the net radiometers. Once irradiance measurements were completed, the sensors were pointed downward to

measure spectral reflected shortwave radiation $R_{sr}(\lambda)$. Since no appreciable variation was observed in the energy spectra of the incoming and reflected radiation over the measurement time, the scans were combined and averaged. Canopy reflectivity $\rho_c(\lambda)$ was calculated as

$$\rho_c(\lambda) = \frac{R_{sr}(\lambda)}{R_s(\lambda)}. \tag{5.6}$$

The total reflected energy and the amount in visible (*VIS*) and near infrared (*NIR*) bands were calculated by means of numerical integration using the trapezoidal method. The differences in reflected energy between the bloomless and waxy isolines were computed and the relative contributions of the *VIS* and *NIR* bands to the total difference were calculated as fractions given by

$$\frac{\Delta VIS}{\Delta Total} = \frac{\int_{400}^{700} R_{sr,B}(\lambda)d\lambda - \int_{400}^{700} R_{sr,W}(\lambda)d\lambda}{\int_{400}^{1100} R_{sr,B}(\lambda)d\lambda - \int_{400}^{1100} R_{sr,W}(\lambda)d\lambda} \tag{5.7}$$

and

$$\frac{\Delta NIR}{\Delta Total} = \frac{\int_{700}^{1100} R_{sr,B}(\lambda)d\lambda - \int_{700}^{1100} R_{sr,W}(\lambda)d\lambda}{\int_{400}^{1100} R_{sr,B}(\lambda)d\lambda - \int_{400}^{1100} R_{sr,W}(\lambda)d\lambda} \tag{5.8}$$

where $R_{sr,W}(\lambda)$ and $R_{sr,B}(\lambda)$ are the spectral reflected shortwave radiation of the waxy and bloomless canopies, respectively.

Leaf epicuticular wax concentration and biometric measurements

Wax concentration and biometric measurements were made when plants were at the flowering stage. The quantity of wax on the leaf blades was determined gravimetrically following the procedure described by Ebercon et al. (1977). Sample leaves were always the first leaf below the flag leaf. One sample consisted of four leaf

blades. Four samples were processed per line. First, the area of the leaf blades was measured using an area scanner (model 3100C, Li-cor, Lincoln, NE). Then, the leaves of one sample were immersed in 100 ml of chloroform for 15 sec. The extracts were evaporated in a closed exhaustion hood over a period of 24 hours at room temperature. The amount of wax was calculated as the mass of residue. Areal density of wax on the leaves was calculated as the mass of residue divided by the sum of the areas of the leaves in the sample. Biometric measurements consisted of plant height and leaf area index (*LAI*). Final plant height (*h*) was measured from the soil to the top of the panicle. Sample size was 25 plants for each line. *LAI* was measured with a canopy analyzer (model LAI-2000, LI-COR, Lincoln, NE). Five *LAI* measurements were made in each plot and averaged.

Additional measurements

Supporting meteorological variables were measured at a height of 2 m from the soil surface in a weather station that was installed near the plots. At this weather station, R_s was measured with a pyranometer (model LI-200, Li-cor, Lincoln, NE), wind speed (u) and direction with a wind monitor (model 05103, R. M. Young, Traverse City, MI), air temperature (T_a) and water vapor pressure (e_a) with a temperature-humidity probe (model HMP45, Vaisala, Vantaa, Finland), and rainfall with a tipping-bucket rain gauge (model TR-525USW, Texas Electronics Inc., Dallas, TX). All sensors were controlled by a data logger (model CR1000, Campbell Scientific, Logan, UT). Measurements were averaged over 30 minutes.

Results and Discussion

The average R_s, T_a, e_a, and u, during the study were 23.9 MJ m^{-2} day^{-1}, 27.8 ^oC, 2.8 kPa, and 2.7 m s^{-1}, respectively. Rainfall contributed a total of 396.7 mm of water during the season. Significant rain events occurred between *DOY* 169 and 172, when a total of 221 mm of water was received by the fields (Fig. 5.1). A drying cycle occurred between *DOY* 190 and 211. Flowering was observed on *DOY* 185.

Final plant height, *LAI*, and *EW* concentration are summarized on Table 5.1. As expected, there was an appreciable difference in *EW* concentration between the lines, but little difference in height and *LAI*. The observed *EW* concentrations are within the range of values previously reported for sorghum in the literature (Ebercon et al., 1977; Jordan et al., 1983).

Table 5.1. Final plant height (*h*), leaf area index (*LAI*), and leaf epicuticular wax concentration for lines used in this study. Measurements were made when the plants were at the flowering stage.

Line	*h* ± SD†	*LAI* ± SD	Wax concentration ± SD
	-------m-------		----------mg dm^{-2}---------
Bloomless Martin	1.2 ± 0.06	4.1 ± 0.09	0.3 ± 0.03
Martin	1.2 ± 0.05	4.3 ± 0.16	2.0 ± 0.18
White Martin	1.2 ± 0.08	4.3 ± 0.24	2.1 ± 0.19

† SD = standard deviation

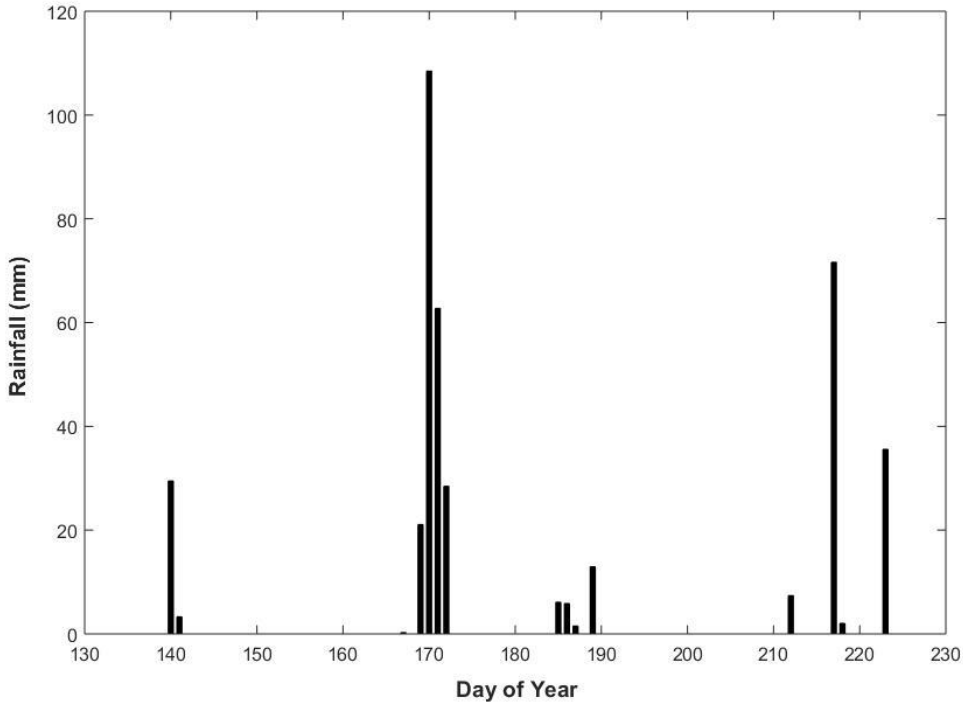

Figure 5.1. Rainfall events during the growing season. Emergence occurred on day of year (*DOY*) 131 and flowering on *DOY* 185.

Spectral energy flux density measurements for *DOY* 196 are presented in Fig.5.2 and integrated values for *DOY* 194, 195, and 196 are given in Table 5.2. Spectral irradiance (Fig. 5.2a) shows that skies were clear during the measurements. The spectral quality of the reflectivity signals shows that the waxy canopies had similar characteristics (Figs. 5.2b and 5.2c). Compared to the bloomless canopy, both waxy canopies had some increased reflectivity in the *VIS* band, especially between 500 and 600 nm, but the majority of the difference in reflected energy originated from the *NIR* band. *NIR* accounted for 86% of the total difference in reflected energy between waxy and bloomless canopies (Table 5.2). Since the effect of waxes on ρ extend across the shortwave *NIR* (Blum, 1975b), the contribution of reflected *NIR* to the total reflected solar energy could be greater than 86% because the measurements presented here are constrained to the resolution of the spectroradiometers used in the study, which only go up to 1100 nm. On average, total canopy reflectivity of the waxy plants was about 3% higher than that of the bloomless canopy. In the *NIR* band the waxy plants had an increase in reflectivity of about 4%, whereas in the *VIS* band the difference between the canopies was less than 1% (Table 5.3). The small difference in reflectivity in the *VIS* band indicates that the wax did not inhibit absorption of photosynthetically active radiation. The reflective spectral characteristics of the canopies are in agreement with the leaf level measurements presented in chapter IV.

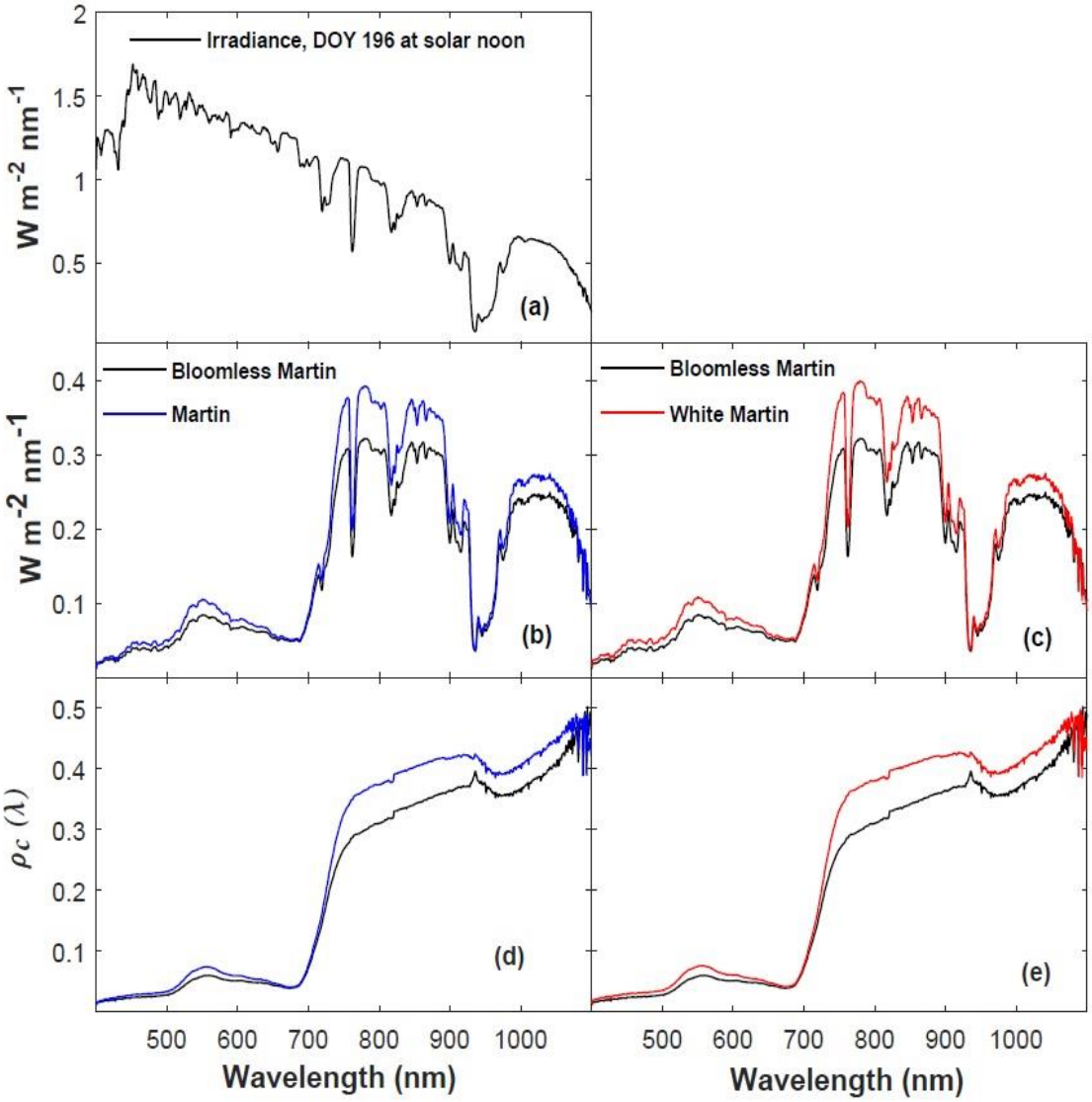

Figure 5.2. Spectral energy flux measurements over the canopies on day of year (*DOY*) 196 at solar noon; (a) spectral solar irradiance [$R_s(\lambda)$], (b) comparison between the energy spectra of reflected solar radiation [$R_{sr}(\lambda)$] of Bloomless Martin and Martin and (c) Bloomless Martin and White Martin. Canopy reflectivity [$\rho_c(\lambda)$] comparisons between the canopies are shown in (d) and (e).

Table 5.2. Integrated reflected energy flux differences between Bloomless Martin, Martin, and White Martin on days of year (*DOY*) 194, 195, and 196.

DOY	$\Delta Total$	ΔVIS	ΔNIR	$\frac{\Delta VIS}{\Delta Total}$	$\frac{\Delta NIR}{\Delta Total}$
	400-1100 nm	**400-700 nm**	**700-1100 nm**		
	----------W m^{-2}----------				
	Bloomless Martin - Martin				
194	-14.85	-2.00	-12.85	0.135	0.865
195	-22.21	-2.84	-19.37	0.128	0.872
196	-15.67	-2.59	-13.08	0.165	0.835
AVG	-17.58	-2.48	-15.10	0.143	0.857
	Bloomless Martin - White Martin				
194	-15.39	-1.32	-14.07	0.086	0.914
195	-20.46	-3.00	-17.46	0.147	0.853
196	-17.25	-3.24	-14.01	0.188	0.812
AVG	-17.70	-2.52	-15.18	0.14	0.86

Table 5.3. Average total, visible (*VIS*), and near infrared (*NIR*) canopy reflectivity (ρ_c) for Bloomless Martin, Martin, and White Martin on days of year (*DOY*) 194, 195, and 196. Measurements were taken at solar noon.

DOY	Line	ρ_c		
		Total	***VIS***	***NIR***
		400-1100 nm	**400-700 nm**	**700-1100 nm**
		----------**%**----------		
194				
	Bloomless Martin	21.3	4.1	34.1
	Martin	23.7	4.5	38.0
	White Martin	23.9	4.3	38.5
195				
	Bloomless Martin	20.1	3.7	32.4
	Martin	23.9	4.3	38.5
	White Martin	23.5	4.3	37.8
196				
	Bloomless Martin	21.1	4.0	33.9
	Martin	23.8	4.6	38.3
	White Martin	24.1	4.7	38.6

Diurnal patterns of R_{sr}, albedo, and LW_e during *DOY* 196 and 204 are shown in Figs. 5.3 and 5.4. Water availability was high on *DOY* 196, whereas on *DOY* 204 it became limiting. On *DOY* 196, the waxy canopies had higher R_{sr}, albedo, and LW_e than the bloomless one (Fig. 5.3). The average difference in R_{sr} between Bloomless Martin and Martin during the day was 13 W m^{-2}, whereas between Bloomless Martin and White Martin, it was 10 W m^{-2}. The average albedo for Bloomless Martin, Martin, and White Martin was 0.18, 0.20, and 0.20, respectively. The differences in LW_e between the canopies indicate that the bloomless canopy was slightly cooler than the waxy canopies.

On *DOY* 204, the waxy canopies also had higher R_{sr} and albedo than the bloomless one, but LW_e was lower (Fig. 5.4). The average difference in R_{sr} between Bloomless Martin and Martin on *DOY* 204 was 6 W m^{-2}, whereas between Bloomless Martin and White Martin it was 12 W m^{-2}. The average albedo for Bloomless Martin, Martin, and White Martin was 0.18, 0.19, and 0.20, respectively. Contrary to what was observed on *DOY* 196, the LW_e data shows that the bloomless canopy was warmer than the waxy ones.

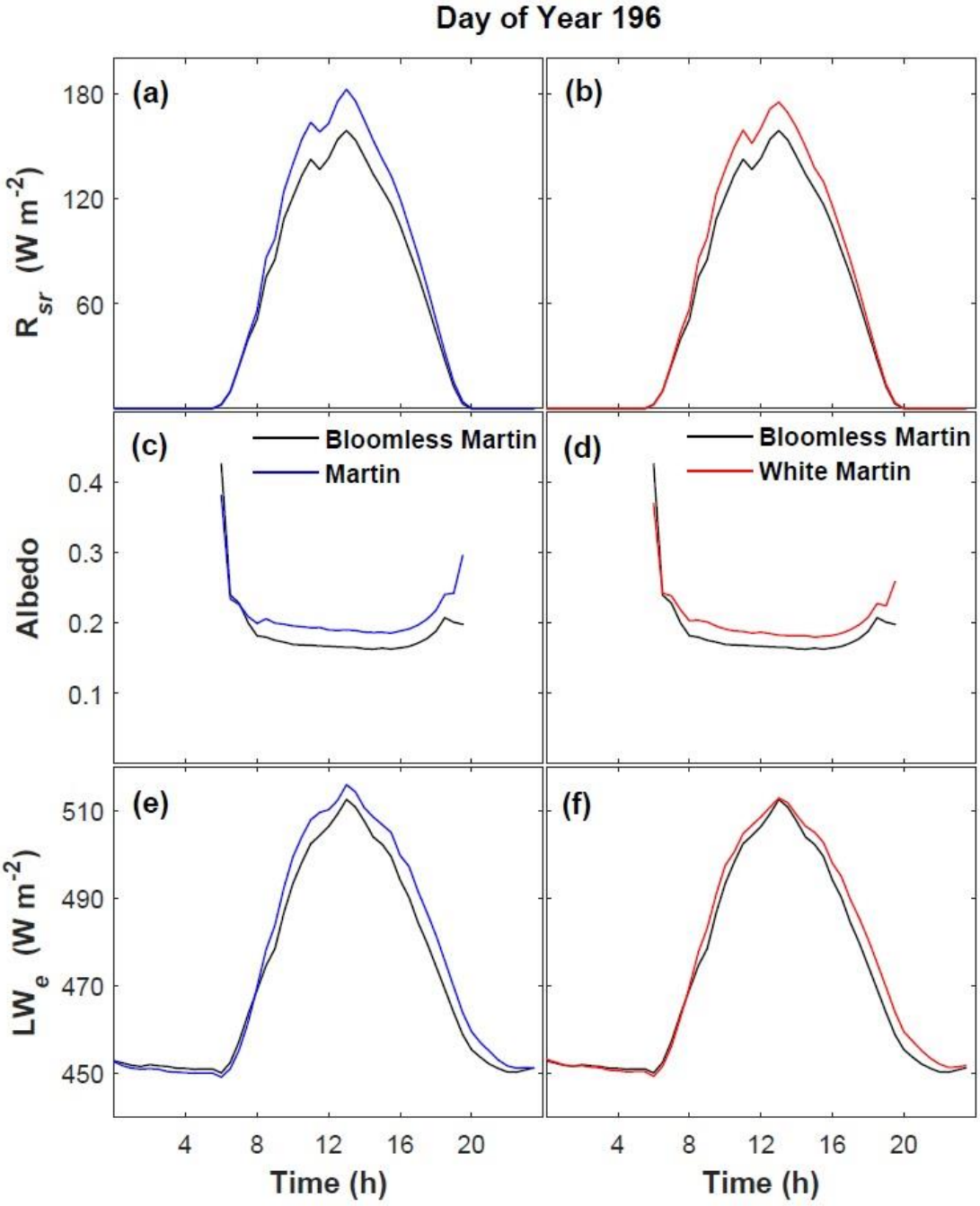

Figure 5.3. Diurnal patterns of reflected shortwave (R_{sr}), albedo, and emitted longwave (LW_e) for (a, c, and e) Bloomless Martin and Martin and (b, d, and f) Bloomless Martin and White Martin on day of year (*DOY*) 196.

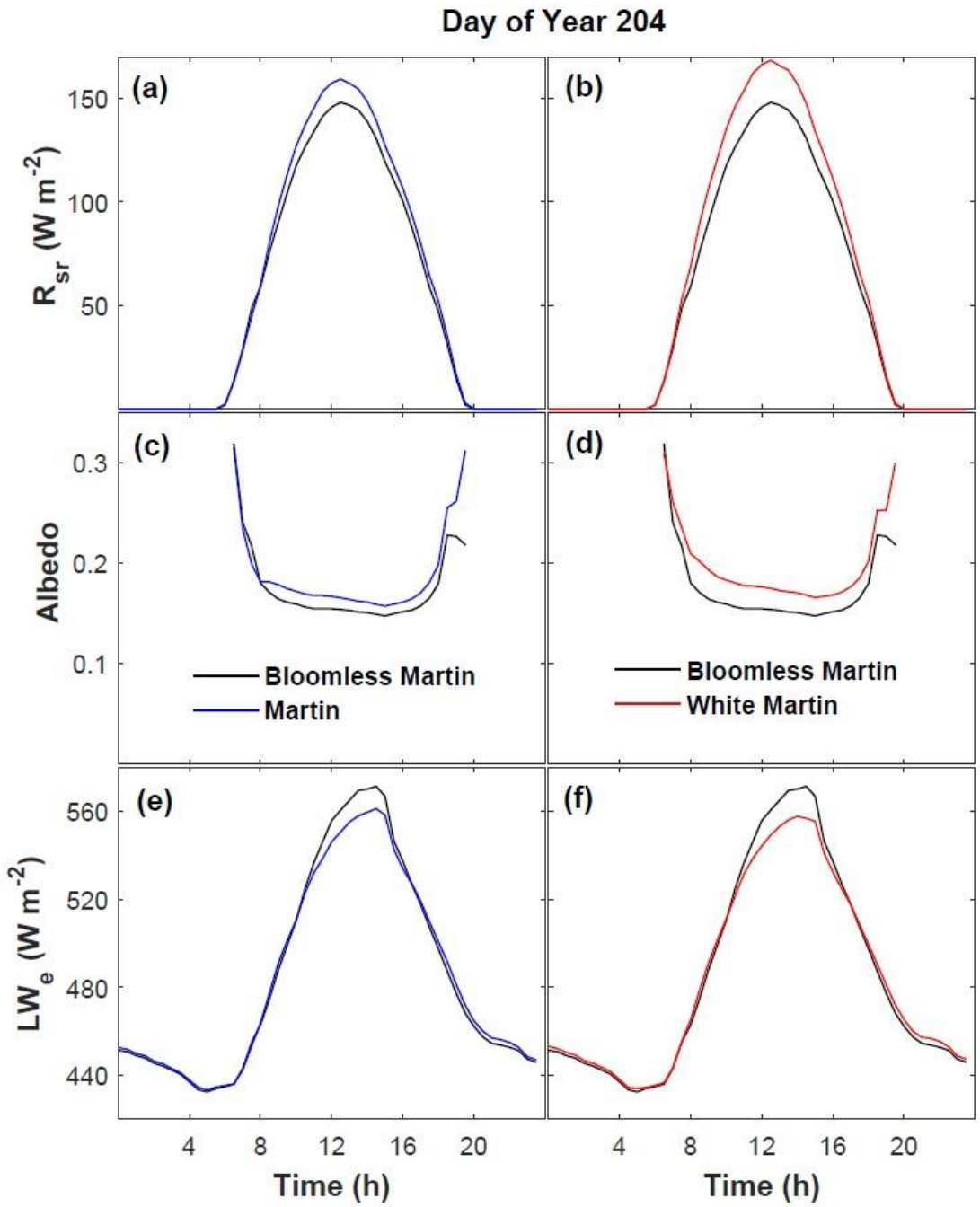

Figure 5.4. Diurnal patterns of reflected shortwave (R_{sr}), albedo, and emitted longwave (LW_e) for (a, c, and e) Bloomless Martin and Martin and (b, d, and f) Bloomless Martin and White Martin on day of year (*DOY*) 204.

The radiation balance of the canopies changed as the plants transitioned from well-watered to drier conditions (Fig. 5.5). The waxy canopies had greater R_{sr}, but lower R_n than the bloomless one throughout this period. Differences in R_n between Bloomless Martin and Martin decreased as drying progressed. The greatest ΔR_n between Bloomless Martin and Martin (Fig. 5.5a) occurred on *DOY* 193 when they differed by 1.04 MJ m^{-2}, which represents a 5% difference in R_n. The average ΔR_n from DOY 190 to 212 between Bloomless Martin and Martin was 0.52 MJ m^{-2}. Differences in R_n between Bloomless Martin and White Martin also declined with drying, but to a lesser degree because of an increase in the difference in albedo (Fig. 5.5b). For Bloomless Martin and White Martin (Fig. 5.5b) the greatest ΔR_n occurred on DOY 192 when R_n differed by 0.72 MJ m^{-2}, which represents a 4% difference in R_n. The average ΔR_n between them was 0.55 MJ m^{-2}. These results are in agreement with those obtained by Blum (1975a), who found that bloomless sorghum canopies had greater R_n than waxy ones by nearly 5%.

The ΔR_{sr} between waxy and bloomless canopies was always negative, indicating that the waxy canopies were reflecting more solar radiation than the bloomless one. Albedo of all the canopies decreased during the drying cycle (Fig. 5.6). That is probably explained by increased transmission through the canopy because of leaf turgor loss and senescing of old leaves, or increased absorption and/or scattering of radiation by the panicle.

On average, from DOY 190 to 212 ΔR_{sr} between Bloomless Martin and Martin was -0.48 MJ m^{-2}. The average ΔR_{sr} between Bloomless Martin and White Martin from *DOY* 190 to 212 was -0.55 MJ m^{-2}. Slopes of regression of R_{sr} vs R_s using 30-minute

averages from *DOY* 190 to 212 indicated that overall, albedos of waxy canopies were 2% higher than the bloomless one (Fig. 5.7).

At the beginning of the drying cycle, ΔLW_e between bloomless and waxy canopies was negative indicating that the bloomless canopy was cooler than waxy ones (Fig. 5.5). On *DOY* 203, ΔLW_e between Bloomless Martin and Martin transitioned to positive values as the bloomless canopy became warmer (Fig. 5.5a). A similar transition between Bloomless Martin and White Martin occurred on *DOY* 201 (Fig. 5.5b). The average ΔLW_e between Bloomless Martin and Martin during *DOY* 190 to 202 was -0.16 MJ m^{-2}, whereas from *DOY* 203 to 212 it was 0.13 MJ m^{-2}. For Bloomless Martin and White Martin ΔLW_e was negative from *DOY* 190 to 200, with an average of -0.15 MJ m^{-2}, and positive from *DOY* 201 to 212, with an average of 0.13 MJ m^{-2}.

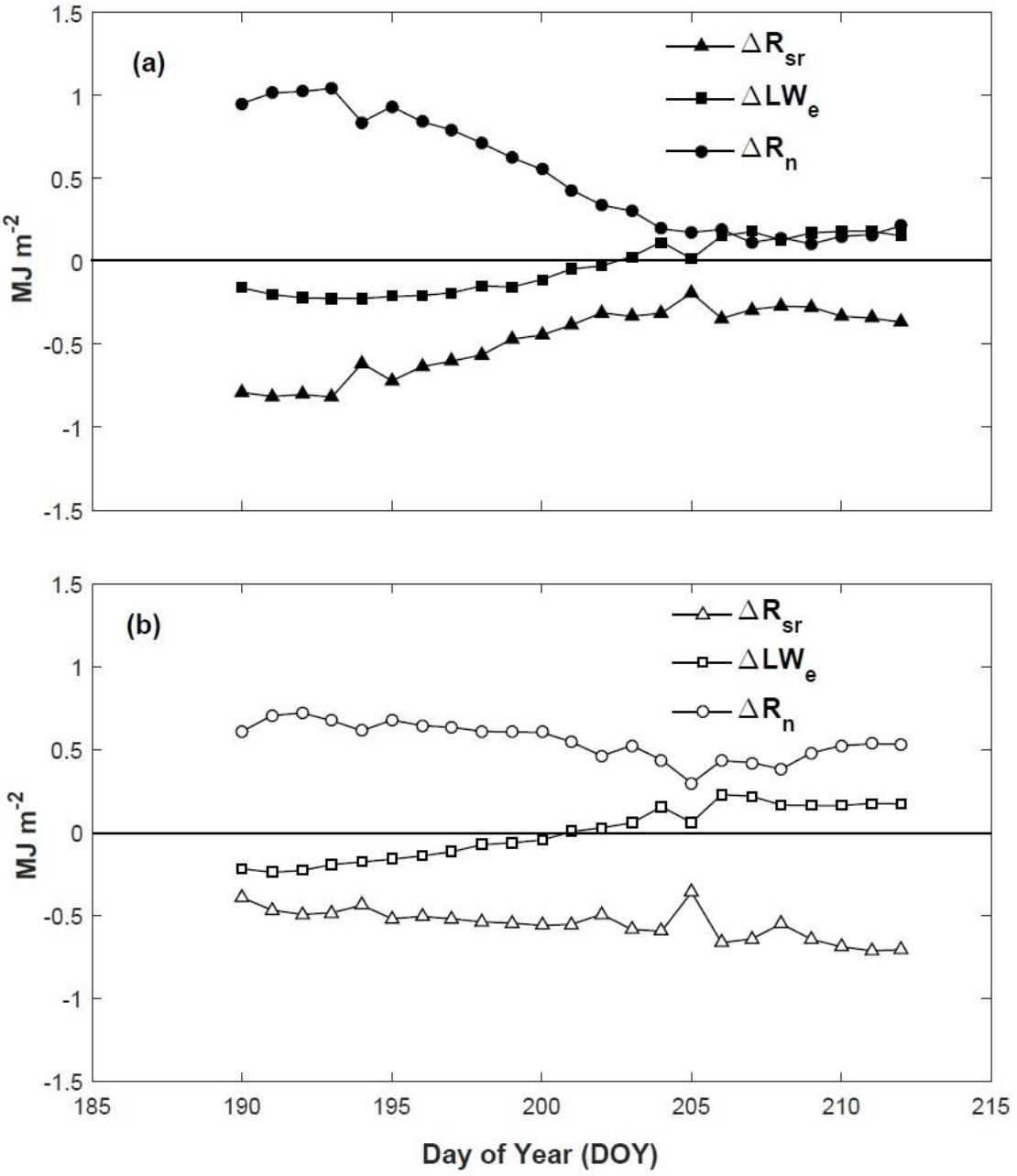

Figure 5.5. Daytime (sunrise to sunset) differences in net radiation (ΔR_n), reflected shortwave (ΔR_{sr}), and emitted longwave (ΔLW_e) between (a) Bloomless Martin and Martin and (b) Bloomless Martin and White Martin. Positive differences indicate that the bloomless canopy had a greater value than the waxy ones.

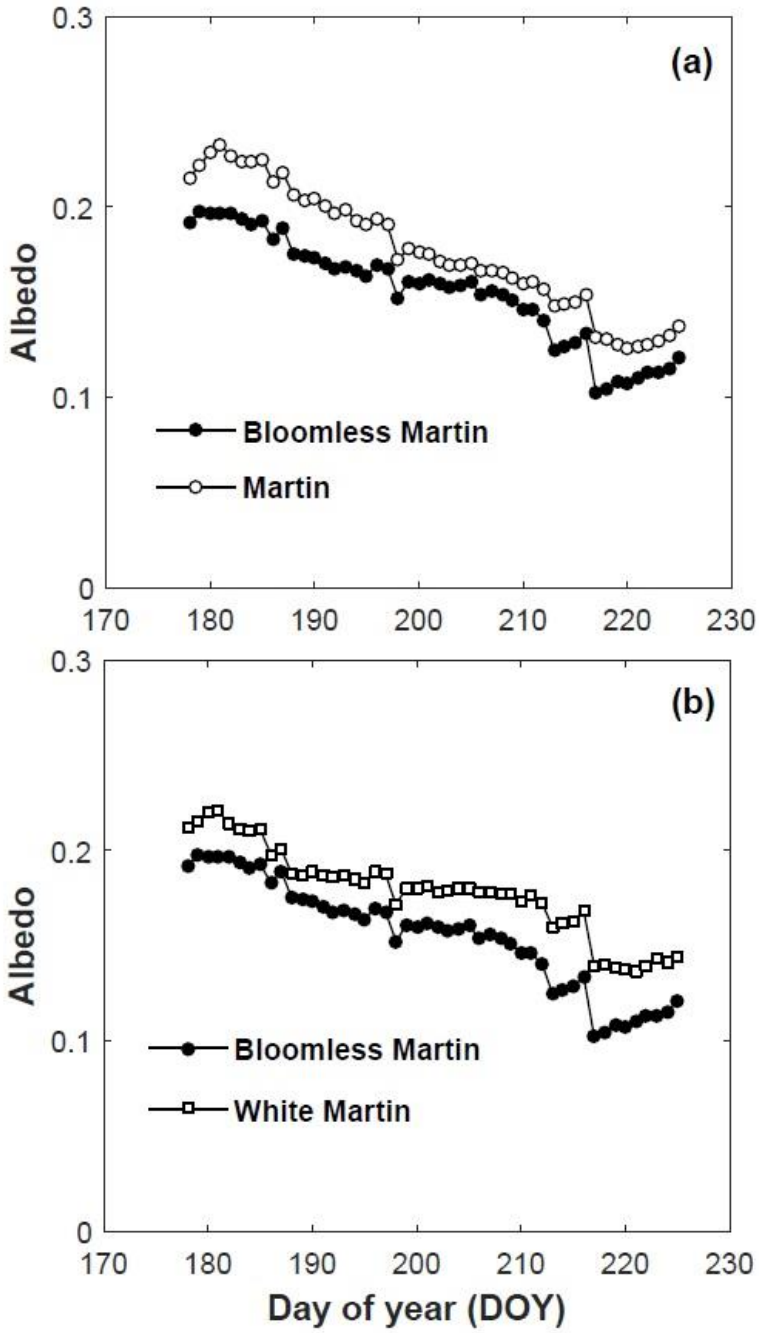

Figure 5.6. Daily albedo values for Bloomless Martin, Martin, and White Martin from day of (*DOY*) 178 to 225. Flowering was observed on *DOY* 185.

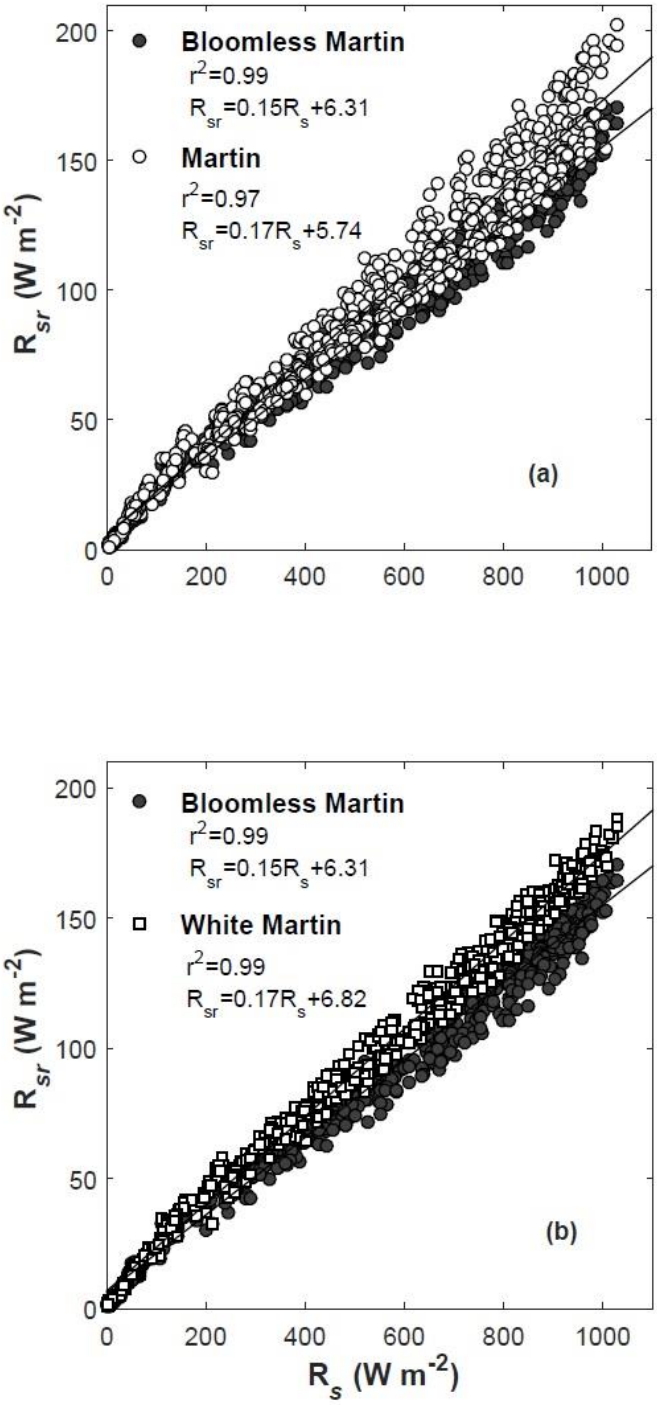

Figure 5.7. Thirty-minute averages of reflected solar radiation (R_{sr}) plotted against solar radiation (R_s) for (a) Bloomless Martin and Martin and (b) Bloomless Martin and White Martin. Values from *DOY* 190 to 212 were included in the linear regression analysis.

Manipulation of the albedo of soil and plant surfaces has received considerable attention in the past. Materials that have high reflectivity such as powdered kaolinite were applied to soils, leaves, and plant canopies with the intent of decreasing the energy load on those surfaces so that their temperature and water use would be reduced (Abou-Khaled et al., 1970; Baradas et al., 1976a, 1976b; Doraiswamy and Rosenberg, 1974; Fuchs et al., 1976; Lemeur and Rosenberg, 1975; Lemeur and Rosenberg, 1976; Oke and Hannel, 1966; Stanhill, 1965; Stanhill et al., 1976). Doraiswamy and Rosenberg (1974) showed that a soybean canopy could be reflectorized by up to 8% with applications of kaolinite, which increased reflectivity mainly in the *VIS* band, decreasing net radiation by about 8% as well. However, as Baradas et al. 1976a and Baradas et al. 1976b later showed, the kaolinite treatments increased the temperature of the canopy due to reduced thermal emissivity and stomatal conductance. The naturally occurring *EW* on the waxy sorghum canopies had a somewhat similar effect. It increased albedo, but mainly in the *NIR* band, and was shown to affect the longwave balance of the canopies. Since the waxes have a negligible effect on emissivity, as seen in chapter IV, the increase in longwave emission by the waxy canopies observed at the beginning of the drying cycle might be explained by lower stomatal conductance.

The results from this study corroborate previous findings that showed that *EW* decreased net radiation of waxy canopies. An overall 2% increase in albedo for waxy canopies was observed in our study, due mainly to higher *NIR* reflectivity compared to the bloomless canopy. Data showed that *EW* were able to reduce R_n without significant effects on absorptivity of *PAR*.

The higher albedo of waxy canopies could have resulted in cooler canopies, and less emitted longwave radiation than the bloomless canopy, but that was not the case when water was readily available. The bloomless canopy in this case was cooler and emitted less longwave radiation than waxy canopies. However, after a nearly 2-week period without rainfall, availability of water became limiting and the bloomless canopy became warmer than the waxy canopies. This suggests that the impact of *EW* on water vapor conductance and plant water relations was more important than albedo in controlling radiation and energy balances. This will be the focus of the next chapter of this dissertation.

CHAPTER VI

EFFECTS OF EPICUTICULAR WAXES ON THE ENERGY BALANCE OF PLANTS

Introduction

In the last two chapters, the effects of epicuticular waxes (*EW*) on leaf spectral properties and on the radiative balance of a canopy were investigated. It was shown that even though *EW* increased the reflectivity of radiant energy from a leaf, the net radiation (R_n) on a leaf is not expected to be significantly affected by *EW* because waxy and bloomless leaves had similar absorptivity for solar radiation and emissivity (ε) of longwave radiation. At the canopy level, however, *EW* were found to reduce R_n of a waxy canopy by 4 to 5% compared to that of bloomless one. The main driver for these differences was reflectivity of solar radiation, which was 2% greater for waxy canopies, mainly in near infrared wavelengths. The longwave radiation balance data indicated that the waxy canopies were warmer than the bloomless one following a rain event, contrary to what would be expected based on differences in albedo, but that pattern switched as the drying cycle progressed with the waxy canopies becoming cooler than the bloomless one. That finding suggests that other mechanisms, effects of *EW* on water vapor conductance and plant water relations, are as important as albedo in controlling radiation and energy balances, and canopy temperature. At the leaf level, *EW* could decrease conductance to water vapor by means of increased thickness of the leaf boundary layer (Sanchez-Diaz et al., 1972), stomatal pore occlusion (Jeffree et al., 1971), and decreased diffusion through the cuticle (O'Toole et al., 1979; Jordan et al., 1984). This reduces

transpiration as shown by Chatterton et al. (1975) who found in a greenhouse study that well-watered bloomless sorghum plants had transpiration rates 26% greater than their well-watered waxy counterparts.

These results pose an interesting challenge in trying to determine how *EW* affects water use and plant temperature. Energy balance theory predicts that increased reflectivity and decreased conductance act synergistically to decrease latent heat fluxes (*LE*) but have opposite effects on canopy temperature (T_c). It is well established that increased reflectivity leads to less heating under radiative load, whereas decreased conductance causes greater heating (Gates, 1980; Campbell and Norman, 1998; Monteith and Unsworth, 2013). If the primary mechanism through which *EW* affect the energy balance of plants is by increased reflectivity, then waxy canopies should have a lower *LE* and be cooler than bloomless canopies. However, if increased reflectivity is of secondary importance and decreased conductance is the dominant mechanism, then waxy canopies should have a lower *LE* and be warmer than bloomless canopies. Additionally, given that *EW* are effective in reducing conductance, it may enable waxy plants to have better control over transpiration and be better coupled to the atmospheric conditions than bloomless plants, which would make them less sensitive to solar radiation as a driver of transpiration.

The objective of this study was to determine whether *EW* affect the energy balance at the field scale and, if that is the case, what mechanisms are governing energy flux differences between waxy and bloomless canopies. To do that, near-isogenic lines

of sorghum contrasting in *EW* load were evaluated at the field level by means of the Bowen ratio energy balance method.

Materials and Methods

Experimental site and plant material

The study was conducted during the 2018 growing season at the Texas A&M AgriLife Research and Extension Center at Corpus Christi, TX (27.7^{o} N, 97.5^{o} W, 16 m above sea level). The soil was classified as Raymondville clay loam (fine, mixed, superactive, hyperthermic Vertic Calciustolls). Average annual minimum and maximum temperature and precipitation are 17.1 ^{o}C, 27.6 ^{o}C, and 805 mm, respectively (https://www.ncdc.noaa.gov/climateatlas/, accessed 24 April 2019). Two near-isogenic lines of sorghum [*Sorghum bicolor* (L.) Moench] contrasting in expression of leaf *EW* content were used. These lines are similar in terms of growth pattern, plant height, and other phenotypic traits. The line Martin has waxy bloom, whereas Bloomless Martin does not. Each line was grown in a 50 by 50 m plot. Row spacing was 0.5 m and followed east-west orientation. The lines were planted on 1 May, day of year (*DOY*) 121, at a population density of 150,000 ha^{-1}. Drip tapes for irrigation were installed in the plots after planting. Emergence occurred on *DOY* 131. Plants were irrigated after emergence to ensure adequate vegetative growth and complete canopy cover of the soil on maturation. Irrigation was withheld after crop establishment so that the plots were rain-fed for the remainder of the growing season. Management practices such as weed and pest control were performed as needed.

Energy balance measurements

The energy balance of the field is given by

$$R_n + LE + H + G = 0 \tag{6.1}$$

where *LE* is the latent heat flux density, *H* is sensible heat flux density, and *G* is the soil heat flux density, all in units of W m^{-2}. The adopted sign convention dictates that fluxes towards the surface are positive, whereas fluxes away from the surface are negative. The *BREB* method was used to evaluate these energy fluxes. The adopted approach is similar to that of Tanner (1960). The Bowen ratio (β) is defined as the ratio of *H* to *LE*, and is expressed as

$$\beta = \frac{H}{LE} \cong \gamma P_a \frac{\Delta T}{\Delta e_a} \tag{6.2}$$

where γ is the psychrometer constant, P_a is the atmospheric pressure, and ΔT and Δe_a are the air temperature and water vapor pressure differences between two heights above the surface, respectively. After substituting Eq. 6.2 into Eq. 6.1, *LE* can be calculated as

$$LE = \frac{-(R_n + G)}{(1 + \beta)} \tag{6.3}$$

H is calculated as a residual in Eq. 6.1 given that R_n, *G* and *LE* are known.

Each plot had its own independent *BREB* system where R_n, *G* and β were measured. R_n was calculated from the output of a four-channel net radiometer (model CNR1, Kipp & Zonen, Delft, Netherlands) as

$$R_n = R_s - R_{sr} + LW_i - LW_e \tag{6.4}$$

where R_s is solar irradiance, R_{sr} is solar radiation reflected by the canopy, LW_i is the incoming atmospheric longwave radiation, and LW_e is the longwave radiation emitted by the canopy. The radiometric canopy temperature (T_c) in °C was calculated as

$$T_c = \{[LW_e - LW_i(1-\varepsilon)]/[\varepsilon\sigma]\}^{0.25} - 273.15 \quad (6.5)$$

where ε is the emissivity of the crop, assumed to be 0.97 (Heilman et al., 1976), and σ is the Stefan-Boltzmann constant. The net radiometers were installed on a mast at a height of 1.8 m above the soil surface.

Soil heat flux was calculated as

$$G = G_{plate} + (\rho_b c_m + C_w\theta)(\frac{\Delta T_s}{\Delta t})Z \quad (6.6)$$

where G_{plate} is the output of a soil heat flux plate installed below the soil surface, T_s is the average soil temperature above the heat flux plates, t is time, ρ_b is the bulk density of the soil, c_m is the specific heat capacity of the soil minerals, C_w is the volumetric heat capacity of water, and θ is the volumetric water content. Heat flux plates (model HFP01, Hukseflux, Delft, Netherlands) were placed at depth (Z) of 8 cm from the soil surface. Thermocouples were installed at 2 and 6 cm to estimate ΔT_s. Water content was measured using 5 cm-long probes (model 5TM, Decagon Devices, Pullman, WA) that were installed horizontally at a depth of 4 cm. In each *BREB* system, G was measured at the center point between rows at two different locations below the net radiometers. The value used for G is the average of those two measurements.

Six-junction copper-constantan thermopiles were constructed to measure ΔT between two intake lines that were separated vertically by 1 m. The devices were aspirated by a fan (model D581L-012GA-1, Micronel, Hagerstown, MD) so that fresh

air was continuously drawn through the intakes. To measure Δe_a, vacuum pumps (model TD-4X2N, Brailsford & CO, Inc., Antrim, NH) were used to drawn air through polyethylene intake tubes (model Bev-A-Line IV, Thermoplastic Processes, Stirling, NJ), and relay-switch (model A21REL-12, Campbell Scientific, Logan, UT) controlled 4-way solenoid valves (model L01SA459B000060, Numatics, Novi, MI) that switched the incoming air streams through temperature-relative humidity probes (model HMP45, Vaisala, Vantaa, Finland). Air entering the sample lines was filtered for dust and insects (model Acro 50 Gelman Sciences, Ann Arbor, MI). After testing, a delay of 25 seconds was chosen between readings from the airstreams after a switch of the controlling valve. Rotameters (model FL-816-VSS, Omega, Norwalk, CT) were used to maintain the flow in the sample lines at 0.75 L min^{-1}. Values of ΔT and Δe_a were measured between the same two heights. Wind speeds (u) were measured with cup anemometers (model 1210D, R. M. Young, Traverse City, MI) installed at the heights where temperature and vapor pressure gradients were measured.

The Bowen ratio masts were installed at the center of the plots. The lower arm of the ΔT and Δe_a intakes was positioned at 0.2 m above the plants. Southeastern winds prevailed during the study. A fetch-to-height ratio of 21:1 was obtained for this configuration, which is an appropriate value for Bowen ratio measurements (Heilman et al., 1989). Data loggers (models CR1000 and CR23X, Campbell Scientific, Logan, UT) controlled the *BREB* systems and the measurements were averaged over a 30-minute period. Daytime totals for the energy fluxes were calculated by integrating the 30-minute averages from sunrise to sunset.

Canopy conductance and decoupling factor

Conductances and the decoupling factor (Ω_c) were evaluated on selected days during daytime from 9 through 17h. The total conductance (g_v) to water vapor transport was calculated as

$$g_v = \frac{P_a LE}{\{\lambda[e_{sat}(T_c) - e_a]\}} \tag{6.7}$$

where λ is the latent heat of vaporization, $e_{sat}(T_c)$ is the saturation water vapor pressure, and e_a is the actual vapor pressure in the atmosphere. It was assumed that g_v consisted of a series network of canopy (g_c) and boundary layer (g_{bl}) conductance. The contributions from the soil surface were neglected because the *LAI* of the plots was greater than 4 and the canopy completely covered the soil. According to Ritchie and Burnett (1971) for sorghum fields where the *LAI* exceeds 2.7 and the ground cover is in excess of 80%, transpiration is much larger than soil evaporation, and is the determinant factor of evapotranspiration (*ET*). Therefore, it is reasonable to estimate g_c as

$$g_c = \frac{g_v g_{bl}}{g_{bl} - g_v}\,. \tag{6.8}$$

The boundary layer conductance for water vapor transport was calculated according to the set of equations given by Campbell and Norman (1998) as

$$g_{bl} = \frac{0.4^2 \hat{\rho} u}{\left\{ln\left[\frac{(z-d)}{z_m}\right]\right\}\left\{ln\left[\frac{(z-d)}{z_v}\right]\right\}} \tag{6.9}$$

where $\hat{\rho}$ is the molar density of air (41.6 mol m^{-3}), z is the height where u was measured, d is the displacement height, z_m is the roughness length for momentum transport, z_v is the roughness length for water vapor transport. Diabatic corrections were neglected because

wind speeds were greater than 3 m s^{-1} (Campbell and Norman, 1998). Parameters d, z_m, and z_v are functions of plant height (h) and were calculated as d=0.65h, z_m=0.1h, and z_v=0.2z_m. Values of Ω_c were calculated according to Jarvis and McNaughton (1986) as

$$\Omega_c = \frac{\frac{s}{\gamma} + 1}{\frac{s}{\gamma} + 1 + \frac{g_{bl}}{g_c}} \tag{6.10}$$

where s is the slope of the saturation water vapor mole fraction curve.

Epicuticular wax concentration and biometric measurements

Wax concentration and biometric measurements were made when plants were at the flowering stage. The quantity of wax on the leaf blades was determined gravimetrically following the procedure described by Ebercon et al. (1977). Sample leaves were always the first leaf below the flag leaf. One sample consisted of four leaf blades. Four samples were processed per line. First, the area of the leaf blades was measured using an area scanner (model 3100C, Li-cor, Lincoln, NE). Then, the leaves of one sample were immersed in 100 mL of chloroform for 15 s. The extracts were evaporated in a closed exhaustion hood over a period of 24 hours at room temperature. The amount of wax was calculated as the mass of residue. Wax concentration on the leaves was calculated as the mass of residue divided by the sum of the areas of the leaves in the sample. Biometric measurements consisted of plant height and leaf area index (*LAI*). Final plant height (h) was measured from the soil to the top of the panicle. Sample size was 25 plants for each line. *LAI* was measured with a canopy analyzer (model LAI-2000, Li-Cor, Lincoln, NE). The *LAI* of each line is represented by the average of 5 readings.

Additional measurements

Supporting meteorological variables were measured at a height of 2 m from the soil surface with a weather station that was installed near the plots. Solar irradiance was measured with pyranometer (model LI-200, Li-cor, Lincoln, NE), wind speed and direction with a wind monitor (model 05103, R. M. Young, Traverse City, MI), air temperature and relative humidity with temperature-humidity probe (model HMP45, Vaisala, Vantaa, Finland), and rainfall with a tipping-bucket rain gauge (model TR-525USW, Texas Electronics Inc., Dallas, TX). All sensors were controlled by a data logger (model CR1000, Campbell Scientific, Logan, UT). Measurements were averaged over 30 minutes.

Stomatal conductance (g_s) was measured on select days using a steady-state porometer (Model SC-1, Decagon Devices, Pullman, WA). The measurements were made on the abaxial side of fully expanded, sunlit, flag leaves. Five leaves were sampled per plot at 1-hour intervals during daytime and their averages were recorded.

Results and Discussion

Climatic conditions during the study are shown in Fig. 6.1. Rainfall was 396.7 mm during the season. Significant rain events occurred between *DOY* 169 and 172, when a total of 221 mm of water were received by the fields. A drying cycle occurred between *DOY* 190 and 212. Flowering was observed on *DOY* 185. Selected days between *DOY* 190 and 212 that characterize a transition from well-watered to mild stress conditions were used to analyze the effects of *EW* on energy fluxes. According to Kanemasu (1977) and Ritchie and Burnett (1971) at this stage sorghum plants are using

water at their maximum and actual *ET* approaches Penman-Monteith reference *ET*. Final plant height, *LAI*, and *EW* concentration are summarized on Table 6.1. There was an appreciable difference in *EW* concentration between the lines, but little difference in height or *LAI*.

Table 6.1. Final plant height (*h*), leaf area index (*LAI*), and leaf epicuticular wax concentration for Bloomless Martin (bloomless) and Martin (waxy). Measurements were taken when the plants were at the flowering stage.

Phenotype	***h* ± SD**†	***LAI* ± SD**	**Wax concentration ± SD**
	----------m----------		**----------mg dm^{-2}----------**
Bloomless	1.2 ± 0.06	4.1 ± 0.09	0.3 ± 0.03
Waxy	1.2 ± 0.05	4.3 ± 0.16	2.0 ± 0.18

† SD = standard deviation

Daytime (sunrise to sunset) energy balance data for *DOY* 190, 197, and 204 are shown in Figs. 6.2, 6.3, and 6.4, respectively. Daily totals are summarized on Table 6.2. *G* was similar for both canopies on these days (Table 6.2).

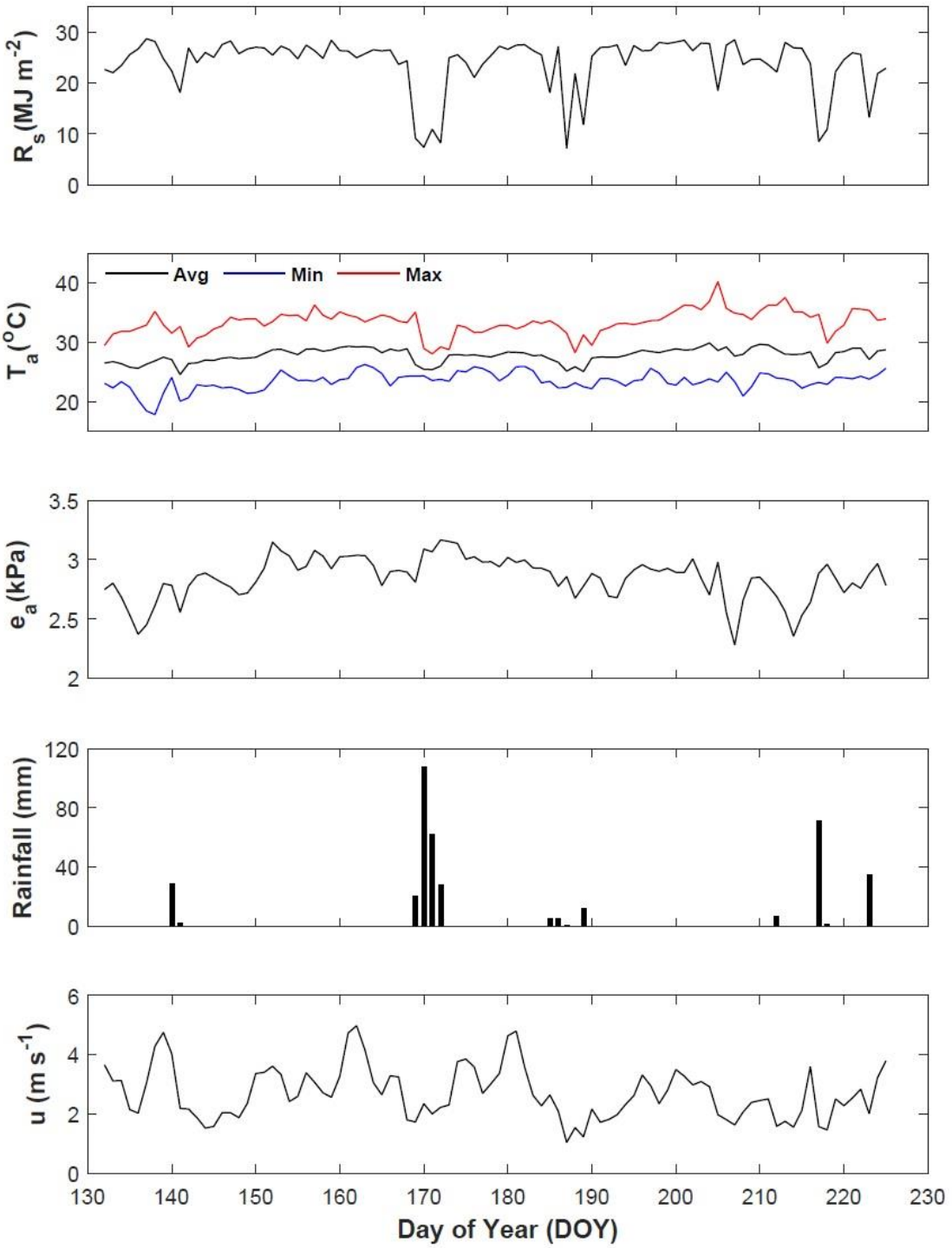

Figure 6.1. Daily (24h) totals of solar radiation (R_s) and rainfall; and average daily values of air temperature (T_a), vapor pressure (e_a), and wind speed (u) during the study. Daily minimum (blue line) and maximum (red line) T_a are plotted for reference. Emergence occurred on day of year (*DOY*) 131 and flowering on *DOY* 185.

Day of year 190 represents the well-watered condition when the majority of the available energy was partitioned to *LE* (Fig. 6.2). The bloomless canopy had greater R_n and *LE* than the waxy one throughout the day, but slightly lower *H*. The average difference between the canopies were 19, 31, and 12 W m^{-2} for R_n, *LE*, and *H*, respectively. In terms of daily totals, the canopies differed in R_n, *LE*, and *H* by 0.95, 1.58 and 0.62 MJ m^{-2} day^{-1}, respectively. This indicates that the phenotypes differed in the way they partitioned R_n into *LE* and *H* by 4.2 and 3.8%, respectively.

The same pattern was observed on *DOY* 197 (Fig. 6.3). The bloomless canopy had greater R_n and *LE* during the day, but lower *H*. On average, the canopies differed in R_n, *LE*, and *H* by 16, 33, and 20 W m^{-2}, respectively. Differences in daily totals between the phenotypes in R_n, *LE*, and *H* were 0.79, 1.65, and 1.02 MJ m^{-2} day^{-1}, respectively. Similarly to what was observed on *DOY* 190, the phenotypes differed in the way they partitioned R_n into *LE* and *H* by 5.7 and 6.3%, respectively.

Significant changes were observed in the diurnal course of *LE* and *H* on *DOY* 204 (Fig. 6.4). The bloomless canopy now had lower *LE* than the waxy one, but greater *H*. R_n was slightly larger for bloomless compared to waxy during the day. On average, the difference between the canopies in R_n, *LE*, and *H* was 4, 53, and 51 W m^{-2}, respectively. In terms of daily totals, the phenotypes differed by in R_n, *LE*, and *H* by 0.20, 2.65 and 2.57 MJ m^{-2} day^{-1}, respectively. As a result, the difference in partitioning of R_n into *LE* and *H* by the phenotypes was 14.5 and 13.2%, respectively.

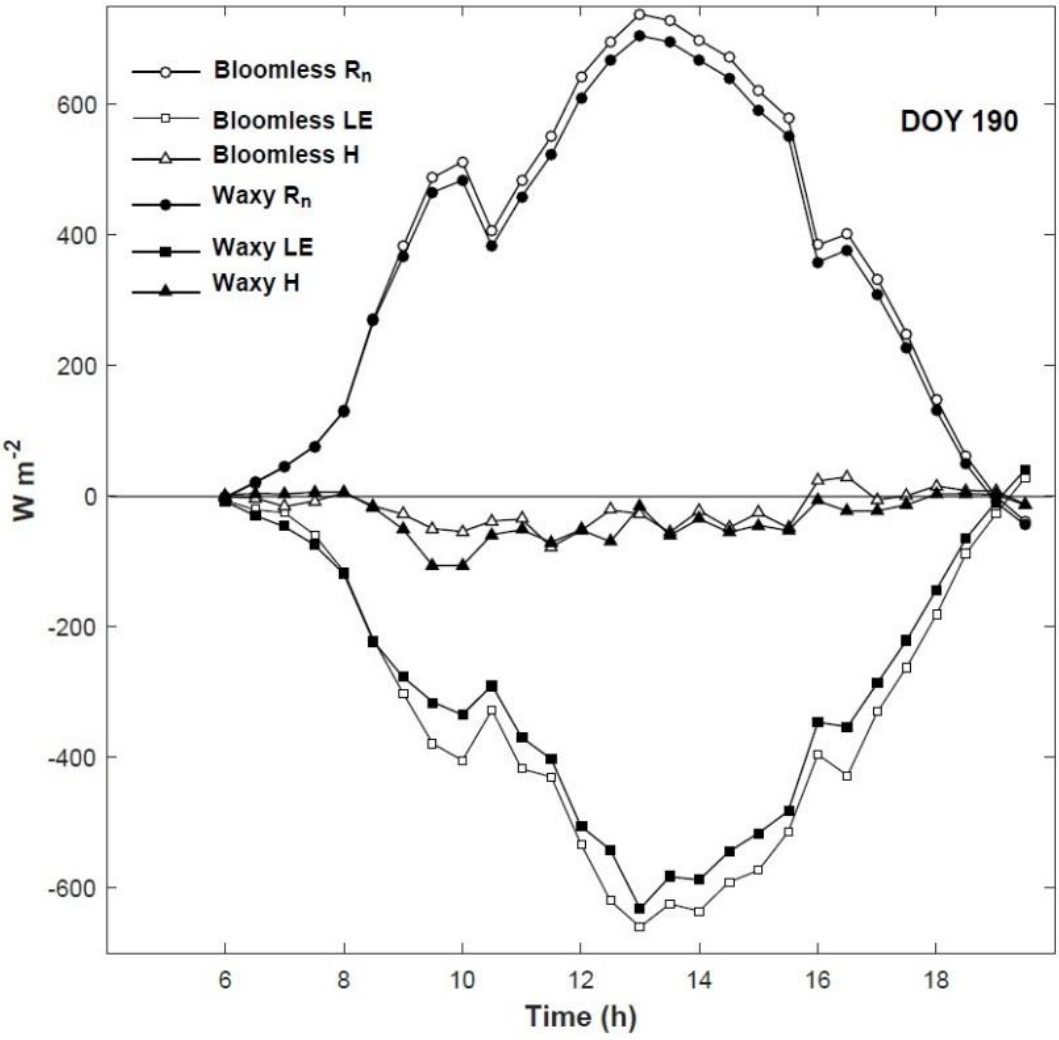

Figure 6.2. Daytime (sunrise to sunset) energy balance components of the bloomless (white markers) and waxy (black markers) plot on day of year (*DOY*) 190. Positive values were assigned to net radiation (R_n) and negative values to sensible (*H*) and latent (*LE*) heat fluxes.

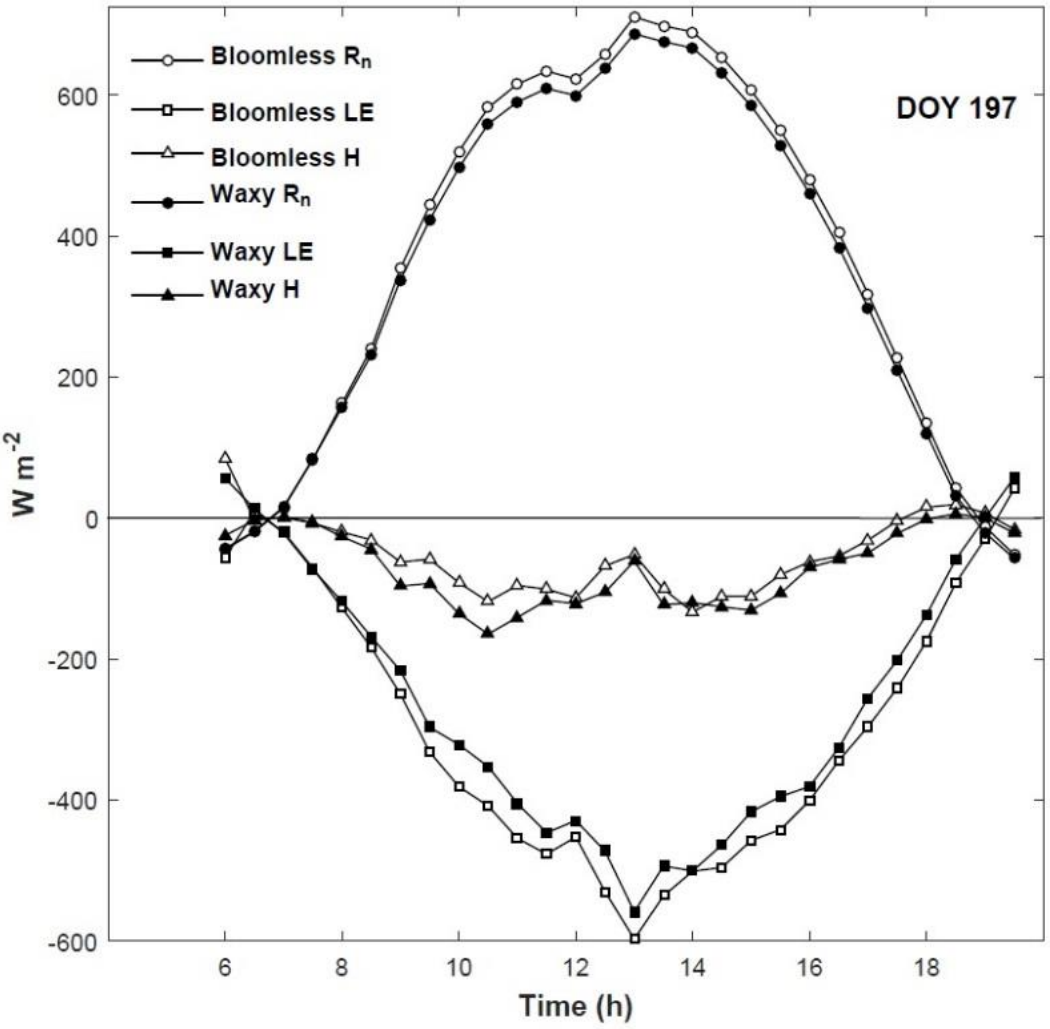

Figure 6.3. Daytime (sunrise to sunset) energy balance components of the bloomless (white markers) and waxy (black markers) plot on day of year (*DOY*) 197. Positive values were assigned to net radiation (R_n) and negative values to sensible (*H*) and latent (*LE*) heat fluxes.

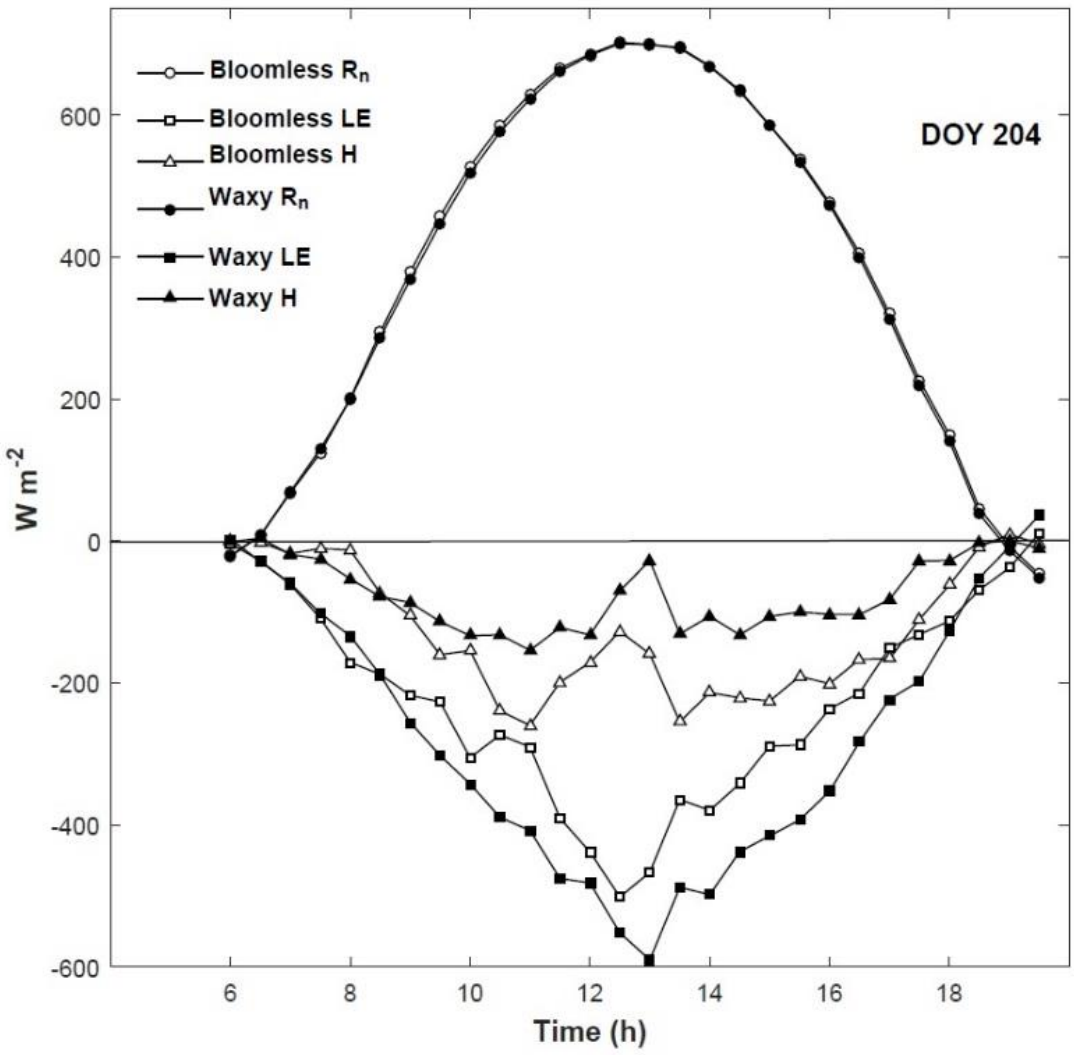

Figure 6.4. Daytime (sunrise to sunset) energy balance components of the bloomless (white markers) and waxy (black markers) plot on day of year (*DOY*) 204. Positive values were assigned to net radiation (R_n) and negative values to sensible (*H*) and latent (*LE*) heat fluxes.

Table 6.2. Daytime (sunrise to sunset) energy balance components of the Bloomless Martin (bloomless) and Martin (waxy) canopies on day of year (*DOY*) 190, 197, and 204. Bowen ratio (β) and the ratios of latent (*LE*), sensible (*H*) and soil heat (*G*) flux to net radiation (R_n) were calculated using the daytime totals.

DOY	Line	R_n	*G*	*LE*	*H*	β	LE/R_n	H/R_n	G/R_n
		---------- MJ m^{-2} day^{-1} ------					---------- % ----------		
190									
	Bloomless	18.48	1.00	16.47	1.01	0.06	89.1	5.5	5.4
	Waxy	17.53	1.01	14.89	1.63	0.11	85.0	9.3	5.7
197									
	Bloomless	18.57	1.12	14.94	2.51	0.17	80.4	13.5	6.0
	Waxy	17.78	0.97	13.29	3.53	0.27	74.7	19.8	5.5
204									
	Bloomless	19.27	1.70	11.27	6.29	0.56	58.5	32.7	8.8
	Waxy	19.08	1.42	13.93	3.72	0.27	73.0	19.5	7.5

Daytime average canopy-air temperature difference (ΔT) data are shown in Fig. 6.5. ΔT was never negative during *DOY* 190 to 212, which indicates that both canopies were warmer than air during the drying cycle. The data shows that from *DOY* 190 to 202 the bloomless canopy was 0.52 ^{o}C cooler than the waxy one on average. On *DOY* 203, there was a change with the waxy canopy becoming cooler than the bloomless canopy, and this condition was maintained in the following days. From *DOY* 203 to 212 the bloomless canopy was 0.38 ^{o}C warmer than the waxy one on average. Bowen ratio data support these observations (Fig. 6.6). The bloomless canopy had lower Bowen ratios than the waxy one on *DOY* 190 and 197 (Figs. 6.6a and 6.6b), but the inverse was observed on *DOY* 204 (Fig. 6.6c). From 9-17h the average β for the bloomless canopy on *DOY* 190, 197, and 204 was 0.07, 0.20, and 0.65, respectively, whereas for the waxy canopy β on *DOY* 190, 197, and 204 was 0.13, 0.28, and 0.28, respectively. These values are similar to the β computed from daytime totals (Table 6.2). This shift in energy fluxes, canopy temperature, and Bowen ratio indicate that the bloomless plants experienced water deficits earlier than the waxy ones, resulting in a change in how R_n was partitioned between *LE* and *H*.

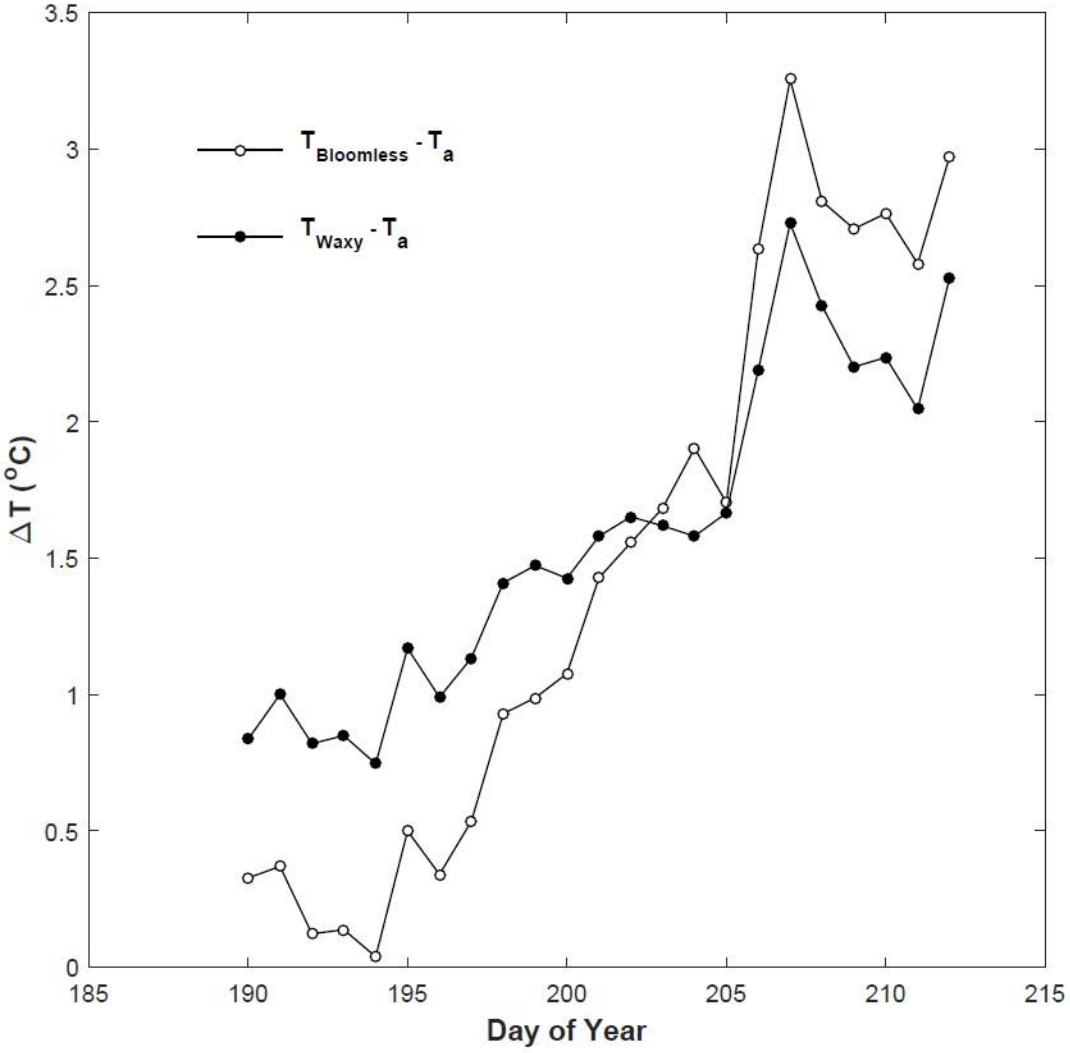

Figure 6.5. Average canopy-air temperature difference (*ΔT*) during daytime (sunrise to sunset) hours. The interval between day of year (*DOY*) 190 to 212 represents a drying cycle. Rainfall events were recorded on *DOY* 189 and 212.

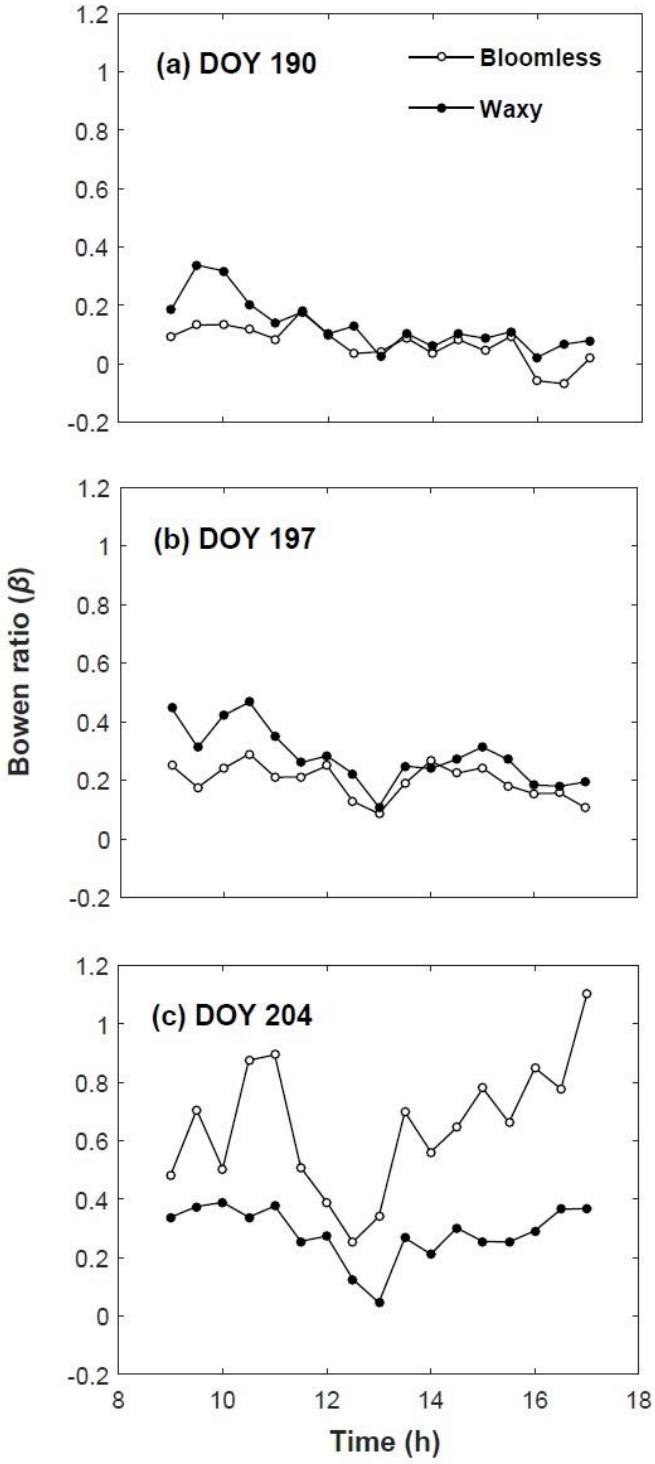

Figure 6.6. Bowen ratio (β) of the bloomless (white markers) and waxy (black markers) plots between 9-17h on day of year (*DOY*) 190, 197, and 204.

Canopy conductance for *DOY* 190, 197, and 204 and stomatal conductance on *DOY* 197 and are shown in Figs. 6.7 and 6.8, respectively. The bloomless canopy had greater g_c than the waxy canopy on *DOY* 190 and 197. On *DOY* 204 g_c decreased for both canopies compared to the other days, but the waxy canopy was able to maintain greater conductance than the bloomless canopy. From 9 to 17h the average g_c for the bloomless canopy on *DOY* 190, 197, and 204 was 0.74, 0.47, and 0.16 mol m^{-2} s^{-1}, respectively; whereas for the waxy canopy g_c on *DOY* 190, 197, and 204 was 0.53, 0.36, and 0.22 mol m^{-2} s^{-1}, respectively. That was also observed at the leaf level, where the abaxial surface of bloomless flag leaves had greater g_s than that of waxy ones on *DOY* 197. The difference between the phenotypes was 0.057 mol m^{-2} s^{-1} on average. Leaf level measurements were not obtained for *DOY* 204. The g_c data indicates that the bloomless canopy had a more appreciable stomatal restriction than the waxy canopy on *DOY* 204.

Values for the canopy decoupling factor for *DOY* 190, 197, and 204 are shown in Fig. 6.9. The bloomless canopy had greater Ω_c than the waxy canopy on *DOY* 190 and 197, though the inverse was observed on *DOY* 204. From 9-17h the average Ω_c for the bloomless canopy on *DOY* 190, 197, and 204 was 0.63, 0.50, and 0.33, respectively, whereas for the waxy canopy Ω_c on *DOY* 190, 197, and 204 was 0.55, 0.44, and 0.40, respectively. Therefore, the waxy canopy was better coupled to the atmosphere than the bloomless one on *DOY* 190 and 197, whereas the bloomless canopy showed better coupling on *DOY* 204.

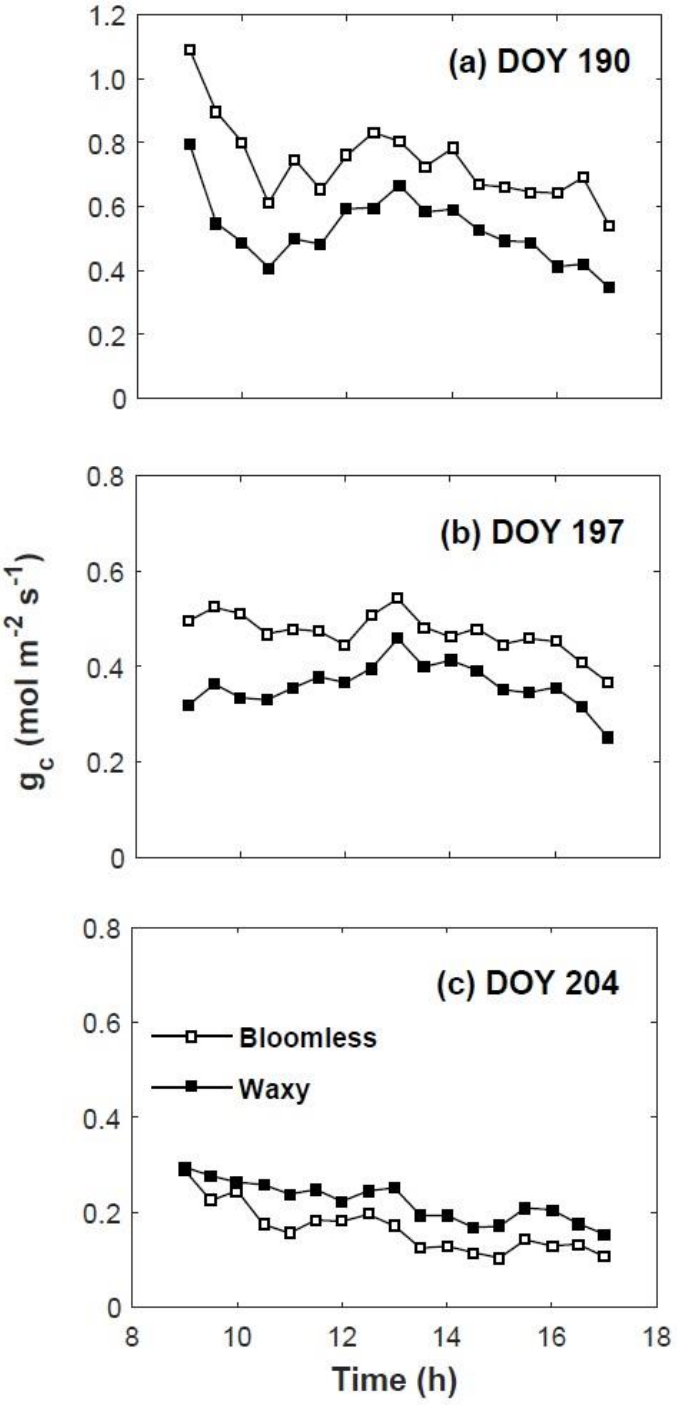

Figure 6.7. Canopy conductance (g_c) of the bloomless (white markers) and waxy (black markers) plots between 9-17h on day of year (*DOY*) 190, 197, and 204.

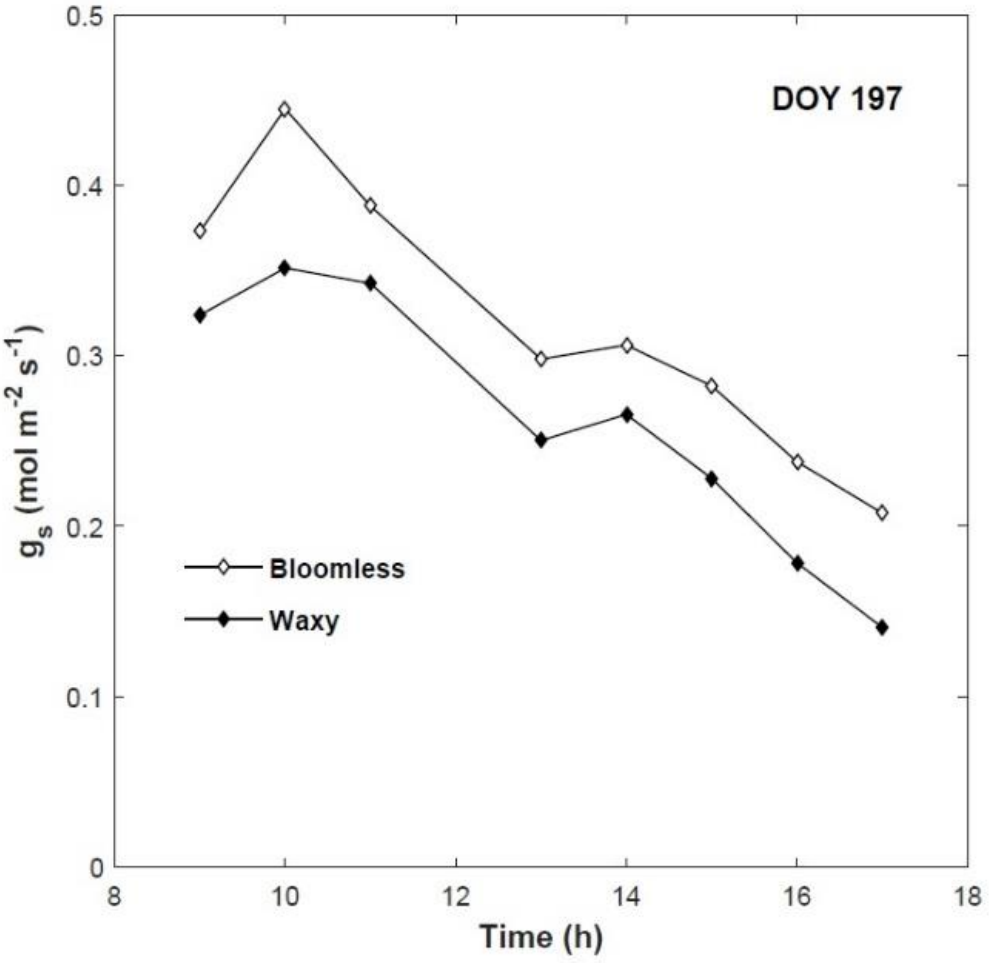

Figure 6.8. Stomatal conductance (g_s) of the bloomless (white markers) and waxy (black markers) plots between 9-17h on day of year (*DOY*) 197. Measurements done on the abaxial side of sunlit flag leaves.

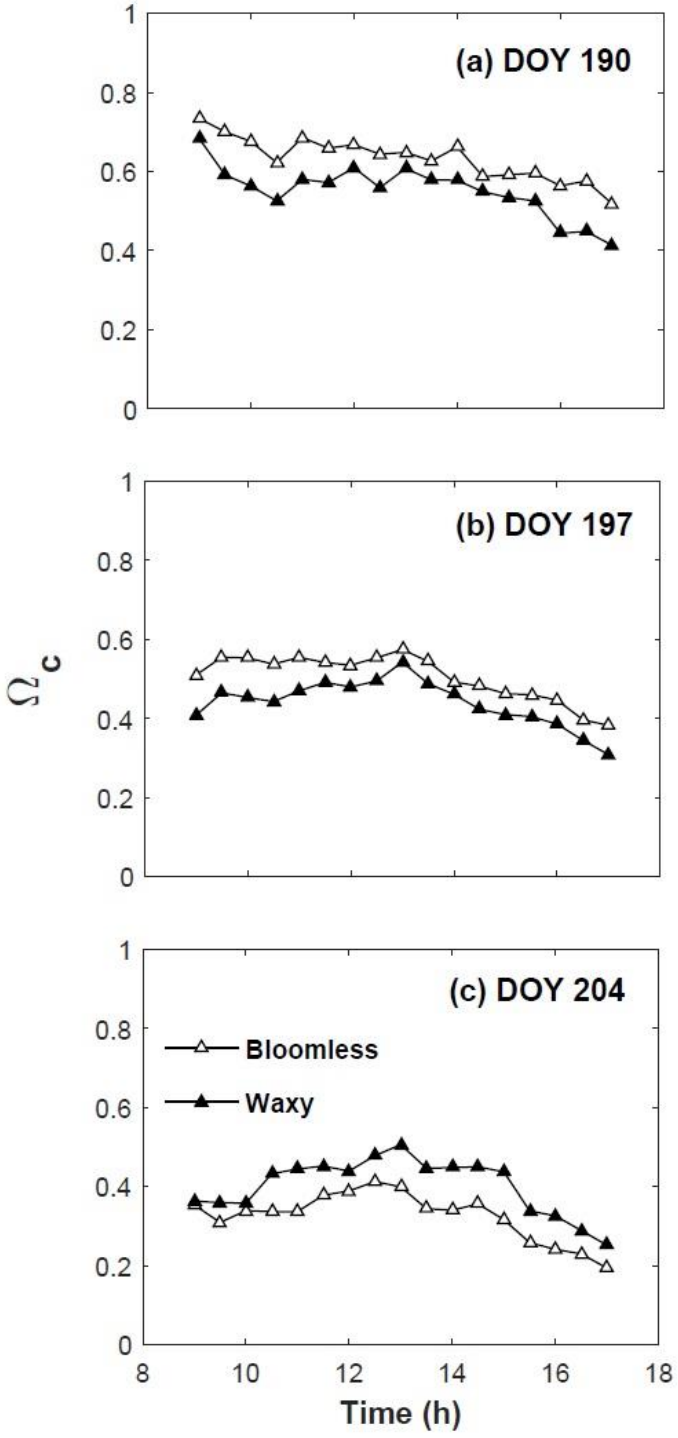

Figure 6.9. Canopy decoupling factor (Ω_c) for the bloomless (white markers) and waxy (black markers) plots between 9-17h on day of year (*DOY*) 190, 197, and 204**.**

Results show that *EW* affected the energy balance of the canopies, and, distinct differences were observed at the beginning and ending of the drying cycle. The data suggests that the observed responses were modulated by rainfall events. Therefore, the effects of *EW* have to be discussed in the context of transient water availability.

When water was non-limiting, i.e. on *DOY* 190 and 197, the bloomless canopy had higher R_n and *LE*, and lower *H*, Bowen ratio, and canopy temperature than the waxy canopy. R_n and g_c in the waxy canopy combined to reduce *LE*, but g_c was the main factor driving the differences between the bloomless and waxy canopies. The reduction in canopy conductance was also reflected in Ω_c. Under well-watered conditions the waxy canopy was better coupled to the atmosphere than the bloomless one. This indicates that the waxy canopy exerted a better control over transpiration and was less sensitive to solar radiation as a driving force for *LE* compared to the bloomless canopy.

When water availability became restrictive, the bloomless canopy had lower *LE*, higher Bowen ratios, and was warmer than the waxy canopy. The decrease in *LE* of the bloomless canopy was caused by reductions in g_c. That caused the bloomless canopy to have lower Ω_c than the waxy one. However, Ω_c in this case should not be interpreted as an indication of better control over transpiration, it just reflects the fact that the bloomless canopy used enough water to induce stomatal closure before the waxy one. Net radiation was similar for both canopies under these conditions. That indicates that the reductions in R_n caused by the waxes were offset by the temperature increase in the bloomless canopy, so that the emission of longwave by the bloomless plot almost equalized the increased reflected solar radiation in the waxy canopy.

The data from this study suggests that the effects of *EW* on the energy balance of plants is that it reduces the rate of water use mostly by means of reducing canopy conductance. On a daily basis, the bloomless canopy used 0.65 and 0.68 mm of water in excess of the waxy one on *DOY* 190 and 197, respectively. Consequently, the waxy canopy had warmer temperatures under well-watered conditions. However, this small reduction on the rate of water use and slightly better coupling to the atmosphere seems to pay off in the long-term. Because the bloomless canopy has poor control of transpiration, it uses water at a faster rate and depletes soil water to the point of stomatal closure earlier than the waxy canopy. That was observed on *DOY* 204. On that day, the waxy canopy used 1.09 mm more water than the bloomless one. Therefore, the bloomless canopy experienced water deficits and became stressed earlier than its waxy counterpart did.

These results show that under well-watered conditions Hypotheses ii was confirmed. *EW* caused a relative decrease in conductance that was greater than the relative increase in albedo, so that the waxy canopy had lower *LE* and higher temperatures than the bloomless canopy. The cooler canopy temperatures and greater *LE* observed for the waxy canopy towards the end of the drying cycle are consequences of a more conservative behavior in terms of water use by that phenotype. An important implication of these results is that they do not suggest that *EW* reduce the overall water use from a field. Instead, *EW* provide a better control over transpiration, helping the plants to extend the amount of time they are not under water deficit stress.

CHAPTER VII

SUMMARY AND CONCLUSIONS

This study demonstrated how epicuticular waxes can affect the radiation and energy balance of plants. At the leaf level, the data shows that increased reflectivity does not imply decreased absorptivity for translucent non-succulent species. Due to reduced transmissivity, waxy and bloomless leaves showed similar absorptivity. The effects of *EW* on emissivity were small as well.

Contrary to what has been traditionally accepted, increased albedo was a mechanism of secondary importance driving differences in energy partitioning between waxy and bloomless plants. Even though waxes caused reductions in net radiation, the amount of energy was small, and does not account for the differences in energy fluxes observed in this study. Instead, the data shows that the primary mechanism through which waxes affect the energy balance of plants is by means of reduced conductance of water vapor. Therefore, the waxy plants had a better control over transpiration and were better coupled to the atmosphere. Consequently, waxy plants use water at a lower rate at the expense of warmer canopy temperatures, while bloomless plants use water at a faster rate and are generally cooler. In the context of dryland agriculture, this could be a good strategy because the bloomless plants depleted water reserves in a shorter period than waxy plants and experienced water deficit stress earlier than the waxy ones.

Different environmental conditions impose different atmospheric demands for water. Consequently, under arid environments plants have higher rates of water use than

in humid environments, and due to scarce rainfall, plants growing in dry areas are under water deficit stress in a shorter time interval than those growing in humid ones. Waxes helped extend the amount of time plants are not under water deficit stress. This period might be stretched or shortened depending on the environment. In arid environments, waxes may give plants a few days of advantage over bloomless plants, whereas in humid environments this could be a little more. However, this will depend on the rainfall frequency of a given location. If rain events occur with a frequency that is much lower than the period it takes for plants to deplete its soil water reserves, then the benefits of waxes with respect to plant water use might be of secondary importance (e.g., decreasing susceptibility to insects, foliar diseases or other abiotic stresses might be a more important role of waxes).

REFERENCES

Abou-Khaled, A., R.M. Hagan, and D.C. Davenport.1970. Effects of kaolinite as a reflective antitranspirant on leaf temperature, transpiration, photosynthesis, and water-use efficiency. Water Resources Research 6:280-289.

Awika, H.O., D.B. Hays, J.E. Mullet, W.L. Rooney, and B.D. Weers. 2017. QTL mapping and loci dissection for leaf epicuticular wax load and canopy temperature depression and their association with QTL for staygreen in Sorghum bicolor under stress. Euphytica 213:207 1-22.

Ball, J.T., I.E. Woodrow, and J.A. Berry. 1987. A model for predicting stomatal conductance and its contribution to the control of photosynthesis under different environmental conditions. In: J. Biggens, editor, Progress in Photosynthesis Research, vol IV. Martinus Nijhoff, Dordrecht, Netherlands. p. 221-224.

Baradas, M.W., B.L. Blad, and N.J. Rosenberg. 1976a. Reflectant induced modification of a soybean canopy radiation balance. IV. Leaf and canopy temperature. Agronomy Journal 68:843-848.

Baradas, M.W., B.L. Blad, and N.J. Rosenberg. 1976b. Reflectant induced modification of a soybean canopy radiation balance. V. Longwave radiation balance. Agronomy Journal 68:848-852.

Blonquist Jr., J.M., J.M. Norman, and B. Bugbee. 2009. Automated measurement of canopy stomatal conductance based on infrared temperature. Agricultural and Forest Meteorology 149:2183-2197.

Blum, A. 1975a. Effect of the Bm gene on epicuticular wax and the water relations of Sorghum bicolor. Israel Journal of Botany 24:50.

Blum, A. 1975b. Effect of the BM gene on epicuticular wax deposition and the spectral characteristics of sorghum leaves. Sabrao Journal 7:45-52.

Bowen, I.S. 1926. The ratio of heat losses by conduction and by evaporation from any water surface. Physical Review 27:779-787.

Campbell, G.S., and J.M. Norman. 1998. An introduction to environmental biophysics, 2nd ed. Springer, New York.

Chatterton, N.J., W.W. Hanna, J.B. Powell, and D.R. Lee. 1975. Photosynthesis and transpiration of bloom and bloomless sorghum. Canadian Journal of Plant Science 55:641-643.

Clarke, J.M., and R.A. Richards. 1988. The effects of glaucousness, epicuticular wax, leaf age, plant height, and growth environment on water loss rates of excised wheat leaves. Canadian Journal of Plant Science 68:975-982.

Cook, G.D., J.R. Dixon, and A.C. Leopold. 1964. Transpiration: its effects on plant leaf temperature. Science 144:546-547.

Doraiswamy, P.C., and N.J. Rosenberg. 1974. Reflectant induced modification of a soybean canopy radiation balance. I. Preliminary tests with a kaolinite reflectant. Agronomy Journal 66:224-228.

Ebercon, A., A. Blum, and W.R. Jordan. 1977. A rapid colorimetric method for epicuticular wax content of sorghum leaves. Crop Science 17:179-180.

Ehrler, W.L., and C.H.M. van Bavel. 1967. Sorghum foliar responses to changes in soil water content. Agronomy Journal 59:243-246.

Febrero, A., S. Fernández, J. Molina-Cano, and J. Araus. 1998. Yield, carbon isotope discrimination, canopy reflectance and cuticular conductance of barley isolines of differing glaucousness. Journal of Experimental Botany 49(326):1575-1581.

Fuchs, M., G. Stanhill, and S. Moreshet. 1976. Effect of increasing foliage and soil reflectivity on the solar radiation balance of wide-row grain sorghum. Agronomy Journal 68:865-871.

Gates, D.M. 1968. Transpiration and leaf temperature. Annual Review of Plant Physiology 19:211-238.

Gates, D.M. 1980. Biophysical ecology. Springer, New York.

Gates, D.M., H.J. Keegan, J.C. Schleter, and V.R. Weidner. 1965. Spectral properties of plants. Applied optics 4:11-20.

Grant, R.H., M.A. Jenks, P.J. Rich, P.J. Peters, and E.N. Ashworth. 1995. Scattering of ultraviolet and photosynthetically active radiation by sorghum bicolor: influence of epicuticular wax. Agricultural and Forest Meteorology 75:263-281.

Hamissou, M., and D.E. Weibel. 2004. The effects of epicuticular wax on the rate of water loss of Sorghum bicolor (L.) Moench. Asian Journal of Plant Sciences 3(6):742-746.

Heilman, J.L, E.T. Kanemasu, N.J. Rosenberg, and B.L. Blad. 1976. Thermal scanner measurement of canopy temperatures to estimate evapotranspiration. Remote Sensing of Environment 5:137-145.

Heilman, J.L., C.L. Brittin, and C.M.U. Neale. 1989. Fetch requirements for bowen ratio measurements of latent and sensible heat fluxes. Agricultural and Forest Meteorology 44:261-273.

Holmes, M.G., and D.R. Keiller. 2002. Effects if pubescence and waxes on the reflectance of leaves in the ultraviolet and photosynthetic wavebands: a comparison of range species. Plant, Cell and Environment 25:85-93.

Jarvis, P.G., and K.G. McNaughton. 1986. Stomatal control of transpiration, scaling up from leaf to region. Advances in Ecological Research 15:1-49.

Jefferson, P.G., D.A. Johnson, and K.H. Asay. 1989. Epicuticular wax production, water status and leaf temperature in Triticeae range grasses of contrasting visible glaucousness. Canadian Journal of Plant Science 69:513-519.

Jeffree, C.E. 2006. The fine structure of the plant cuticle. In: M. Riederer and C. Müller, editors, Biology of the plant cuticle. Blackwell Publishing Ltd., Iowa. p. 11-110.

Jeffree, C.E., R.P.C. Johnson, and P.G. Jarvis. 1971. Epicuticular wax in the stomatal antechamber of Sitka Spruce and its effects on the diffusion of water vapour and carbon dioxide. Planta 98:1-10.

Jenks, M.A., and E.N. Ashworth. 1999. Plant epicuticular waxes: function, production, and genetics. Horticultural Reviews 23:1-68.

Johnson, D.A., R.A. Richards, and N.C. Turner. 1983. Yield, water relations, gas exchange, and surface reflectance of near-isogenic wheat lines differing in glaucousness. Crop Science 23:318-325.

Johnson, I.R. 2013. PlantMod: exploring the physiology of plant canopies. IMJ Software, Dorrigo, NSW, Australia. www.imj.com.au/software/plantmod.

Jones, H.G. 2014. Plants and microclimate: a quantitative approach to environmental plant physiology, 3rd ed. Cambridge University Press, UK.

Jordan, W.R., R.L. Monk, F.R. Miller, D.T. Rosenow, L.E. Clark, and P.J. Shouse. 1983. Environmental physiology of sorghum. I. Environmental and genetic control of epicuticular wax load. Crop Science 23:552-558.

Jordan, W.R., P.J. Shouse, A. Blum, F.R. Miller, and R.L. Monk. 1984. Environmental physiology of sorghum. II. Epicuticular wax load and cuticular transpiration. Crop Science 24:1168-1173.

Kanemasu, E.T. 1977. Evapotranspiration from corn, sorghum, soybean, and winter wheat. Kansas Agricultural Experiment Station Research Reports Vol. 0: Iss. 12. https://doi.org/10.4148/2378-5977.7277.

Kanemasu, E.T., and Arkin, G.F. 1974. Radiant energy and light environment of crops. Agricultural Meteorology 14:211-215.

Kirkham, M.B. 2014. Principles of soil and plant water relations, 2nd ed. Elsevier Academic Press, Waltham, MA.

Körner, C., J.A. Scheel, and H. Bauer. 1979. Maximum leaf diffusive conductance in vascular plants. Photosynthetica 13:45-82.

Lange, O.L. 1959. Untersuchungen über Wärmehaushalt und Hitzeresistenz mauretanischer Wüsten- und Savannenpflanzen. Flora 147:595-651.

Lemeur, R., and N.J. Rosenberg. 1975. Reflectant induced modification of a soybean canopy radiation balance. II. A quantitative and qualitative analysis of radiation reflected from a green soybean canopy. Agronomy Journal 67:301-306.

Lemeur, R., and N.J. Rosenberg. 1976. Reflectant induced modification of a soybean canopy radiation balance. III. A comparison of the effectivenessof celite and kaolinite reflectants. Agronomy Journal 68:30-35.

Monteith, J.L. 1965. Evaporation and environment. In: Symposia of the Society for Experimental Biology, 19. Cambridge University Press, Cambridge, 205-234.

Monteith, J.L., and M.H. Unsworth. 2013. Principles of environmental physics, 4th ed. Academic Press, MA, USA.

Oke, T.R., and F.G. Hannell. 1966. Variations of temperature within a soil. Weather 21:21-28.

O'Toole, J.C., R.T. Cruz, J.N. Seiber. 1979. Epicuticular wax and cuticular resistance in Rice. Physiologia Plantarum 47:239-244.

Penman, H.L. 1948. Natural evaporation from open water, bare soil and grass. Proceedings of the Royal Society of London A193:120-145.

Powel, P., D.E. Weibel, A. Sotamayor, and M. Alameda. 1977. Increased susceptibility of bloomless sorghum to foliar pathogens. Sorghum Newsletter 20:76-77.

Premachandra, G.S., D.T. Hahn, J.D. Axtell, and R.J. Joly. 1994. Epicuticular wax load and water use efficiency in bloomless and sparse bloom mutants of Sorghum bicolor L. Environmental and Experimental Botany 34:293–301.

Reicosky, D.A., and J.W. Hanover. 1978. Physiological effects of surface waxes. I. Light reflectance for glaucous and non-glaucous Picea punges. Plant Physiology 62:101-104.

Richards, R.A., H.M. Rawson, and D.A. Johnson. 1986. Glaucousness in wheat: its development and effect on water-use efficiency, gas exchange and photosynthetic tissue temperatures. Australian Journal of Plant Physiology 13:465-73.

Ritchie, J.T., and E. Burnett. 1971. Dryland evaporative flux in a subhumid climate: II. Plant influences. Agronomy Journal 63:56-62.

Rosenberg, N.J., B.L. Blad, and S.B. Verma. 1983. Microclimate: The biological environment, 2nd ed. John Wiley & Sons, Inc., New York.

Sanchez-Diaz, M.F., J.D. Hesketh, and P. J. Kramer. 1972. Wax filaments on sorghum leaves as seen with a scanning electron microscope. Journal of the Arizona Academy of Science 7(1):6-7.

Saneoka, H., and S. Ogata. 1987. Relationship between water use efficiency and cuticular wax deposition in warm season forage crops grown under water deficit conditions. Soil Science and Plant Nutrition 33(3):439-448.

Shepherd, T., and D.W. Griffiths. 2006. The effects of stress on plant cuticular waxes. New Phytologist 171:469-499.

Shuttleworth, W.J., and J.S. Wallace. 1985. Evaporation from sparse crops: an energy combination theory. Quarterly Journal of the Royal Meteorological Society 111:839-855.

Stanhill, G. 1965. Observations of the reduction of soil temperatures. Agricultural Meteorology 2(3):197-203.

Stanhill, G., S. Moreshet, and M. Fuchs. 1976. Effect of increasing foliage and soil reflectivity on the yield and water use efficiency of grain sorghum. Agronomy Journal 68:329-332.

Tanner, C.B. 1960. Energy balance approach to evapotranspiration of crops. Soil Science Society of America Proceedings 24:1-9.

Thornley, J.H.M., and I.R. Johnson. 2000. Plant and crop modelling. Blackburn Press, New Jersey.